ISSN 1520-295X

Quintuple Friction Pendulum Isolator Behavior, Modeling and Validation

by
Donghun Lee and Michael C. Constantinou

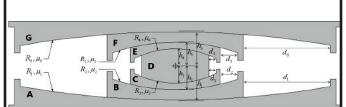
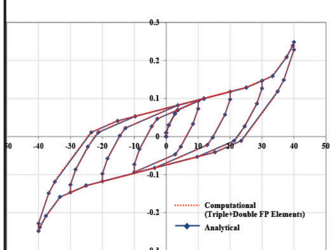

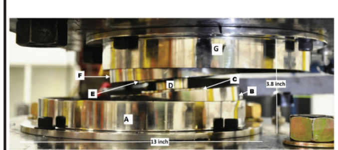
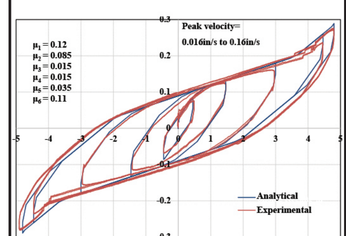

Technical Report MCEER-15-0007

December 28, 2015

This research was conducted at the University at Buffalo, State University of New York, and was supported by MCEER Thrust Area 3, Innovative Technologies.

Quintuple Friction Pendulum Isolator Behavior, Modeling and Validation

by

Donghun Lee[1] and Michael C. Constantinou[2]

Publication Date: December 28, 2015
Submittal Date: June 28, 2015

Technical Report MCEER-15-0007

MCEER Thrust Area 3, Innovative Technologies

1 Ph.D. Candidate, Department of Civil, Structural and Environmental Engineering, University at Buffalo, State University of New York
2 SUNY Distinguished Professor, Department of Civil, Structural and Environmental Engineering, University at Buffalo, State University of New York

MCEER
University at Buffalo, State University of New York
212 Ketter Hall, Buffalo, NY 14260
E-mail: *mceer@buffalo.edu*; WWW Site: *http://mceer.buffalo.edu*

PREFACE

MCEER is a national center of excellence dedicated to the discovery and development of new knowledge, tools and technologies that equip communities to become more disaster resilient in the face of earthquakes and other extreme events. MCEER accomplishes this through a system of multidisciplinary, multi-hazard research, education and outreach initiatives.

Headquartered at the University at Buffalo, State University of New York, MCEER was originally established by the National Science Foundation (NSF) in 1986, as the first National Center for Earthquake Engineering Research (NCEER). In 1998, it became known as the Multidisciplinary Center for Earthquake Engineering Research (MCEER), from which the current name, MCEER, evolved.

Comprising a consortium of researchers and industry partners from numerous disciplines and institutions throughout the United States, MCEER's mission has expanded from its original focus on earthquake engineering to one which addresses the technical and socioeconomic impacts of a variety of hazards, both natural and man-made, on critical infrastructure, facilities, and society.

MCEER investigators derive support from the State of New York, National Science Foundation, Federal Highway Administration, National Institute of Standards and Technology, Department of Homeland Security/Federal Emergency Management Agency, other state governments, academic institutions, foreign governments and private industry.

This report describes the Quintuple Friction Pendulum Isolator, which is a spherical sliding isolator with six sliding surfaces. Analytical models of behavior are presented to describe the force-displacement loop for two general cases of geometric and frictional parameters. The analytical model is useful in performing simplified calculations and in verifying more complex computational models. Computational models are also presented which may be implemented in commercial software. A model isolator was tested and the results are used to validate the analytical and computational models.

ABSTRACT

This report describes the behavior of the Quintuple Friction Pendulum Isolator, a spherical sliding isolator with six sliding surfaces, five effective pendula and nine regimes of operation that allow for complex multi-stage adaptive behavior, depending on the amplitude of displacement. An analytical model is presented that is capable of tracing the behavior of the isolator in two general configurations of geometric and frictional properties. This analytical model is useful for verifying computational models and in performing simplified calculations for analysis and design. A computational model that can be implemented in program SAP2000 is also presented and verified by comparison to the analytical model. Two configurations of a model Quintuple Friction Pendulum Isolator have been tested and the results have been used to validate the analytical and computational models.

ACKNOWLEDGEMENTS

The tested Quintuple FP Isolator was designed and manufactured by Earthquake Protection Systems, Inc., Vallejo, CA. The authors and MCEER gratefully acknowledge and thank Mr. Gregory Nielsen of Arup, Los Angeles who reviewed the report for accuracy and completeness.

TABLE OF CONTENTS

LIST OF FIGURES

LIST OF TABLES

SECTION 1
INTRODUCTION

The Quintuple Friction Pendulum (FP) Isolator is an extension of the Triple FP Isolator (Morgan, 2007; Fenz and Constantinou, 2008a and 2008b) and consists of six spherical sliding surfaces. It offers a more complex multi-stage behavior and smoother transition between regimes than the Triple FP Isolator. It is envisioned as another isolator in the arsenal of isolators available to the engineer to choose from when very large displacement capacities are needed and when complex multi-stage behavior improves performance.

Table 1-1 illustrates the evolution of the Friction Pendulum Isolator and presents information on the number of effective pendula and the number of sliding regimes (or stages) of behavior. The Single FP Isolator (Zayas et al, 1987; Mokha et al, 1991) is characterized by a single sliding surface, one effective pendulum and has one stage of operation. The Double FP Isolator (Fenz and Constantinou, 2006) offers the important advantages of reduced heating effects and increased displacement capacity for a given plan dimension, and can be configured for limited adaptive behavior (although then with the requirement for articulation, which would reduce the axial load capacity). It has two effective pendula and three sliding regimes. The Triple FP Isolator has the same advantages as the Double FP Isolator and also an increased capability for adaptive behavior. It has three effective pendula and five sliding regimes. The Quintuple FP Isolator will be shown to have five effective pendula and nine sliding regimes. The increased number of pendula and sliding regimes increases the adaptability of behavior at the expense of increased complexity in modeling its behavior. The number of effective pendula denotes the name of each isolator. Note that the schematics of isolators in Table 1-1 show the Double FP Isolator having an articulated slider as it is needed for adaptive behavior (Fenz and Constantinou, 2006). Removal of the articulation requires certain friction and geometric constraints that reduce the isolator to having the same behavior as the Single FP Isolator. Also, the Triple and Quintuple FP Isolators are shown to lack articulation for the inner most part–the rigid slider–as articulation would render the bearings unstable (Sarlis and Constantinou, 2013).

TABLE 1-1 Evolution of Friction Pendulum Isolator and Number of Effective Pendula and Sliding Regimes

	Single FP	Double FP	Triple FP	Quintuple FP
Configuration		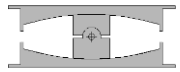	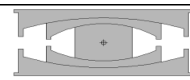	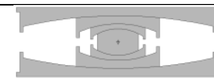
Number of effective pendula	1	2	3	5
Number of sliding regimes	1	3	5	9

The existence of the Quintuple FP Isolator was postulated by Tsai et al (2010) who studied isolators with multiple sliding surfaces and presented a computational plasticity-based model of behavior. Tsai et al (2010) also presented simple algebraic force-displacement relations that only apply for the loading branch and provide no information for unloading.

This paper presents a treatment of the Quintuple Friction Pendulum Isolator that includes:

1) Analytical force-displacement relations for all sliding regimes which are valid for the loading and the unloading branches of the hysteresis loop, and for two general configurations of geometric and frictional properties. These relations may be used to perform simplified calculations in accordance with the Equivalent Lateral Force (ELF) procedure of the ASCE 7 Standard (ASCE, 2010). They can also be used to verify computational models for use in response history analysis.

2) A computational model that can be readily utilized in commercially available software, with examples developed in program SAP2000 (Computers and Structures, 2014).

3) Test results on two configurations of a model Quintuple FP Isolator that are used to validate the analytical and computational models presented.

SECTION 2

ANALYTICAL FORCE-DISPLACEMENT RELATIONS

Figure 2-1 presents a cross section of the Quintuple FP Isolator and defines the geometric and frictional parameters. Note that quantities R_i, i=1 to 6 are the radii of curvature of the six concave surfaces and quantities μ_i, i=1 to 6 are the coefficients of friction at the six sliding interfaces. The analytical force-displacement relations are derived using the approach of Fenz and Constantinou (2008a) and Morgan (2007) in which only equilibrium of horizontal and vertical forces is used. This necessitates certain geometric and frictional constraints. A model for general geometric and frictional parameters further requires consideration of equilibrium of moments and results in a much higher complexity without any practical significance as shown by Sarlis and Constantinou (2013).

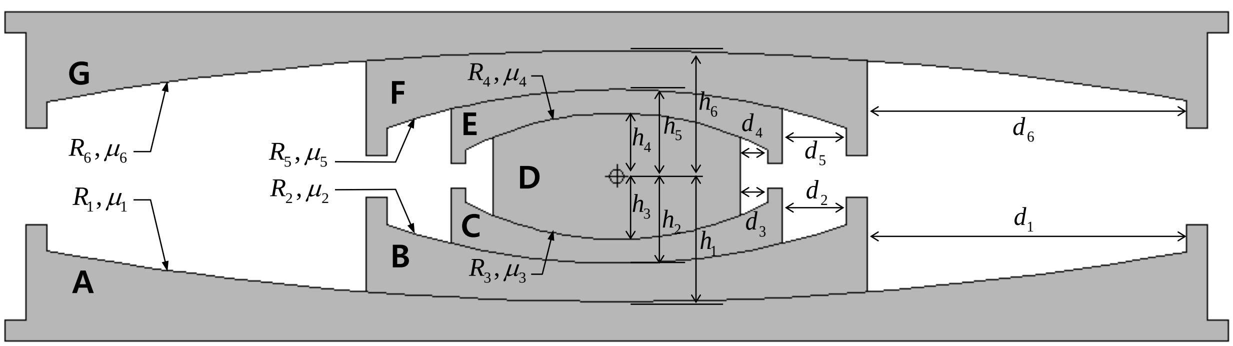

FIGURE 2-1 Cross Section of Quintuple Friction Pendulum Isolator

The basic assumptions of the theory for the Quintuple FP Isolators parallel those for the Triple FP Isolator in the model of Fenz and Constantinou (2008a). They are as follows where quantity $R_{eff,i}$ is the effective radius of curvature and d_i^* is the actual displacement capacity.

$$R_{eff,i} = R_i - h_i \tag{1}$$

$$d_i^* = d_i \left(R_{eff,i} / R_i \right) \tag{2}$$

1) The effective radii satisfy the condition: $R_{eff3} = R_{eff4} << R_{eff2} \leq R_{eff5} << R_{eff1} \leq R_{eff6}$.

2) The coefficients of friction satisfy either of the following two conditions:

   a. Configuration 1, where $\mu_3 = \mu_4 < \mu_5 \le \mu_2 < \mu_6 \le \mu_1$.

   b. Configuration 2, where $\mu_3 = \mu_4 < \mu_2 \le \mu_5 < \mu_6 \le \mu_1$.

   Note that configuration 2 is achieved by interchanging plates C and E of configuration 1 as shown in Figure 2-1. Also, the combination of conditions $\mu_3 = \mu_4$ and $R_{eff\,3} = R_{eff\,4}$ ensures that initiation of motion occurs simultaneously on interfaces 3 and 4 (per Figure 2-1). Any other combination of these four parameters would have resulted in behavior that cannot be exactly predicted by the model presented herein and would require a more complex treatment (Sarlis and Constantinou, 2013). Note that configurations 1 and 2 also encompass the simpler configuration where $\mu_3 = \mu_4 < \mu_5 = \mu_2 < \mu_6 \le \mu_1$, which is characterized by four effective pendula and seven regimes of operation.

3) The displacement capacity of each surface is such that there is gradual stiffening at large displacement. For both configurations, motion on outer surfaces should initiate prior to reaching the restrainers of the inner surfaces (for example, motion on sliding surface 1 should initiate prior to reaching the restrainer of part B, etc.) which leads to the following conditions:

$$\frac{d_1^*}{R_{eff\,1}} + \frac{d_2^*}{R_{eff\,2}} > \mu_1 - \mu_2 \;,\quad \frac{d_1^*}{R_{eff\,1}} + \frac{d_2^*}{R_{eff\,2}} + \frac{d_3^*}{R_{eff\,3}} > \mu_2 - \mu_3$$
$$\frac{d_5^*}{R_{eff\,5}} + \frac{d_6^*}{R_{eff\,6}} > \mu_6 - \mu_5 \;,\quad \frac{d_4^*}{R_{eff\,4}} + \frac{d_5^*}{R_{eff\,5}} + \frac{d_6^*}{R_{eff\,6}} > \mu_5 - \mu_4 \tag{3}$$

4) Sliding should initiate on the surface of highest friction prior to the onset of any stiffening (i.e. prior to contacting any of the displacement restrainers). This leads to the requirement that

$$d_6^* > (\mu_1 - \mu_6) R_{eff\,6} \tag{4}$$

5) For the special case of Configuration 2 where $R_{eff1} < R_{eff6}$, the following condition is also needed:

$$\mu_5 - \mu_2 > \left(\frac{d_1^*}{R_{eff1}} + \frac{d_2^*}{R_{eff2}} \right) - \left(\frac{d_5^*}{R_{eff5}} + \frac{d_6^*}{R_{eff6}} \right) \quad (5)$$

Details of the derivation of the force-displacement relations are presented in Appendix A. Summaries of the relations are presented in Table 2-1 for Configuration 1 and in Table 2-2 for Configuration 2. Details of the unloading branch of each loop are presented in Appendix A. Representative force-displacement relations based on the algebraic equations of Tables 2-1 and 2-2 will be presented in the next section together with results of computational analysis.

Note that configurations 1 and 2 only differ in that regimes 2 and 3 and regimes 8 and 9 are interchanged. This leads to small differences in the loops, which will be illustrated in examples.

TABLE 2-1 Force-Displacement Relation of Quintuple FP Isolator of Configuration 1

Requirements		$\mu_3 = \mu_4 < \mu_5 \le \mu_2 < \mu_6 \le \mu_1$
Regime	Conditions	Force-displacement relation
I	Motion starts on surfaces 3 and 4. Motion occurs on surfaces 3 and 4.	$F = \frac{W}{R_{eff3} + R_{eff4}} u + \frac{F_{f3} R_{eff3} + F_{f4} R_{eff4}}{R_{eff3} + R_{eff4}}$ Valid until: $F^{\mathrm{I}} = F_{f5}$, $u^{\mathrm{I}} = (\mu_5 - \mu_3) R_{eff3} + (\mu_5 - \mu_4) R_{eff4}$
II	Motion stops on 4 and starts on 5. Motion occurs on surfaces 3 and 5.	$F = \frac{W}{R_{eff3} + R_{eff5}} u + \frac{F_{f3} R_{eff3} + F_{f4} R_{eff4} + F_{f5} (R_{eff5} - R_{eff4})}{R_{eff3} + R_{eff5}}$ Valid until: $F^{\mathrm{II}} = F_{f2}$, $u^{\mathrm{II}} = u^{\mathrm{I}} + (F_{f2} - F_{f5}) \times \left[(R_{eff3} + R_{eff5}) / W \right]$
III	Motion stops on 3 and starts on 2. Motion occurs on surfaces 2 and 5.	$F = \frac{W}{R_{eff2} + R_{eff5}} u + \frac{F_{f2} (R_{eff2} - R_{eff3}) + F_{f3} R_{eff3} + F_{f4} R_{eff4} + F_{f5} (R_{eff5} - R_{eff4})}{R_{eff2} + R_{eff5}}$ Valid until: $F^{\mathrm{III}} = F_{f6}$, $u^{\mathrm{III}} = u^{\mathrm{II}} + (F_{f6} - F_{f2}) \times \left[(R_{eff2} + R_{eff5}) / W \right]$

IV	Motion stops on 5 and starts on 6. Motion occurs on surfaces 2 and 6.	$F=\frac{W}{R_{eff\,2}+R_{eff\,6}}u+\frac{F_{f\,2}\left(R_{eff\,2}-R_{eff\,3}\right)+F_{f\,3}R_{eff\,3}}{R_{eff\,2}+R_{eff\,6}}\ldots$ $+\frac{F_{f\,4}R_{eff\,4}+F_{f\,5}\left(R_{eff\,5}-R_{eff\,4}\right)+F_{f\,6}\left(R_{eff\,6}-R_{eff\,5}\right)}{R_{eff\,2}+R_{eff\,6}}$ Valid until: $F^{\mathrm{IV}}=F_{f\,1},\ u^{\mathrm{IV}}=u^{\mathrm{III}}+\left(F_{f\,1}-F_{f\,6}\right)\times\left[\left(R_{eff\,2}+R_{eff\,6}\right)/W\right]$
V	Motion stops on 2 and starts on 1. Motion occurs on surfaces 1 and 6.	$F=\frac{W}{R_{eff\,1}+R_{eff\,6}}u+\frac{F_{f\,1}\left(R_{eff\,1}-R_{eff\,2}\right)+F_{f\,2}\left(R_{eff\,2}-R_{eff\,3}\right)+F_{f\,3}R_{eff\,3}}{R_{eff\,1}+R_{eff\,6}}\ldots$ $+\frac{F_{f\,4}R_{eff\,4}+F_{f\,5}\left(R_{eff\,5}-R_{eff\,4}\right)+F_{f\,6}\left(R_{eff\,6}-R_{eff\,5}\right)}{R_{eff\,1}+R_{eff\,6}}$ Valid until: $F^{\mathrm{V}}=F_{dr6}=\frac{W}{R_{eff\,6}}d_6^*+F_{f\,6}$, $u^{\mathrm{V}}=u_{dr6}=u^{\mathrm{IV}}+\left(F_{dr6}-F_{f\,1}\right)\times\left[\left(R_{eff\,1}+R_{eff\,6}\right)/W\right]$
VI	Motion reaches end on 6 and stops. Motion starts on 5. Motion occurs on surfaces 1 and 5.	$F=\frac{W}{R_{eff\,1}+R_{eff\,5}}\left(u-u_{dr6}\right)+F_{dr6}$ Valid until: $F^{\mathrm{VI}}=F_{dr1}=\frac{W}{R_{eff\,1}}d_1^*+F_{f\,1}$, $u^{\mathrm{VI}}=u_{dr1}=u_{dr6}+\left(F_{dr1}-F_{dr6}\right)\times\left[\left(R_{eff\,1}+R_{eff\,5}\right)/W\right]$
VII	Motion reaches end on 1 and stops. Motion starts on 2. Motion occurs on surfaces 2 and 5.	$F=\frac{W}{R_{eff\,2}+R_{eff\,5}}\left(u-u_{dr1}\right)+F_{dr1}$ Valid until: $F^{\mathrm{VII}}=F_{dr5}=W\left(\frac{d_5^*}{R_{eff\,5}}+\frac{d_6^*}{R_{eff\,6}}\right)+F_{f\,5}$, $u^{\mathrm{VII}}=u_{dr5}=u_{dr1}+\left(F_{dr5}-F_{dr1}\right)\times\left[\left(R_{eff\,2}+R_{eff\,5}\right)/W\right]$
VIII	Motion reaches end on 5 and stops. Motion starts on 4. Motion occurs on surfaces 2 and 4.	$F=\frac{W}{R_{eff\,2}+R_{eff\,4}}\left(u-u_{dr5}\right)+F_{dr5}$ Valid until: $F^{\mathrm{VIII}}=F_{dr2}=W\left(\frac{d_1^*}{R_{eff\,1}}+\frac{d_2^*}{R_{eff\,2}}\right)+F_{f\,2}$, $u^{\mathrm{VIII}}=u_{dr2}=u_{dr5}+\left(F_{dr2}-F_{dr5}\right)\times\left[\left(R_{eff\,2}+R_{eff\,4}\right)/W\right]$

IX	Motion reaches end on 2 and stops. Motion starts on 3. Motion occurs on surfaces 3 and 4.	$F = \frac{W}{R_{eff3} + R_{eff4}}\left(u - u_{dr2}\right) + F_{dr2}$ Valid until: $F^{\text{IX}} = \frac{W}{R_{eff3} + R_{eff4}}\left(u^{\text{IX}} - u_{dr2}\right) + F_{dr2}$ $u^{\text{IX}} = d_1^* + d_2^* + d_3^* + d_4^* + d_5^* + d_6^*$

TABLE 2-2 Force-Displacement Relation of Quintuple FP Isolator of Configuration 2

Requirements		$\mu_3 = \mu_4 < \mu_2 \le \mu_5 < \mu_6 \le \mu_1$
Regime	Conditions	Force-displacement relation
I	Motion starts on surfaces 3 and 4. Motion occurs on surfaces 3 and 4.	$F = \frac{W}{R_{eff3} + R_{eff4}}u + \frac{F_{f3}R_{eff3} + F_{f4}R_{eff4}}{R_{eff3} + R_{eff4}}$ Valid until: $F^{\text{I}} = F_{f2}$, $u^{\text{I}} = \left(\mu_2 - \mu_3\right)R_{eff3} + \left(\mu_2 - \mu_4\right)R_{eff4}$
II	Motion stops on 3 and starts on 2. Motion occurs on surfaces 2 and 4.	$F = \frac{W}{R_{eff2} + R_{eff4}}u + \frac{F_{f3}R_{eff3} + F_{f4}R_{eff4} + F_{f2}\left(R_{eff2} - R_{eff3}\right)}{R_{eff2} + R_{eff4}}$ Valid until: $F^{\text{II}} = F_{f5}$, $u^{\text{II}} = u^{\text{I}} + \left(F_{f5} - F_{f2}\right)\times\left[\left(R_{eff2} + R_{eff4}\right)/W\right]$
III	Motion stops on 4 and starts on 5. Motion occurs on surfaces 2 and 5.	$F = \frac{W}{R_{eff2} + R_{eff5}}u + \frac{F_{f2}\left(R_{eff2} - R_{eff3}\right) + F_{f3}R_{eff3} + F_{f4}R_{eff4} + F_{f5}\left(R_{eff5} - R_{eff4}\right)}{R_{eff2} + R_{eff5}}$ Valid until: $F^{\text{III}} = F_{f6}$, $u^{\text{III}} = u^{\text{II}} + \left(F_{f6} - F_{f5}\right)\times\left[\left(R_{eff2} + R_{eff5}\right)/W\right]$
IV	Motion stops on 5 and starts on 6. Motion occurs on surfaces 2 and 6.	$F = \frac{W}{R_{eff2} + R_{eff6}}u + \frac{F_{f2}\left(R_{eff2} - R_{eff3}\right) + F_{f3}R_{eff3}}{R_{eff2} + R_{eff6}}\ldots$ $+\frac{F_{f4}R_{eff4} + F_{f5}\left(R_{eff5} - R_{eff4}\right) + F_{f6}\left(R_{eff6} - R_{eff5}\right)}{R_{eff2} + R_{eff6}}$ Valid until: $F^{\text{IV}} = F_{f1}$, $u^{\text{IV}} = u^{\text{III}} + \left(F_{f1} - F_{f6}\right)\times\left[\left(R_{eff2} + R_{eff6}\right)/W\right]$

V	Motion stops on 2 and starts on 1. Motion occurs on surfaces 1 and 6.	$F=\frac{W}{R_{eff1}+R_{eff6}}u+\frac{F_{f1}\left(R_{eff1}-R_{eff2}\right)+F_{f2}\left(R_{eff2}-R_{eff3}\right)+F_{f3}R_{eff3}}{R_{eff1}+R_{eff6}}\ldots$ $+\frac{F_{f4}R_{eff4}+F_{f5}\left(R_{eff5}-R_{eff4}\right)+F_{f6}\left(R_{eff6}-R_{eff5}\right)}{R_{eff1}+R_{eff6}}$ Valid until: $F^{\text{V}}=F_{dr6}=\frac{W}{R_{eff6}}d_6^*+F_{f6}$, $u^{\text{V}}=u_{dr6}=u^{\text{IV}}+\left(F_{dr6}-F_{f1}\right)\times\left[\left(R_{eff1}+R_{eff6}\right)/W\right]$
VI	Motion reaches end on 6 and stops. Motion starts on 5. Motion occurs on surfaces 1 and 5.	$F=\frac{W}{R_{eff1}+R_{eff5}}\left(u-u_{dr6}\right)+F_{dr6}$ Valid until: $F^{\text{VI}}=F_{dr1}=\frac{W}{R_{eff1}}d_1^*+F_{f1}$, $u^{\text{VI}}=u_{dr1}=u_{dr6}+\left(F_{dr1}-F_{dr6}\right)\times\left[\left(R_{eff1}+R_{eff5}\right)/W\right]$
VII	Motion reaches end on 1 and stops. Motion starts on 2. Motion occurs on surfaces 2 and 5.	$F=\frac{W}{R_{eff2}+R_{eff5}}\left(u-u_{dr1}\right)+F_{dr1}$ Valid until: $F^{\text{VII}}=F_{dr2}=W\left(\frac{d_1^*}{R_{eff1}}+\frac{d_2^*}{R_{eff2}}\right)+F_{f2}$, $u^{\text{VII}}=u_{dr2}=u_{dr1}+\left(F_{dr2}-F_{dr1}\right)\times\left[\left(R_{eff2}+R_{eff5}\right)/W\right]$
VIII	Motion reaches end on 2 and stops. Motion starts on 3. Motion occurs on surfaces 3 and 5.	$F=\frac{W}{R_{eff3}+R_{eff5}}\left(u-u_{dr2}\right)+F_{dr2}$ Valid until: $F^{\text{VIII}}=F_{dr5}=W\left(\frac{d_5^*}{R_{eff5}}+\frac{d_6^*}{R_{eff6}}\right)+F_{f5}$, $u^{\text{VIII}}=u_{dr5}=u_{dr2}+\left(F_{dr5}-F_{dr2}\right)\times\left[\left(R_{eff3}+R_{eff5}\right)/W\right]$
IX	Motion reaches end on 5 and stops. Motion starts on 4. Motion occurs on surfaces 3 and 4.	$F=\frac{W}{R_{eff3}+R_{eff4}}\left(u-u_{dr5}\right)+F_{dr5}$ Valid until: $F^{\text{IX}}=\frac{W}{R_{eff3}+R_{eff4}}\left(u^{\text{IX}}-u_{dr5}\right)+F_{dr5}$ $u^{\text{IX}}=d_1^*+d_2^*+d_3^*+d_4^*+d_5^*+d_6^*$

SECTION 3
MODELING QUINTUPLE FRICTION PENDULUM ISOLATORS FOR RESPONSE HISTORY ANALYSIS

The analytical algebraic model presented in Tables 2-1 and 2-2 is useful in quickly constructing force-displacement loops of the quintuple FP Isolator to better understand its behavior, in performing simplified calculations of response based on the Equivalent Lateral Force (ELF) procedure of the ASCE 7 Standard (ASCE, 2010) and in verifying more complex computational methods used in response history analysis. Moreover, the model may be used to develop a computational tri-axial model (biaxial horizontal motion under varying vertical load) based on the procedures presented in Ray et al (2013). However, of interest to the profession is the availability of a verified computational model of the isolator that can be readily utilized in available commercial software. Two such models are described in this section. Both utilize elements available in program SAP2000 (Computers and Structures, 2014). The first of these models utilizes a combination of five Single Friction Pendulum elements and additional gap elements. The second model utilizes a combination of one Double Friction Pendulum and one Triple Friction Pendulum elements.

3.1 Series Model Based on Single FP Elements

This model uses a series representation of up to five pendula based on the paradigm of Fenz and Constantinou (2008c) in modeling the Triple FP Isolator in SAP2000, although the model can be implemented in any program. The five pendula are needed in the general case where five different values of friction and/or five different values of the effective radius describe the isolator behavior (say in configuration 1 when $\mu_3 = \mu_4 < \mu_5 < \mu_2 < \mu_6 < \mu_1$). The number of needed pendula reduces depending on the number of friction values and effective radii. For example, a case with $R_{eff3} = R_{eff4}$, $R_{eff2} = R_{eff5}$, $R_{eff1} = R_{eff6}$ and $\mu_3 = \mu_4 < \mu_5 = \mu_2 < \mu_6 = \mu_1$ would require only three pendula as the isolator effectively behaves as a Triple FP Isolator.

Figure 3-1 illustrates the model. Each single FP element is characterized by: (a) a linear elastic spring of stiffness $W/\bar{R}_{eff}$ where W is the instantaneous axial load on the isolator, (b) a friction force $\bar{\mu}W$ where $\bar{\mu}$ is a coefficient of friction that may be dependent on the velocity and (c) a gap element with displacement capacity, $\bar{d}$, that is related to the displacement capacity of each sliding surface.

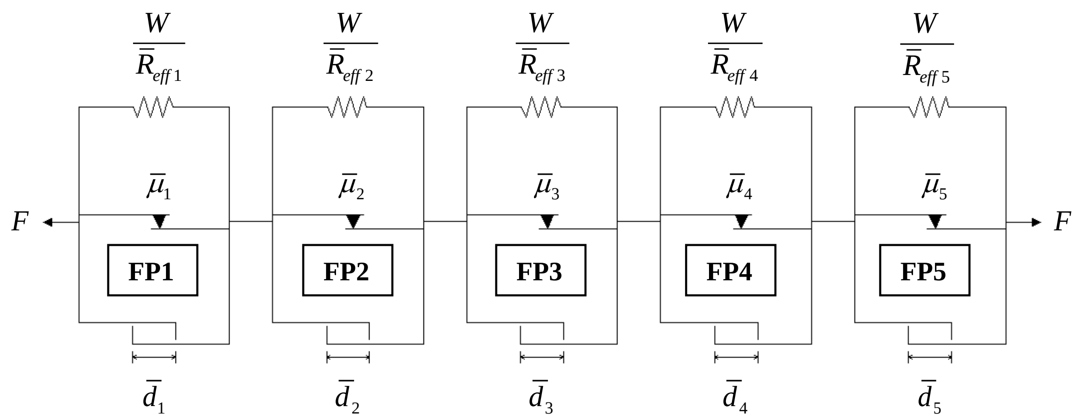

FIGURE 3-1 Representation of Series Model of Quintuple Friction Pendulum Isolator

TABLE 3-1a Parameters Used in Series Model with Five Single FP Elements to Represent the Behavior of the Quintuple FP Isolator of Configuration 1

Element	Coefficient of friction	Radius of curvature	Displacement capacity
Single FP1	$\bar{\mu}_1 = \mu_3 = \mu_4$	$\bar{R}_{eff1} = R_{eff3} + R_{eff4}$	$\bar{d}_1 = d^*_{total} - \left(\bar{d}_2 + \bar{d}_3 + \bar{d}_4 + \bar{d}_5 + \bar{d}_6\right)$
Single FP2	$\bar{\mu}_2 = \mu_5$	$\bar{R}_{eff2} = R_{eff5} - R_{eff4}$	$\bar{d}_2 = \left(\frac{d^*_5}{R_{eff5}} + \frac{d^*_6}{R_{eff6}}\right)\left(R_{eff5} - R_{eff4}\right)$
Single FP3	$\bar{\mu}_3 = \mu_2$	$\bar{R}_{eff3} = R_{eff2} - R_{eff3}$	$\bar{d}_3 = \left(\frac{d^*_1}{R_{eff1}} + \frac{d^*_2}{R_{eff2}}\right)\left(R_{eff2} - R_{eff3}\right)$
Single FP4	$\bar{\mu}_4 = \mu_6$	$\bar{R}_{eff4} = R_{eff6} - R_{eff5}$	$\bar{d}_4 = d^*_6\left(1 - \frac{R_{eff5}}{R_{eff6}}\right)$
Single FP5	$\bar{\mu}_5 = \mu_1$	$\bar{R}_{eff5} = R_{eff1} - R_{eff2}$	$\bar{d}_5 = d^*_1\left(1 - \frac{R_{eff2}}{R_{eff1}}\right)$

Note: $d^*_{total} = d^*_1 + d^*_2 + d^*_3 + d^*_4 + d^*_5 + d^*_6$ is the displacement capacity of the isolator

The parameters in the series model are selected to represent the actual behavior of the isolator as revealed in the analytical model of Tables 2-1 and 2-2. The force-displacement relation of the series model of Figure 3-1 may be easily constructed and is shown in Figure 3-2. Comparison of this loop to the model described in Tables 2-1 and 2-2 leads to relations presented in Table 3-1a and 3-1b that define the parameters of the model.

TABLE 3-1b Parameters Used in Series Model with Five Single FP Elements to Represent the Behavior of the Quintuple FP Isolator of Configuration 2

Element	Coefficient of friction	Radius of curvature	Displacement capacity
Single FP1	$\bar{\mu}_1 = \mu_3 = \mu_4$	$\bar{R}_{eff\,1} = R_{eff\,3} + R_{eff\,4}$	$\bar{d}_1 = d^*_{total} - \left(\bar{d}_2 + \bar{d}_3 + \bar{d}_4 + \bar{d}_5 + \bar{d}_6\right)$
Single FP2	$\bar{\mu}_2 = \mu_2$	$\bar{R}_{eff\,2} = R_{eff\,2} - R_{eff\,3}$	$\bar{d}_2 = \left(\frac{d^*_1}{R_{eff\,1}} + \frac{d^*_2}{R_{eff\,2}}\right)\left(R_{eff\,2} - R_{eff\,3}\right)$
Single FP3	$\bar{\mu}_3 = \mu_5$	$\bar{R}_{eff\,3} = R_{eff\,5} - R_{eff\,4}$	$\bar{d}_3 = \left(\frac{d^*_5}{R_{eff\,5}} + \frac{d^*_6}{R_{eff\,6}}\right)\left(R_{eff\,5} - R_{eff\,4}\right)$
Single FP4	$\bar{\mu}_4 = \mu_6$	$\bar{R}_{eff\,4} = R_{eff\,6} - R_{eff\,5}$	$\bar{d}_4 = d^*_6\left(1 - \frac{R_{eff\,5}}{R_{eff\,6}}\right)$
Single FP5	$\bar{\mu}_5 = \mu_1$	$\bar{R}_{eff\,5} = R_{eff\,1} - R_{eff\,2}$	$\bar{d}_5 = d^*_1\left(1 - \frac{R_{eff\,2}}{R_{eff\,1}}\right)$

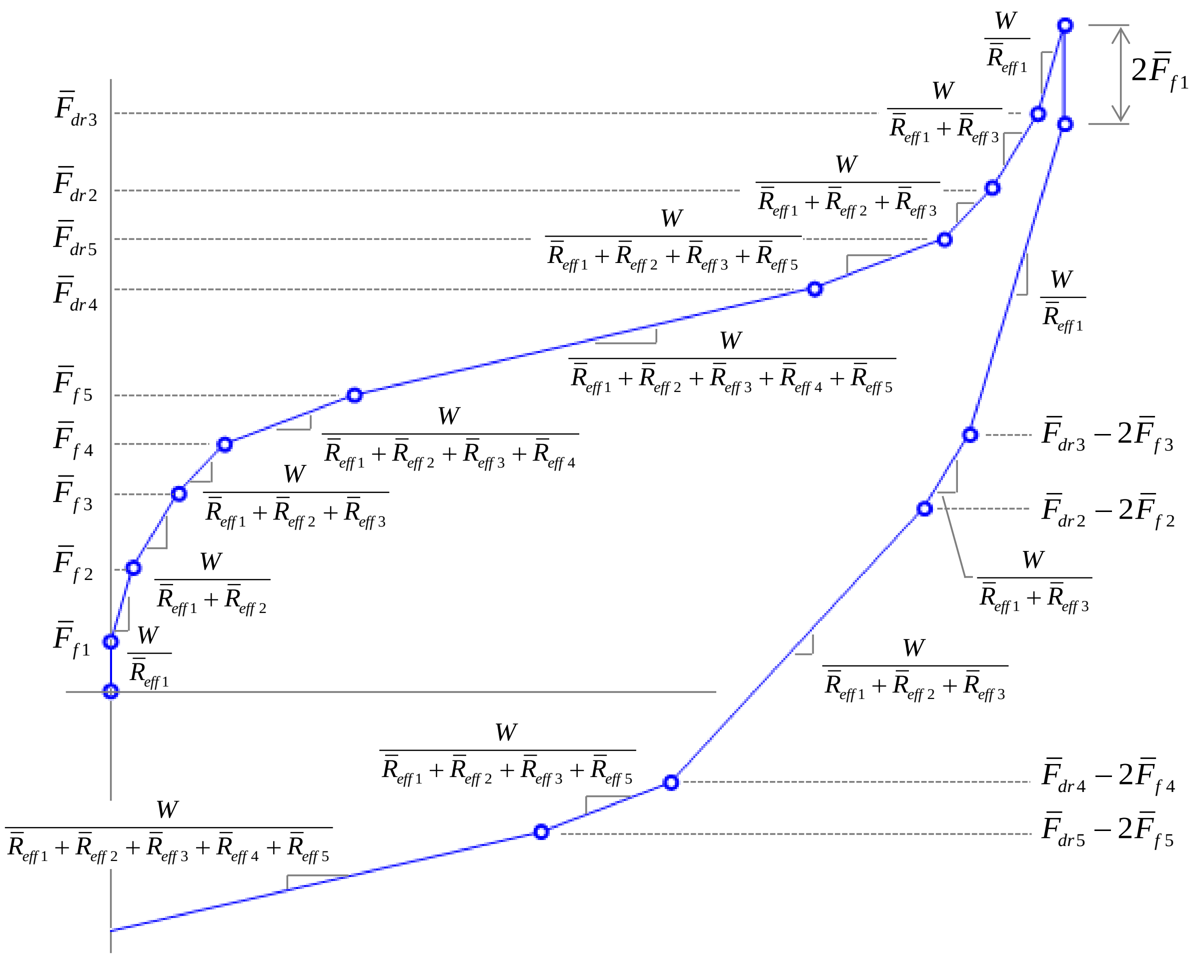

FIGURE 3-2 Force-Displacement Relation of Series Model with Five Single FP Elements

The series model with five single FP elements shown in Figure 3-1 can be implemented as an assembly of vertically-connected single FP elements and gap elements in commercial software SAP2000. Admittedly, however, this modeling approach is complicated because it would require 37 nodes, 27 rigid beam elements, four additional boundary supports, five single FP elements and at least 16 gap elements to model the tri-axial behavior of the bearing (see Fenz and Constantinou, 2008c for the similar case of the Triple FP Isolator). Figure 3-3 illustrates the model with five single FP elements. The figure also shows that this element may be reduced to a pair of one Triple FP and one Double FP elements, of which the Triple FP element exist in the most recent version of program SAP2000, and the Double FP Element may be simulated as a subversion of the Triple FP element in program SAP2000.

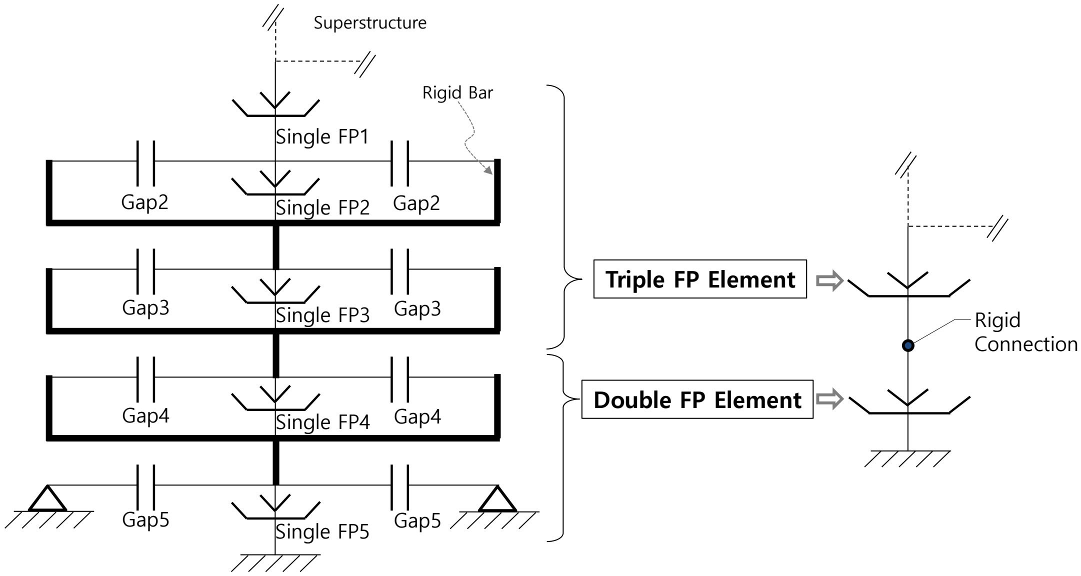

FIGURE 3-3 Series Model of Quintuple FP Isolator with (a) Five Single FP Elements in Series and (b) Pair of Double and Triple FP Elements

3.2 Series Model Based on Combination of Triple FP and Double FP Elements

The series model with five Single FP elements shown in Figure 3-3 can be represented by a pair of one Double and one Triple FP Isolator element as shown in Figure 3-4. These two elements are already available in program SAP2000 (the Double FP element is a subversion of the Triple FP element). However, their use in modeling the Quintuple FP Isolator requires that the Double and Triple FP element parameters be correctly specified.

The Triple FP element will be used to represent the behavior of an idealized Triple FP Isolator with the parameters shown in Figure 3-4(a) and the Double FP element will be used to represent the behavior of an idealized Double FP element with the parameters shown in Figure 3-4(b). Note that the parameters of this idealized isolator will be determined so that the two elements represent the behavior of the actual isolator. The assembly of these two elements consists of five pendula that produce the same behavior as the series model of Figure 3-1.

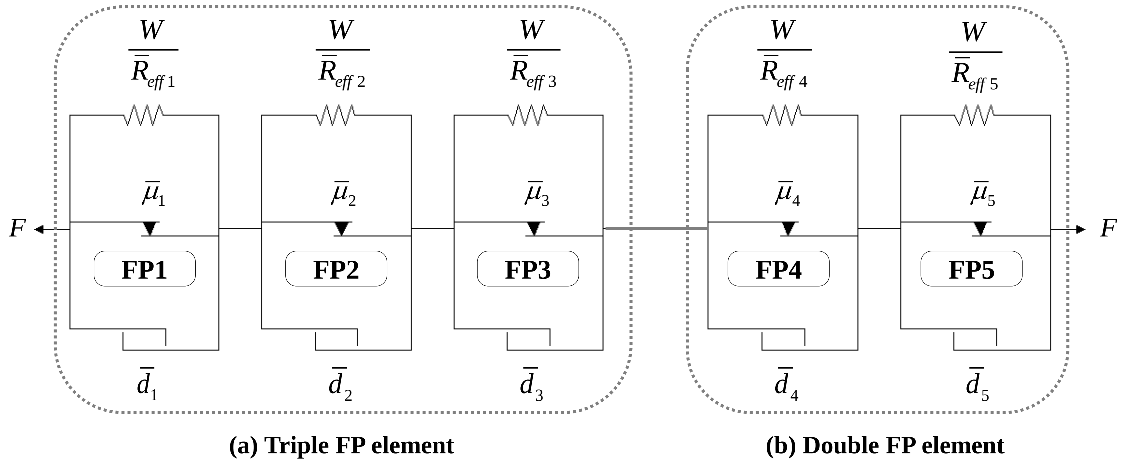

FIGURE 3-4 Parameters of (a) Triple FP Element and (b) Double FP Element Representing a Quintuple FP Isolator

TABLE 3-2 Parameters Used in Series Model with One Triple and One Double FP Element to Represent the Behavior of the Quintuple FP Isolator

Element	Surface	Coefficient of friction	Radius of curvature	Displacement capacity
Triple FP element	Inner surfaces	$\tilde{\mu}_2 (= \tilde{\mu}_3) = \mu_3 (= \mu_4)$	$\tilde{R}_{eff\,2} (= \tilde{R}_{eff\,3}) = R_{eff\,3} (= R_{eff\,4})$	$\tilde{d}_2 = \tilde{d}_3 = \left[d^*_{total} - \left(\tilde{d}_1 + \tilde{d}_4 + \tilde{d}_5 + \tilde{d}_6 \right) \right] / 2$
	Outer top surface	$\tilde{\mu}_4 = \mu_5$	$\tilde{R}_{eff\,4} = R_{eff\,5}$	$\tilde{d}_4 = d^*_5 + \frac{R_{eff\,5}}{R_{eff\,6}} d^*_6$
	Outer bottom surface	$\tilde{\mu}_1 = \mu_2$	$\tilde{R}_{eff\,1} = R_{eff\,2}$	$\tilde{d}_1 = d^*_2 + \frac{R_{eff\,2}}{R_{eff\,1}} d^*_1$
Double FP element	Upper surface	$\tilde{\mu}_5 = \mu_6$	$\tilde{R}_{eff\,5} = R_{eff\,6} - R_{eff\,5}$	$\tilde{d}_5 = d^*_6 \left(1 - \frac{R_{eff\,5}}{R_{eff\,6}} \right)$
	Lower surface	$\tilde{\mu}_6 = \mu_1$	$\tilde{R}_{eff\,6} = R_{eff\,1} - R_{eff\,2}$	$\tilde{d}_6 = d^*_1 \left(1 - \frac{R_{eff\,2}}{R_{eff\,1}} \right)$

$d^*_{total} = d^*_1 + d^*_2 + d^*_3 + d^*_4 + d^*_5 + d^*_6$

The parameters of Triple FP and Double FP elements are derived using the actual parameters of the Quintuple FP Isolator are presented in Table 3-2. For the Triple FP element, the parameters are derived by use of the following: (a) the relation between the actual parameters of the Triple FP Isolator and the series model with three single FP pendula presented in Fenz and Constantinou (2008c), and (b) the relation between the first three pendula of the series model in Figure 3-1 to the actual parameters of Quintuple FP Isolator.

3.3 Model Verification

To verify the computational models presented, a case of the Quintuple FP Isolator in Configuration 1 is modeled in program SAP2000, analyzed to obtain force-displacement relations and then compared to the predictions of the analytical model. Table 3-3 presents the parameters of the example Quintuple FP Isolator. For the analysis, a simple seismically-isolated structure was constructed and analyzed in SAP2000. The lateral force-displacement relation was obtained by imposing a history of displacement at a control point. Details are provided in Appendix B. A second example of Configuration 2 will also be presented and discussed. The second example consists of an isolator with the same geometric and frictional characteristics as the example of Configuration 1, but with μ_2=0.03 and μ_5=0.06.

TABLE 3-3 Parameters of Analyzed Quintuple FP Isolator of Configuration 1

Radius (inch)		Height (inch)		Friction Coefficient		Displacement Capacity (inch)	
R_1	238	h_1	8	μ_1	0.10	d_1	14
R_2	50	h_2	6	μ_2	0.06	d_2	6
R_3	24	h_3	4	μ_3 (= μ_4)	0.01	d_3	2.25
R_4	24	h_4	4			d_4	2.25
R_5	50	h_5	6	μ_5	0.03	d_5	6
R_6	156	h_6	8	μ_6	0.07	d_6	14

Figure 3-5 compares force-displacement loops obtained by the computational SAP2000 model to that constructed using the analytical model of Table 2-1 for the example of Configuration 1. The five Single FP element model and the Triple-Double FP element model gave exactly the same results so only the results of the latter are shown in Figure 3-5. The loops were constructed to a displacement of 40inch, which is in regime IX and just short of the displacement capacity of 41.1inch. Loops at intermediate amplitudes of displacement are also shown in Figure 3-5. The transition points between regimes are identified in the graphs. Evidently, the SAP2000 computational model predicts exactly the behavior of the isolator as determined by the analytical model of Table 2-1.

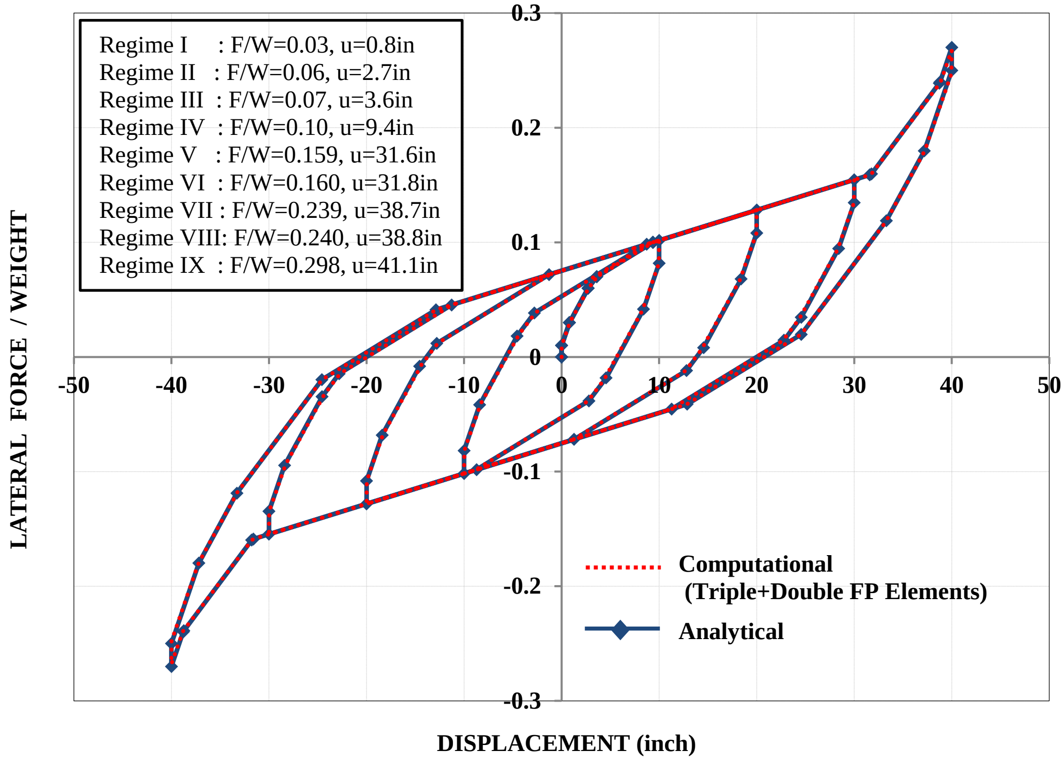

FIGURE 3-5 Comparison of Analytical and Computational Force-Displacement Loops for Example of Configuration 1 in Table 3-3

The example of Configuration 2 also resulted in identical analytical and computational force-displacement loops. However, the behavior of the isolator of Configuration 2 was the same as that of Configuration 1 except for some small difference in the stiffening regimes which are related to differences in the sliding regimes as revealed in Tables 2-1 and 2-2. Accordingly, only results of the analytical model are presented in order to expose differences between the two configurations. The comparison of loops for the configurations is presented in Figure 3-6. The small difference between the two configurations is highlighted by zooming on the stiffening regimes. Analysis of isolators with different geometric and frictional properties revealed generally small differences in the force-displacement loops between the two configurations. An example of the largest differences calculated is for a case for which the loops are presented in Figure 3-7. Configurations 1 is the same as that of Table 3-3 in terms of frictional and geometric properties but for the radius of surface 5 being R_5=120inch instead of 50inch and coefficient of friction μ_5=0.02 instead of 0.03. Configuration 2 has the properties of surfaces 2 and 5 interchanged.

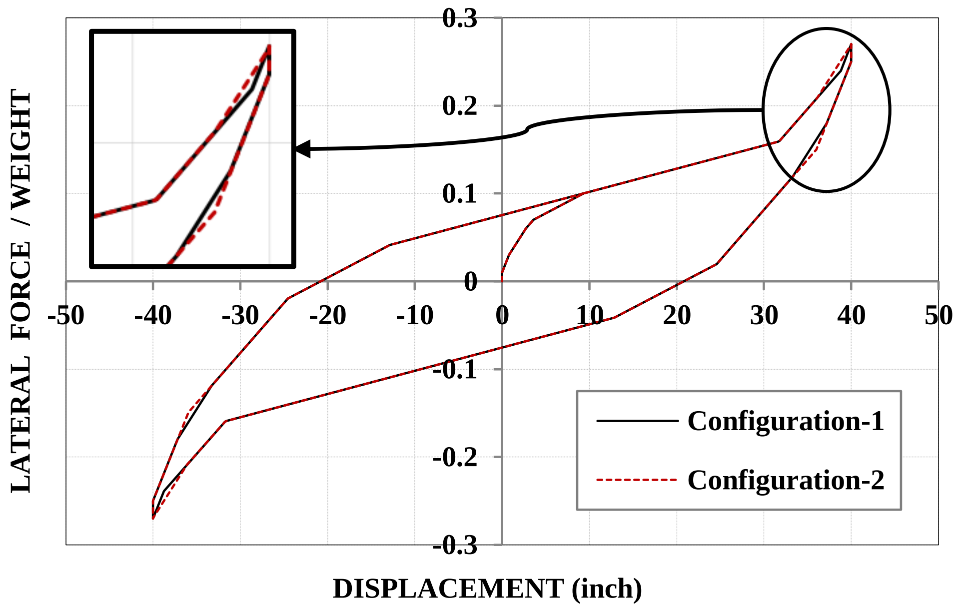

FIGURE 3-6 Comparison of Analytical Force-Displacement Loops for Examples of Configurations 1 and 2 per Table 3-3

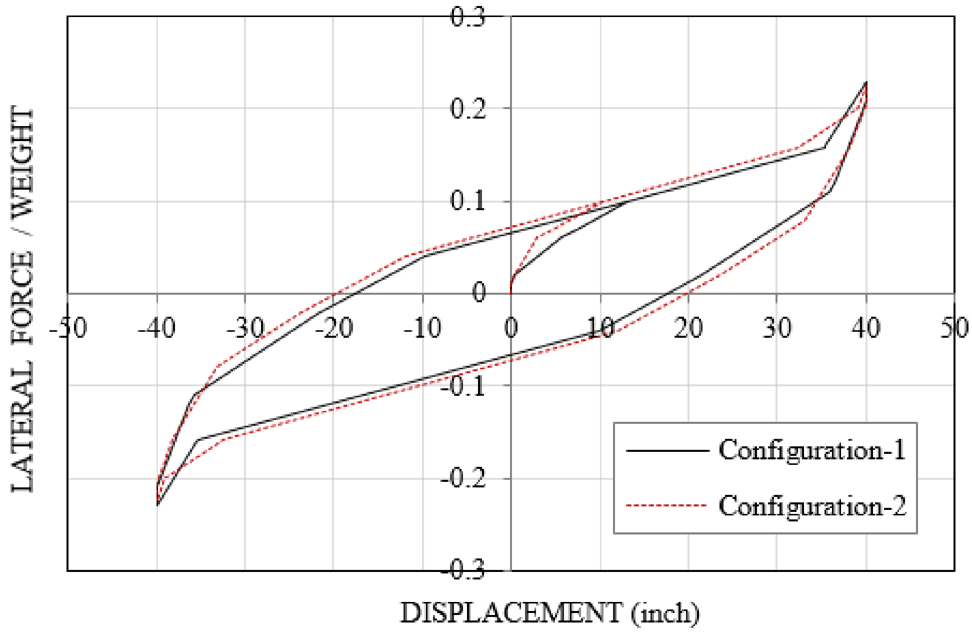

FIGURE 3-7 Comparison of Analytical Force-Displacement Loops for Examples of Configurations 1 and 2 per Table 3-3 but with R_5=120in. and μ_5=0.02

The results in Figures 3-6 and 3-7 demonstrate small differences between configurations 1 and 2. Nevertheless, the force-displacement relations of the two configurations are governed by different sets of equations, respectively given in Tables 2-1 and 2-2.

The presented results provide verification for the computational model in program SAP2000. Nevertheless, the analytical model and the computational model in program SAP2000 require validation by comparison to experimental data. This is provided in the next section where test results are presented.

SECTION 4
MODEL VALIDATION

A model Quintuple FP Isolator was tested in the bearing test machine at the University at Buffalo (Kasalanati and Constantinou, 1999). Table 4-1 presents the properties of the tested isolator. Two configurations were tested, 1 and 2. Configuration 2 was created by simply interchanging the position of parts C and E per Figure 2-1 and resulted in a change in the distribution of friction values. Note the values of the friction coefficient in Table 4-1 were measured in the experiments and are typical of very low speed conditions and an axial load W=20kip. The values of friction varied a little during the testing as will be discussed later. An image of the tested isolator, deformed in the bearing testing machine is shown in Figure 4-1. Its basic dimensions (height of 3.8in is for the un-deformed position) and the seven parts of the bearings are shown in the figure (also, see Figure B-3 for detailed dimensions).

TABLE 4-1 Parameters of Tested Quintuple FP Isolator (Values of Friction are for Configuration 1. Values in Parenthesis are for Configuration 2.)

Radius (inch)		Height (inch)		Friction Coefficient		Displacement Capacity (inch)	
R_1	18	h_1	1.4	μ_1	0.12 (0.12)	d_1	1.5
R_2	8	h_2	1.2	μ_2	0.085 (0.035)	d_2	1.3
R_3	2	h_3	0.9	μ_3	0.015 (0.015)	d_3	0.55
R_4	2	h_4	0.9	(= μ_4)		d_4	0.55
R_5	8	h_5	1.2	μ_5	0.035 (0.085)	d_5	1.3
R_6	18	h_6	1.4	μ_6	0.11 (0.11)	d_6	1.5

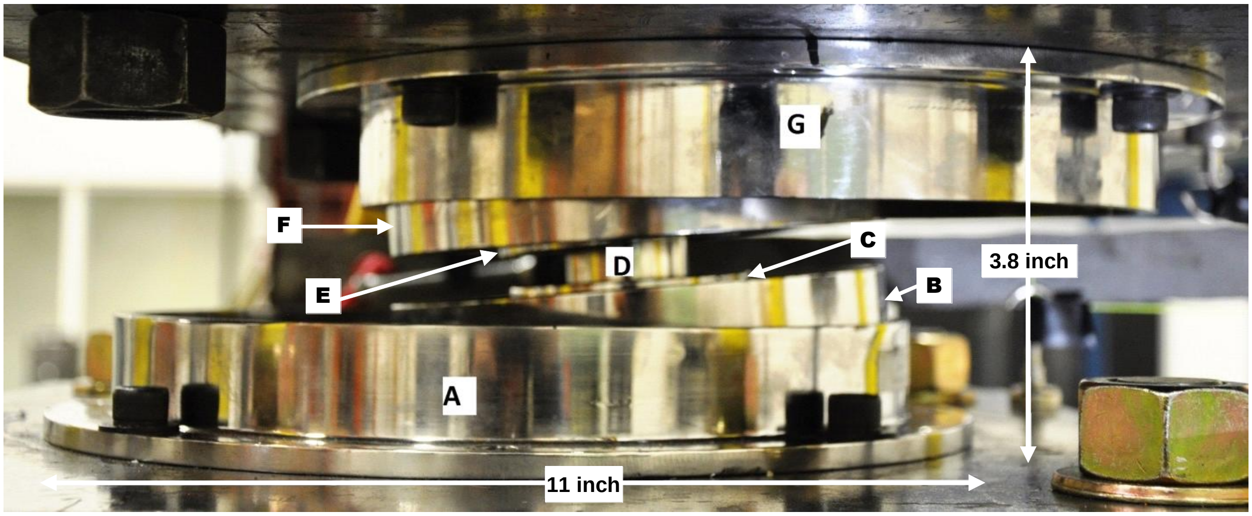

FIGURE 4-1 Image of Deformed Quintuple FP Isolator in Testing Machine

Testing of the isolator was first conducted under quasi-static conditions (harmonic motion of frequency equal to 0.005Hz, peak velocity of 0.16in/sec) so that the coefficient of friction remained essentially constant (Coulomb friction). Accordingly, the tested isolator clearly exhibited the nine regimes of operation and allowed for comparison to the analytical model. Subsequently testing was conducted under dynamic conditions to reveal the smooth behavior that results from the velocity dependence of the coefficient of friction.

Testing of the isolator was conducted under a specified constant load *W*=20kip. Table 4-2 presents the conducted test program. The peak displacement was 5.0inch that represented a limit of the test machine. The displacement capacity of the isolator was 5.58inch. The isolator was deformed up to regime VIII.

TABLE 4-2 Test Matrix for Quintuple FP Isolator

Configuration	Test no.	Vertical load (kip)	Displacement amplitude (in)	Frequency (Hz)	No. of cycles	Regime
1	1	20	0.5	0.005	2	III
	2	20	1.5	0.005	2	V
	3	20	3.0	0.005	2	V
	4	20	4.5	0.005	2	VII
	5	20	5.0	0.005	2	VIII
2	6	20	5.0	0.005	2	VIII

During testing it was observed that parts of the isolator exhibited some rotation about the vertical axis and, as a result of that, they had small out-of-plane motion. This resulted in slight variation of the displacement at each of the transition points between regimes (uncertainty on what the displacement exactly is).

Figure 4-2 presents a comparison of experimental and analytical results for the tests of Configuration 1 in Table 4-1. Only the results of the analytical model are presented since the computational model obtained in SAP2000 produces exactly the same results as the analytical model. The values of friction coefficients used in the analytical model are those in Table 4-1. In reality the values of friction varied in the loops at various amplitudes as a result of the velocity dependence of the coefficient of friction. Note that velocity in the five tests shown in Figure 4-2 varied from a peak value of 0.016 to 0.16in/sec, a range over which there is some effect of velocity. This explains the observed “smoothness” of the experimental loops whereas the analytical loops show sharper transition from one regime to the next. Nevertheless, the analytical results are in good agreement with the experimental results.

The experimental results of Figure 4-2 (and also in results presented later in this report under faster motion conditions) show an uneven behavior as if there is a momentary stop of motion in the stiffening regime of operation. It is not precisely known what caused this behavior but experimental results and advanced theory presented in Sarlis and Constantinou (2013) indicate that this may be caused by small differences in the values of friction at surfaces 3 and 4. Note that the theory presented in this report is based on the assumption that these two values of friction are equal.

The single test of the isolator in Configuration 2 produced practically the same force-displacement loop as that of Configuration 1, and both were accurately predictable by the analytical model. Instead of comparing the force-displacement loops for the two configurations in this slow test, a comparison is made when the two isolators were tested under dynamic conditions.

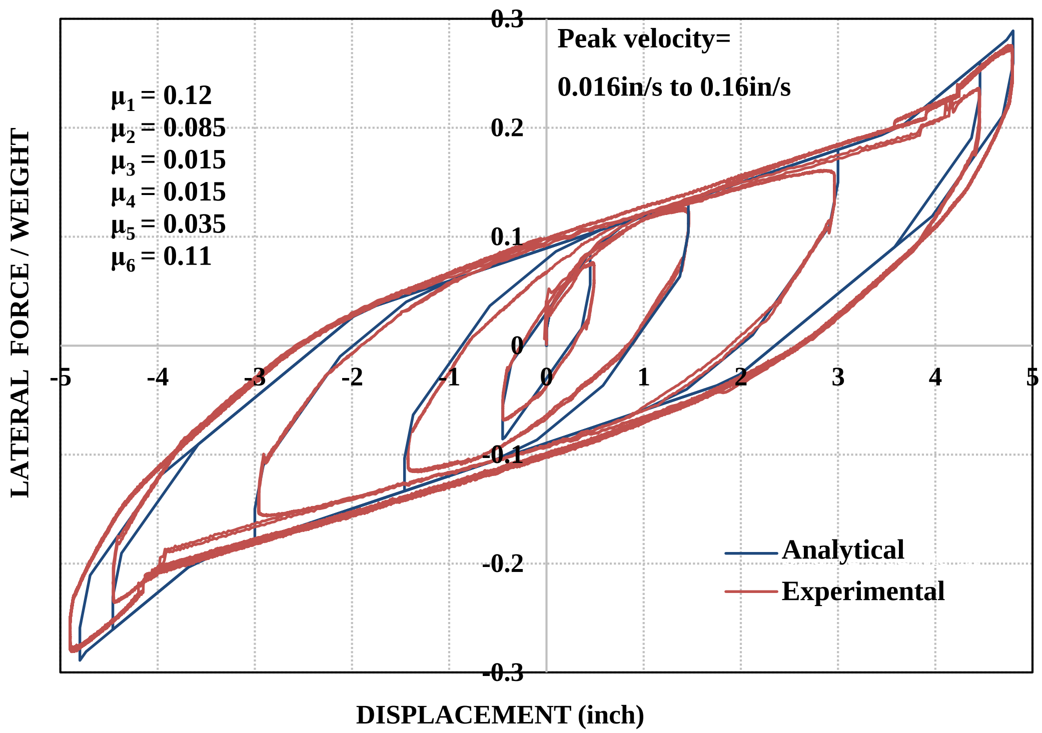

FIGURE 4-2 Experimental and Analytical Force-Displacement Loops of Isolator in Configuration 1

Additional tests were conducted on the isolators of Configuration 1 and 2 under the same load but larger velocity of motion in order to reveal the behavior of the isolators under dynamic conditions. Test results are presented in Figures 4-3 and 4-4. Testing was conducted by first imposing a slow motion to the maximum displacement over a period of 70sec, then pausing for 10sec and then imposing two and a half cycles of harmonic motion of frequency of 0.1Hz and amplitude of either 3 or 5inch. The peak velocity of motion was either 1.9 or 3.1 in/sec. Figure 4-3 shows the results for Configuration 1 in the test at peak velocity of 1.9in/sec, and Figures 4-4 and 4-5 show the results in Configurations 1 and 2 in the tests at peak velocity of 3.1in/sec. The history of imposed motion is included in the graphs of Figures 4-3 to 4-5. The graphs also include the loops obtained in the quasi-static testing at the same amplitude of motion for comparison. The results clearly illustrate the effect of velocity in affecting friction (increase) and in causing the loops to have smooth transitions between regimes.

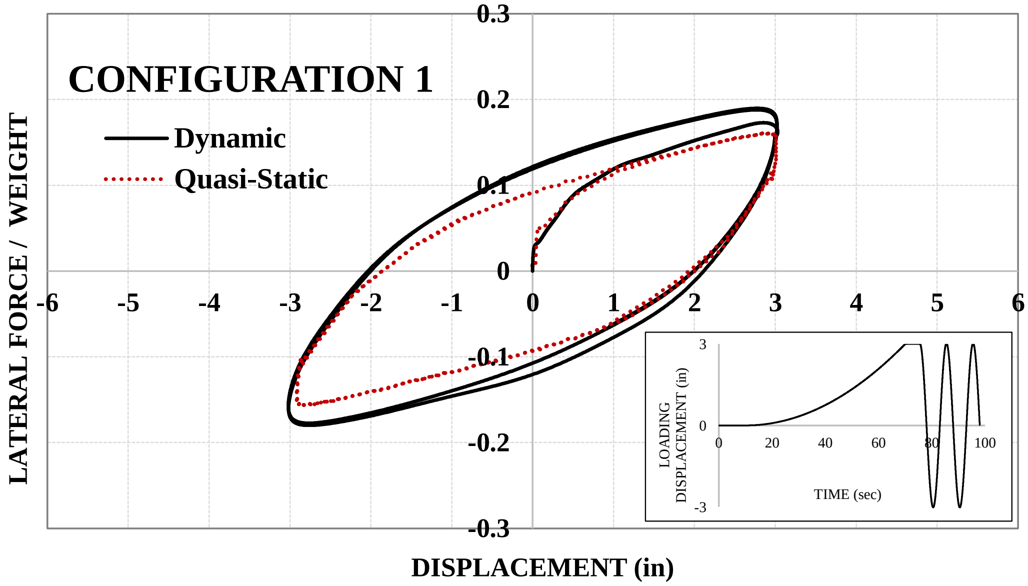

FIGURE 4-3 Experimental Force-Displacement Loops of Isolator in Configuration 1 for Quasi-Static Test and at Peak Velocity of 1.9in/sec

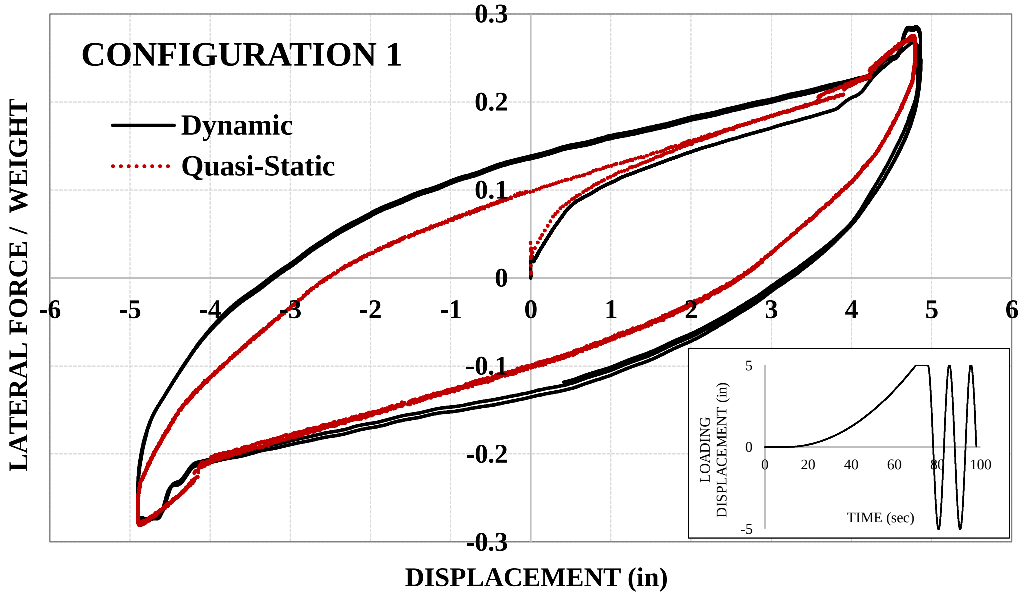

FIGURE 4-4 Experimental Force-Displacement Loops of Isolator in Configuration 1 for Quasi-Static Test and at Peak Velocity of 3.1in/sec

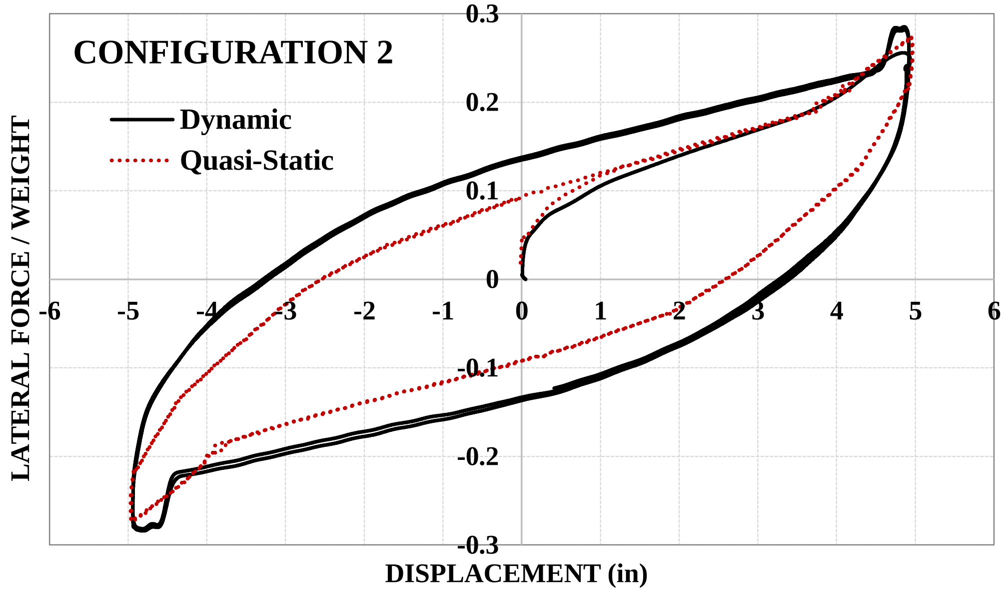

FIGURE 4-5 Experimental Force-Displacement Loops of Isolator in Configuration 2 for Quasi-Static test and at Peak Velocity of 3.1in/sec

Prediction by the computational model of the force-displacement loops under dynamic conditions requires (a) knowledge of the coefficient of friction-velocity relations for each sliding surface, and (b) a procedure for specifying these properties in the Triple-Double model of the isolator in program SAP2000. It is generally assumed that the coefficient of friction follows the relation

$$\mu = \mu_{FAST} - (\mu_{FAST} - \mu_{SLOW})\,\mathrm{e}^{-aV} \qquad (6)$$

where μ_{FAST} and μ_{SLOW} are values of the coefficient of sliding friction valid for large velocity and for quasi-static conditions, respectively, *V* is the velocity of sliding, and “a” is the rate parameter used to describe the velocity-dependence of friction.

Specification of the three parameters of the model for each sliding surface is complicated by the fact that the Triple FP bearing model in program SAP2000 (also the models of Morgan, 2007 and Fenz and Constantinou, 2008a) does not truly trace the motion on the four sliding surfaces but rather simulates the behavior through the motion of the three effective pendula. The result is that the sliding velocity is not precisely known at each sliding surface but it can be estimated by the procedure described in Fenz and Constantinou (2008c) and with details provided in Sarlis and Constantinou (2010). This requires the specification of fictitious values for the rate parameter for the three effective pendula. This is further complicated by the fact that the manual of program SAP2000 does not provide details and does not present verification examples. A comparison of the results produced by the Triple FP element in the program and the validated series model of Fenz and Constantinou (2008c) implemented in SAP2000 resulted in essentially the same results and, therefore, it is believed that the values of the rate parameter for the Triple FP element in SAP2000 should be specified using the approach outlined in Fenz and Constantinou (2008a) and Sarlis and Constantinou (2010).

TABLE 4-3 Values of Friction Coefficient and Rate Parameter Used in Analysis of Isolator of Configuration 1 (Top Table Reports Properties of Isolator; Bottom Table Reports Parameters of Computational Model)

Quintuple Isolator	μ_1	μ_2	$\mu_3 = \mu_4$	μ_5	μ_6
μ_{SLOW}	0.12	0.085	0.015	0.035	0.11
μ_{FAST}	0.16	0.11	0.04	0.09	0.15
Rate parameter a (sec/inch)	4.0	3.6	3.0	3.6	4.0
Triple-Double Model	$\tilde{\mu}_1$	$\tilde{\mu}_2 = \tilde{\mu}_3$	$\tilde{\mu}_4$	$\tilde{\mu}_5$	$\tilde{\mu}_6$
$\tilde{\mu}_{SLOW}$	0.085	0.015	0.035	0.11	0.12
$\tilde{\mu}_{FAST}$	0.11	0.04	0.09	0.15	0.16
Rate parameter $\tilde{a}$ (sec/inch)	3.0	1.5	3.0	2.0	2.0

The computational model of the Quintuple FP Isolator described in Appendix B requires the use of three nodes interconnected by two Triple FP elements, one of which has been reduced to behave as a Double FP element (this is done by specifying artificial values of the radius and friction to impede motion of the inner sliding surfaces-see Table B-2b). Accordingly, the division of velocity for the sliding surfaces of the Quintuple FP model should be based on approach described in Fenz and Constantinou (2006) for the Double FP element and in Fenz and Constantinou (2008c) for the Triple FP element. Table 4-3 presents values of friction and the rate parameter used in an analysis of the tested isolator of Configuration 1. Note that the values of the rate parameter were assumed for each sliding surface to have a value in a range consistent with what is typically assumed in analysis (e.g., Sarlis and Constantinou, 2010).

There are three sources of uncertainty in the data of Table 4-3: (a) unlike the case of quasi-static conditions, the actual values of friction at high velocity (μ_{FAST}) are not directly measured (uncertain due to the smoothness of the experimental loops) but assumed although some information was obtained from the recorded loops, (b) the actual values of the rate parameter for each sliding surface are not known but rather assumed, and (c) the values of the rate parameter in the computational model are approximate as the velocities are not directly computed but rather estimated on the basis of a simplified theory.

Figure 4-6 presents comparisons of experimental and computational force-displacement loops of the tested isolator of Configuration 1 (with the properties of Table 4-3–also see Table B-2 for other details) in the two tests at velocities of 1.9 and 3.1in/sec. The comparison is good given the several sources of uncertainty in the values of the model parameters and the fact that the sliding velocities are small (portions of the peak velocity of testing) so that there is considerable variability of friction, which would not be dominant in testing with much higher velocity. (Unfortunately, testing at higher velocities could not be performed due to instabilities in the control mechanism of the testing machine). Nevertheless, it is noted that changes in the specified values of the rate parameter resulted in noticeable changes in the computed loops for the motions used in the testing (up to 3.1in/sec) but the effects where minor or insignificant when the peak velocity was larger than 10in/sec.

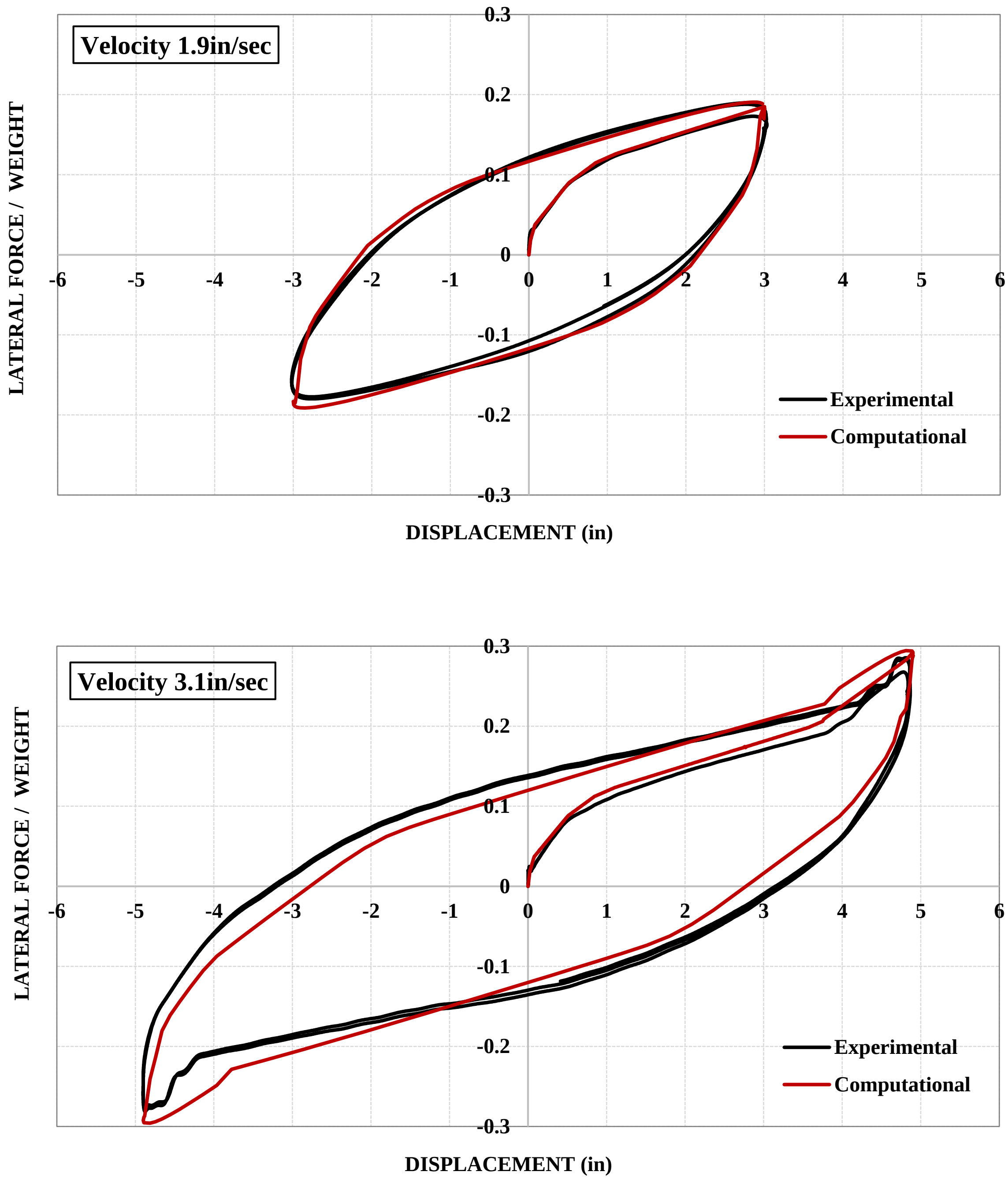

FIGURE 4-6 Comparison of Experimental and Computational Force-Displacement Loops of Isolator in Configuration 1 at Peak Test Velocities of 1.9 and 3.1in/sec

SECTION 5
CONCLUSIONS

The behavior of the Quintuple Friction Pendulum Isolator has been investigated. This isolator has six spherical sliding surfaces, five effective pendula and nine regimes of operation that allow for complex adaptive behavior and smooth transition between regimes of operation. Analytical models of behavior have been presented for two configurations that are envisioned to include all cases of interest in applications. Moreover, a computational model has been developed that is readily implementable in computer program SAP2000. Comparison of results obtained by the computational and analytical model provided verification of the computational model.

A model isolator was tested and the results were compared to predictions of the analytical and computational models. The comparison demonstrated the validity of the analytical model and of the computational model. It is believed that this isolator will be a useful addition to the arsenal of isolators available to the engineer for use in the seismic protection of structures.

SECTION 6
REFERENCES

American society of Civil Engineers (ASCE), 2010. *Minimum Design Loads for Buildings and Other Structures*, ASCE 7-10. Reston, VA.

Computers and Structures Inc. (2014). *SAP2000: Static and Dynamic Finite Element Analysis of Structures* (Version 17.1.1), Computers and Structures Inc., Berkeley, CA.

Fenz DM, Constantinou MC (2006). Behavior of the Double Concave Friction Pendulum Bearing, *Earthquake Engineering and Structural Dynamics*, **35**(11), 1403-1424, DOI: 10.1002/eqe.589.

Fenz DM, Constantinou MC (2008a). Spherical Sliding Isolation Bearings with Adaptive Behavior: Theory, *Earthquake Engineering and Structural Dynamics*, **37**(2), 163-183, DOI: 10.1002/eqe.751.

Fenz DM, Constantinou MC (2008b). Spherical Sliding Isolation Bearings with Adaptive Behavior: Experimental Verification, *Earthquake Engineering and Structural Dynamics*, **37**(2), 185-208, DOI: 10.1002/eqe.750.

Fenz DM, Constantinou MC (2008c). Modeling Triple Friction Pendulum Bearings for Response History Analysis, *Earthquake Spectra*, **24**(4), 1011-1028

Kasalanati A, Constantinou MC (1999). *Experimental Study of Bridge Elastomeric and Other Isolation and Energy Dissipation Systems with Emphasis on Uplift Prevention and High Velocity Near Source Seismic Excitation*, *Technical Report MCEER-99-0004*, Multidisciplinary Center for Earthquake Engineering Research, University at Buffalo, Buffalo, NY.

Mokha A, Constantinou MC, Reinhorn AM, Zayas VA (1991). Experimental Study of Friction-Pendulum Isolation System, ASCE, *J. Struct. Eng.*, **117**(4), 1201-1217.

Morgan TA (2007). The Use of Innovative Base Isolation Systems to Achieve Complex Seismic Performance Objectives, Ph.D. Dissertation, Department of Civil and Environmental Engineering, University of California, Berkeley, CA.

Ray T, Sarlis AS, Reinhorn AM, Constantinou MC (2013). Hysteretic Models for Sliding Bearings with Varying Frictional Force, *Earthquake Engineering and Structural Dynamics*, **42**(15), 2341-2360, DOI: 10.1002/eqe.2373.

Sarlis AS, Constantinou MC (2010). *Modeling Triple Friction Pendulum Isolators in Program SAP2000*, supplement to *MCEER Report 05-009*, document distributed to the engineering community together with executable version of program and example files, University at Buffalo, NY.

Sarlis AS, Constantinou MC (2013). *Model of Triple Friction Pendulum Bearing for General Geometric and Frictional Parameters and for Uplift Conditions*, *Technical Report MCEER-13-0010*, Multidisciplinary Center for Earthquake Engineering Research, University at Buffalo, Buffalo, NY.

Tsai CS, Lin YC, Su HC (2010). Characterization and modeling of multiple friction pendulum isolation system with numerous sliding interfaces, *Earthquake Engineering and Structural Dynamics*, **39**(13), 1463-1491, DOI: 10.1002/eqe1044.

Zayas VA, Low SS, Mahin SA (1987). *The FPS Earthquake Resisting System: Experimental Report, Report No. UCB/EERC-87/01*, Earthquake Engineering Research Center, University of California Berkeley, Berkeley, CA.

APPENDIX A

DERIVATION OF FORCE-DISPLACEMENT RELATIONS FOR CONFIGURATION 1

The derivation of the force-displacement relation of the quintuple FP Isolator is presented in detail for configuration 1. The force-displacement relation is derived from the equilibrium and geometric considerations following the paradigm of Fenz and Constantinou (2006 and 2008a) and distinguishing the relation in accordance with the sliding regime. In what follows, *W* is the normal load acting at the center of the top plate of the bearing, *F* is the horizontal force, $F_f = \mu W$ is the friction force, μ is assumed constant and independent of the conditions of motion (Coulomb friction) and *S* is the resultant force acting perpendicularly to a sliding surface. Moreover, the following quantities are defined in which *i*=1 to 6:

The effective radius of curvature

$$R_{eff,i} = R_i - h_i \quad \text{(A-1)}$$

The actual displacement capacity of each sliding surface:

$$d_i^* = d_i \left(R_{eff,i} / R_i \right) \quad \text{(A-2)}$$

A-1 Sliding Regime I

Sliding Regime I begins with sliding on surfaces 3 and 4 which are characterized by the least friction forces. Motion initiates when horizontal force is equal to friction force on surface 2 and 3 ($F = F_{f3} = F_{f4}$). The displaced shape (with the sliding surfaces highlighted in red) and the free body diagram (FBD) of parts C and E during Sliding Regime I are shown in Figure A-1.

Equilibrium in the vertical and horizontal directions of the FBD of part C in Figure A-1 (b) results in:

$$W + F_{f3}\sin\theta_3 - S_3\cos\theta_3 = 0 \quad \text{(A-3a)}$$

$$F_{f3}\cos\theta_3 + S_3\sin\theta_3 - F = 0 \quad \text{(A-3b)}$$

From geometry, the relative displacement of slider C, u_3, is

$$u_3 = R_{eff\,3} \sin \theta_3 \tag{A-4}$$

Assuming small rotations (so that $\cos\theta \approx 1$ and $\sin\theta \approx \theta$) and rearranging equations (A-3) and (A-4), the following is derived for force F :

$$F = \frac{W}{R_{eff\,3}} u_3 + F_{f\,3} \tag{A-5}$$

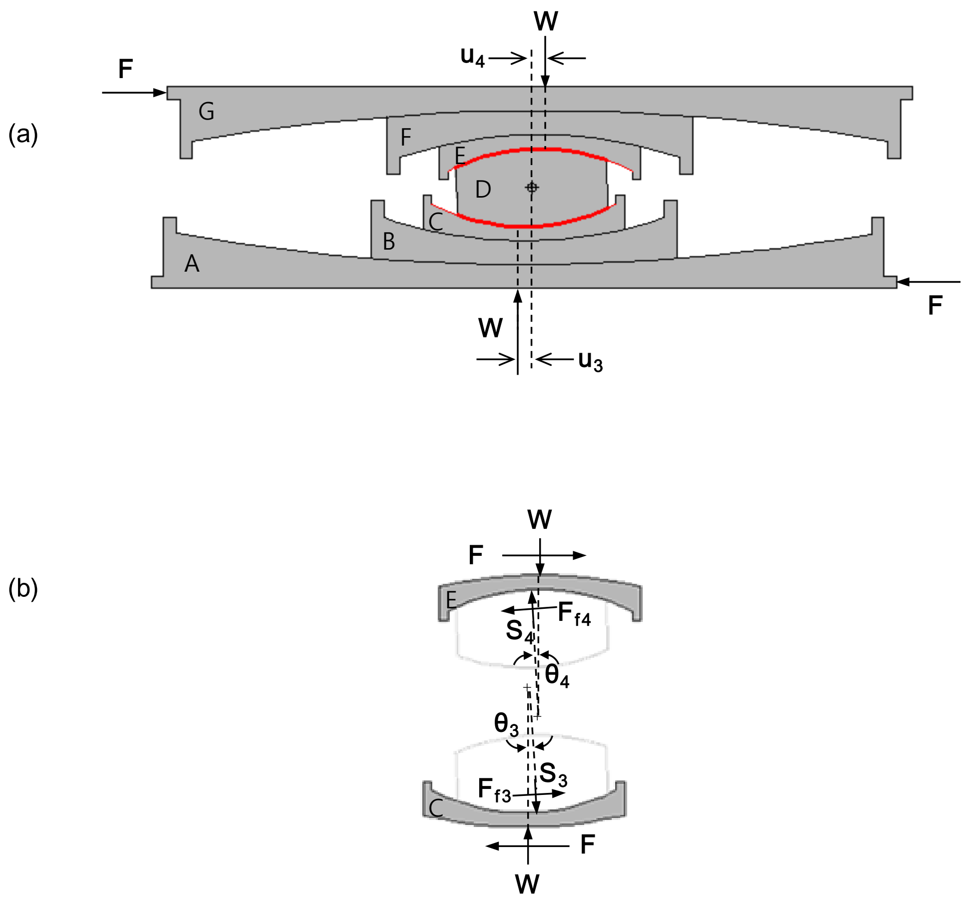

FIGURE A-1   Displaced Shape (a) and Free Body Diagrams (b) of the Quintuple FP Isolator During Sliding Regime I

Similarly, equilibrium for part E leads to:

$$F = \frac{W}{R_{eff\,4}} u_4 + F_{f\,4} \tag{A-6}$$

Since $u = u_3 + u_4$ and $u_1 = u_2 = u_5 = u_6 = 0$, combination of equations (A-5) and (A-6) results in

$$F = \frac{W}{R_{eff\,3} + R_{eff\,4}} u + \frac{F_{f3} R_{eff\,3} + F_{f4} R_{eff\,4}}{R_{eff\,3} + R_{eff\,4}} \tag{A-7}$$

The force-displacement loop in regime I is shown in Figure A-2. Note that on reversal motion the force drops by $2F_{f3}\left(= 2F_{f4}\right)$. This regime is valid until a displacement u=u^{I} is reached.

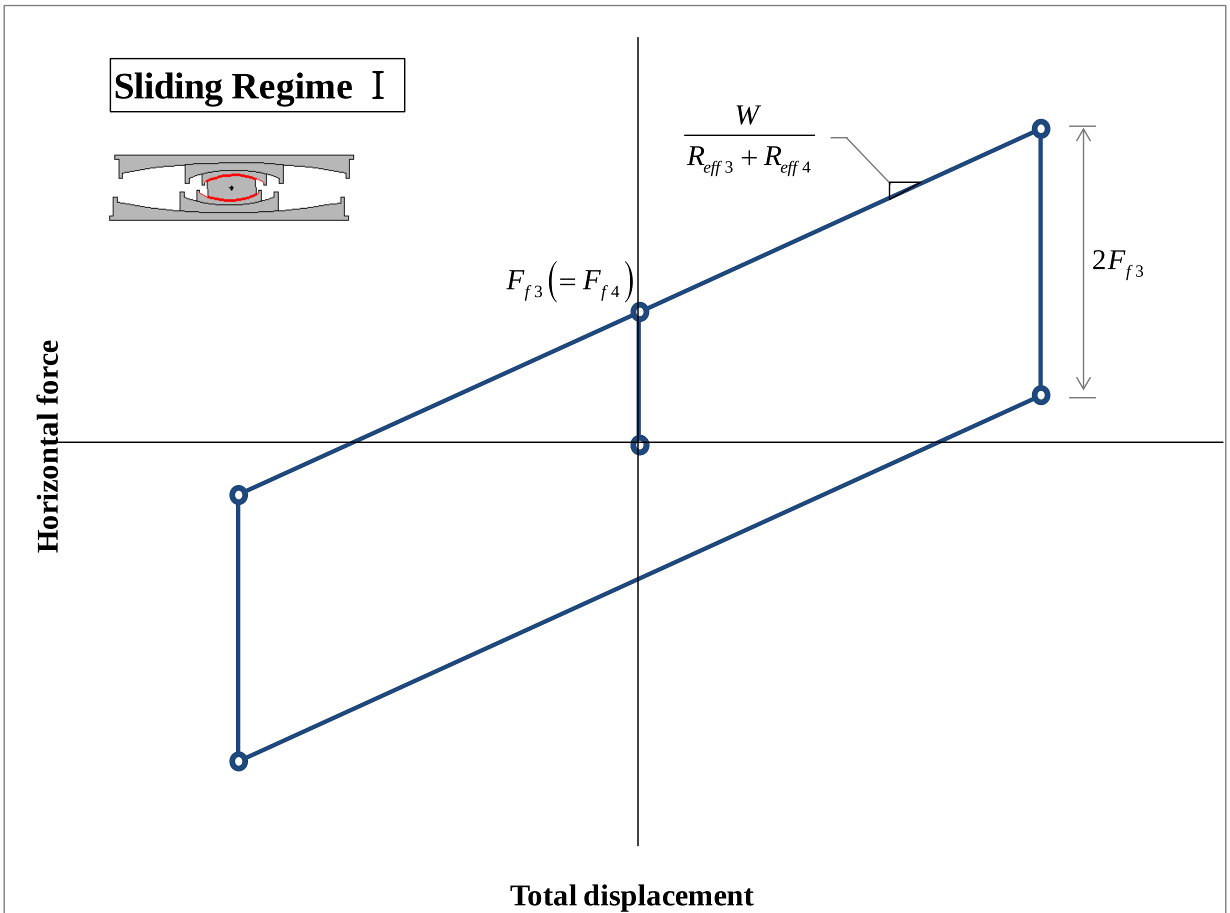

FIGURE A-2 Force-Displacement Relationship in Sliding Regime I

A-2 Sliding Regime II

Sliding regime II initiates when the lateral force $F = F_{f5}$, motion on surface 4 stops, motion initiates on surface 5 and motion continues on surface 3 as shown in Figure A-3(a). This sequence of motion is required for compatibility of displacements and is consistent with what occurs in the Triple FP Isolator.

The transition displacement between sliding regimes I and II, u^{I}, is obtained by solving equation (A-7) for the displacement u when force $F = F_{f5}$:

$$u^{\mathrm{I}} = (\mu_5 - \mu_3) R_{eff3} + (\mu_5 - \mu_4) R_{eff4} \qquad \text{(A-8)}$$

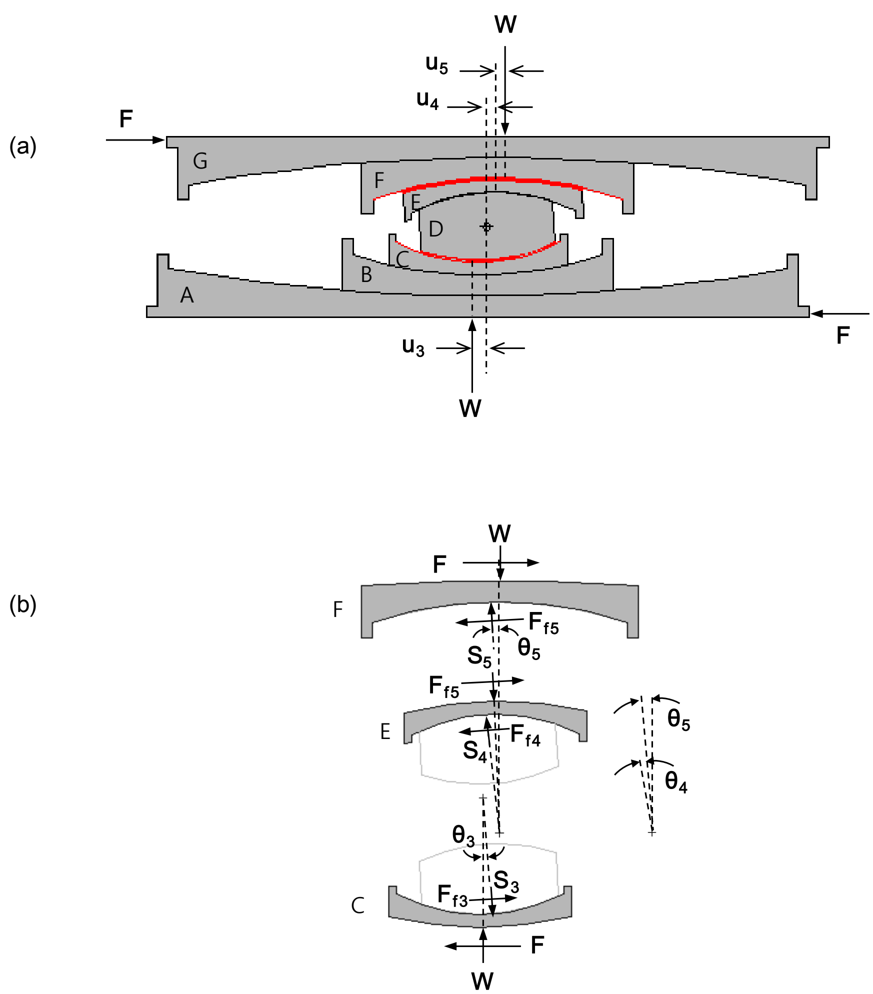

FIGURE A-3 Displaced Shape (a) and Free Body Diagrams (b) of the Quintuple FP Isolator During Sliding Regime II

Based on the FBD of Figure A-3(b) and geometric considerations in similarity to the presentation for regime I, the following is obtained:

$$u_4 = R_{eff\,4} \sin\theta_4 \qquad \text{(A-9a)}$$

$$u_5 = R_{eff\,5} \sin\theta_5 \qquad \text{(A-9b)}$$

$$F = \frac{W}{R_{eff\,3}} u_3 + F_{f\,3} \qquad \text{(A-10a)}$$

$$F = \frac{W}{R_{eff\,5}} u_5 + F_{f\,5} \qquad \text{(A-10b)}$$

$$S_5 \cos\theta_5 + F_{f\,4} \sin(\theta_4 + \theta_5) - S_4 \cos(\theta_4 + \theta_5) - F_{f\,5} \sin\theta_5 = 0 \qquad \text{(A-11a)}$$

$$S_4 \sin(\theta_4 + \theta_5) + F_{f\,4} \cos(\theta_4 + \theta_5) - S_5 \sin\theta_5 - F_{f\,5} \cos\theta_5 = 0 \qquad \text{(A-11a)}$$

Assuming small rotations, the force-displacement relation is obtained as,

$$F = W\left(\frac{u_4}{R_{eff\,4}} + \frac{u_5}{R_{eff\,5}}\right) + F_{f\,4} \qquad \text{(A-12)}$$

Combining equations (A-10) and (A-12) and using $u = u_3 + u_4 + u_5$, the force-displacement relation in regime II is obtained:

$$F = \frac{W}{R_{eff\,3} + R_{eff\,5}} u + \frac{F_{f\,3} R_{eff\,3} + F_{f\,4} R_{eff\,4} + F_{f\,5}\left(R_{eff\,5} - R_{eff\,4}\right)}{R_{eff\,3} + R_{eff\,5}} \qquad \text{(A-13)}$$

This relationship is shown in Figure A-4 together with that of regime I for completeness. This regime is valid until a displacement $u = u^{II}$ is reached.

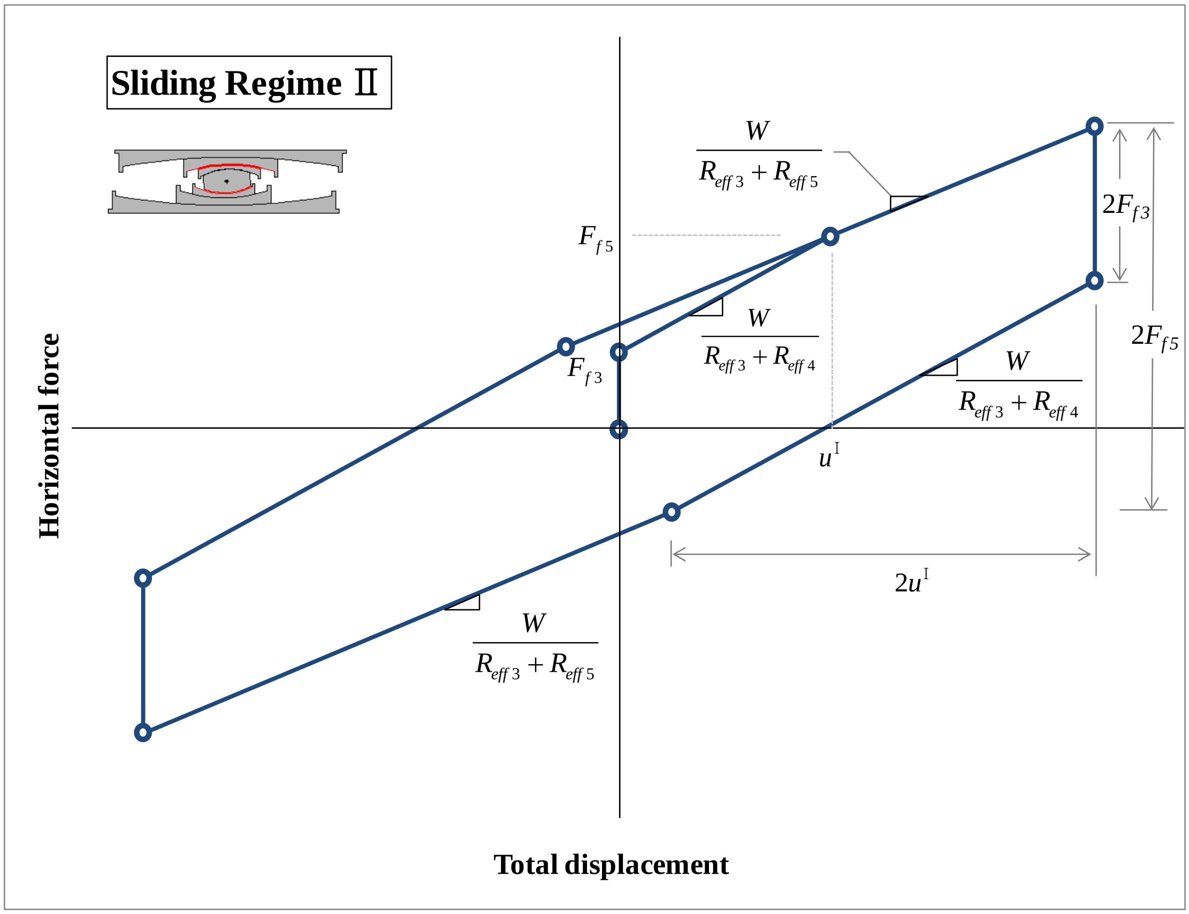

FIGURE A-4 Force-Displacement Relationship in Sliding Regime II

A-3 Sliding Regime III

The sliding regime III initiates when the lateral force $F = F_{f2}$, motion stops on surface 3, motion begins on surface 2 and motion continues on surface 4 as shown in Figure A-5(a). The transition occurs at a displacement u^{II} obtained by solving equation (A-13) for displacement u when $F = F_{f2}$:

$$u^{\mathrm{II}} = u^{\mathrm{I}} + \left(F_{f2} - F_{f5}\right) \times \left[\left(R_{eff3} + R_{eff5}\right) / W\right] \qquad \text{(A-14)}$$

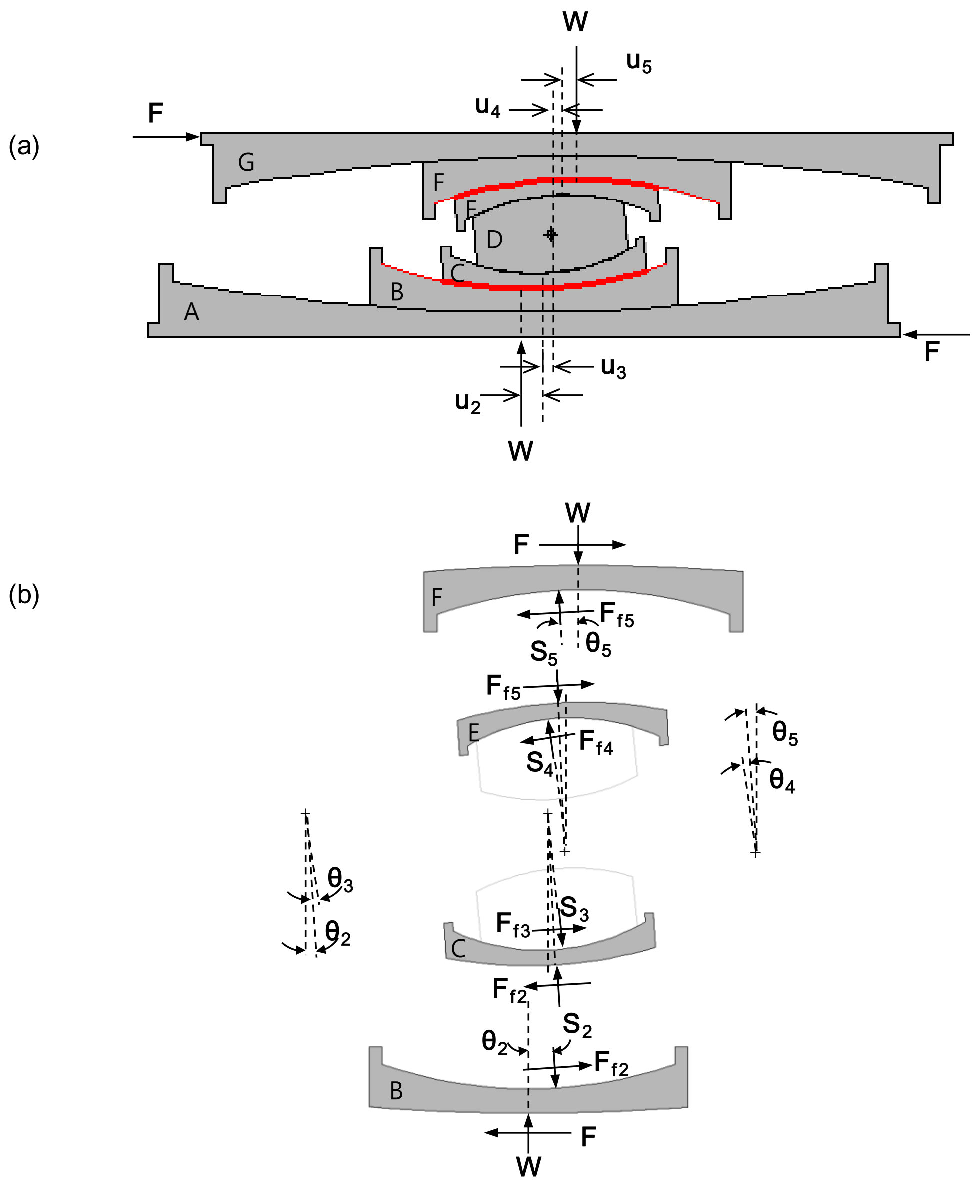

FIGURE A-5   Displaced Shape (a) and Free Body Diagrams (b) of the Quintuple FP Isolator During Sliding Regime III

Based on the FBD of Figure A-5(b) and geometric considerations in similarity to the presentation for regimes I and II, the following is obtained:

$$u_2 = R_{eff\,2} \sin\theta_2 \tag{A-15a}$$

$$u_3 = R_{eff\,3} \sin\theta_3 \tag{A-15b}$$

$$F = \frac{W}{R_{eff\,2}} u_2 + F_{f\,2} \tag{A-16}$$

$$F = W\left(\frac{u_2}{R_{eff\,2}} + \frac{u_3}{R_{eff\,3}}\right) + F_{f3} \tag{A-17}$$

The force-displacement relationship in sliding regime III is finally obtained by combining equations (A-10b), (A-12), (A-16) and (A-17) and using $u = u_2 + u_3 + u_4 + u_5$:

$$F = \frac{W}{R_{eff\,2} + R_{eff\,5}}u + \frac{F_{f2}\left(R_{eff\,2} - R_{eff\,3}\right) + F_{f3}R_{eff\,3} + F_{f4}R_{eff\,4} + F_{f5}\left(R_{eff\,5} - R_{eff\,4}\right)}{R_{eff\,2} + R_{eff\,5}} \tag{A-18}$$

This relationship is shown in Figure A-6 together with those for regimes II and III. This regime is valid until a displacement $u=u^{III}$ is reached.

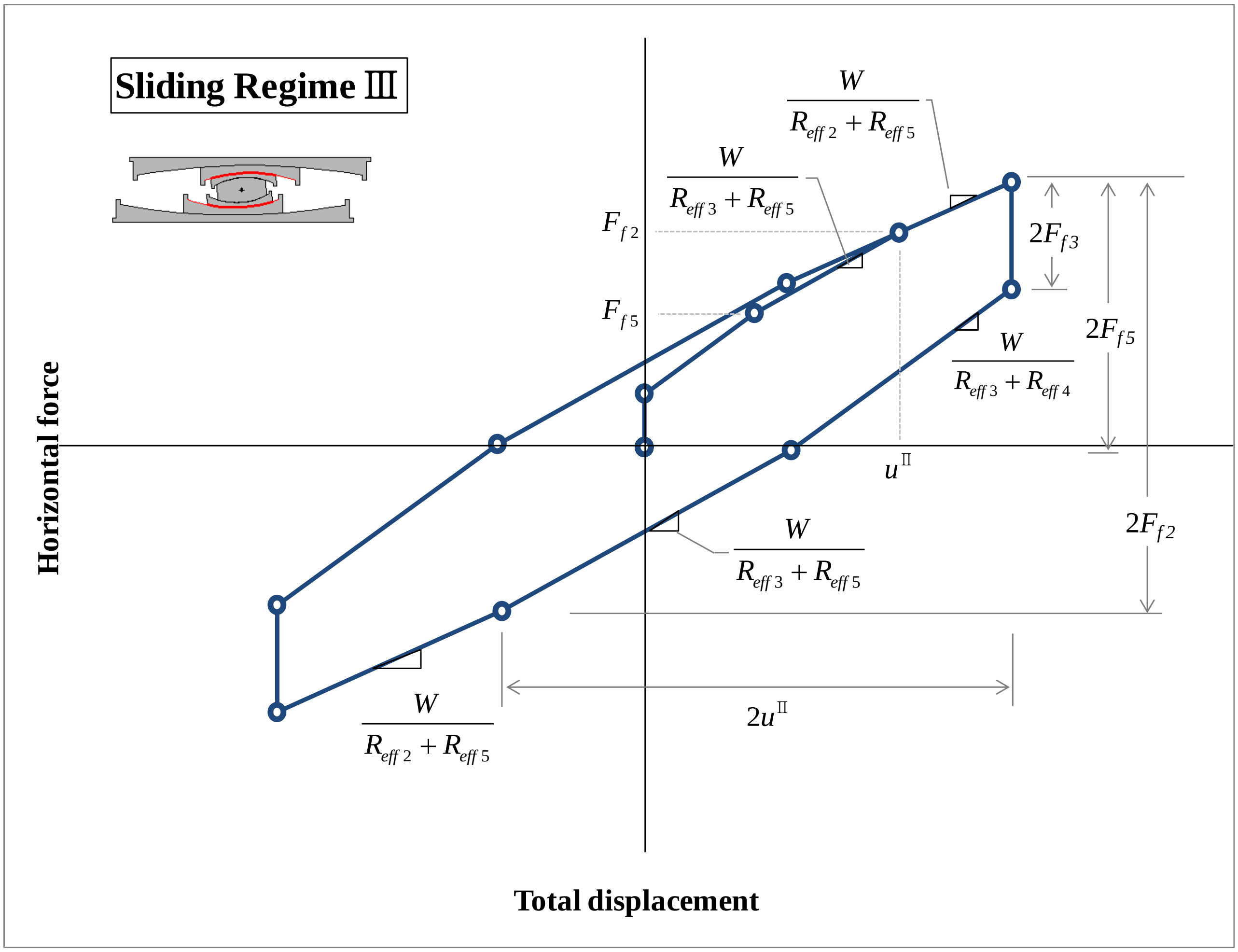

FIGURE A-6 Force-Displacement Relationship in Sliding Regime III

A-4 Sliding Regime IV

The sliding regime IV initiates when the lateral force $F = F_{f6}$, motion stops on surface 5, motion begins on surface 6 and motion continues on surface 2 as shown in Figure A-7(a). The transition occurs at a displacement u^{III} obtained by solving equation (A-18) for displacement u when $F = F_{f6}$:

$$u^{\mathrm{III}} = u^{\mathrm{II}} + \left(F_{f6} - F_{f2}\right) \times \left[\left(R_{eff2} + R_{eff5}\right)/W\right] \quad \text{(A-19)}$$

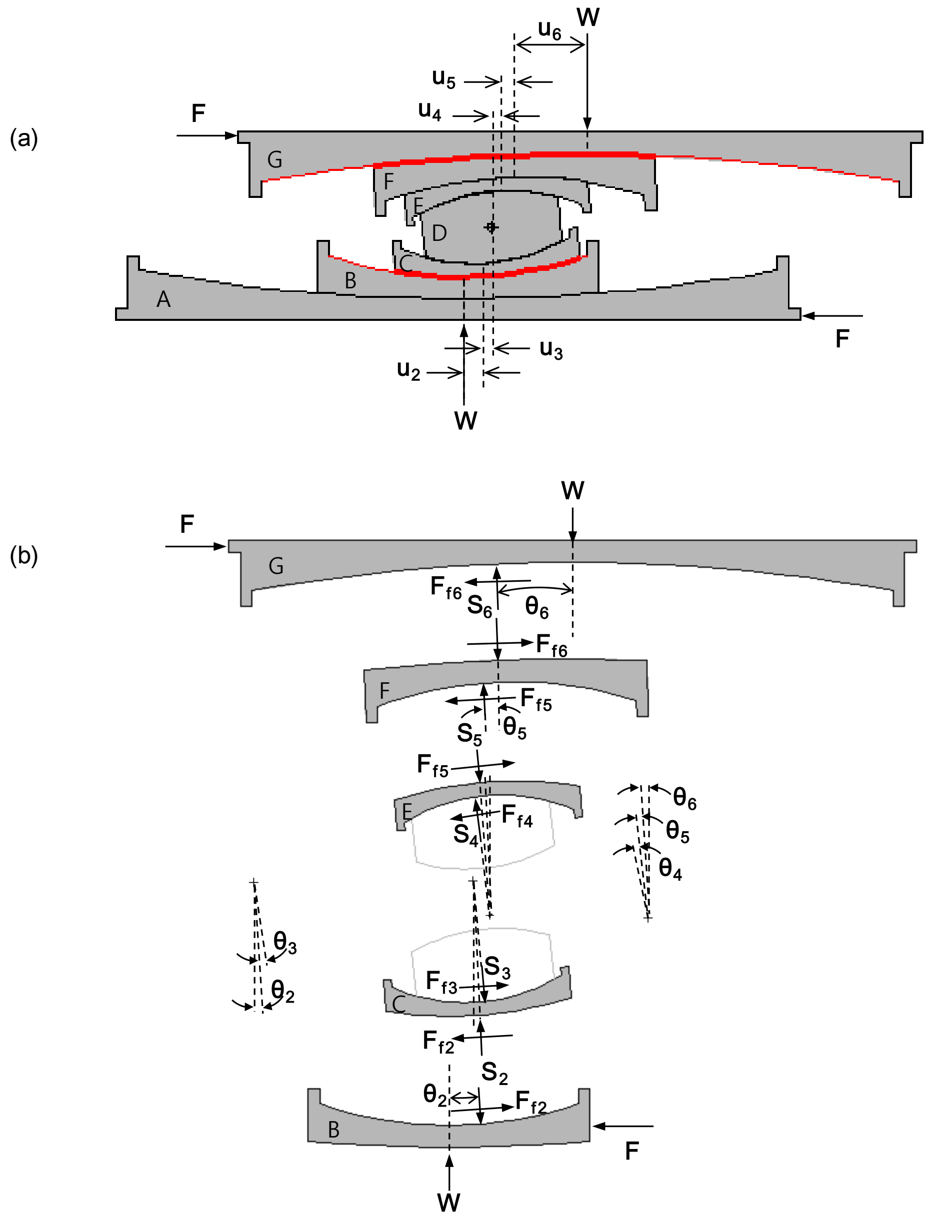

FIGURE A-7 Displaced Shape (a) and Free Body Diagrams (b) of the Quintuple FP Isolator During Sliding Regime IV

Based on the FBD of Figure A-7(b) and geometric considerations in similarity to the presentation for regimes I to III, the following is obtained:

$$u_6 = R_{eff\,6} \sin\theta_6 \qquad \text{(A-20)}$$

$$F = \frac{W}{R_{eff\,6}} u_6 + F_{f\,6} \qquad \text{(A-21)}$$

$$F = W\left(\frac{u_5}{R_{eff\,5}} + \frac{u_6}{R_{eff\,6}}\right) + F_{f\,5} \qquad \text{(A-22)}$$

The equilibrium equations for part E are obtained by considering the FBD shown in Figure A-7(b) and accounting for the its rotation:

$$S_5 \cos(\theta_5 + \theta_6) + F_{f\,4} \sin(\theta_4 + \theta_5 + \theta_6) - S_4 \cos(\theta_4 + \theta_5 + \theta_6) - F_{f\,5} \sin(\theta_5 + \theta_6) = 0 \qquad \text{(A-23a)}$$

$$S_4 \sin(\theta_4 + \theta_5 + \theta_6) + F_{f\,4} \cos(\theta_4 + \theta_5 + \theta_6) - S_5 \sin(\theta_5 + \theta_6) - F_{f\,5} \cos(\theta_5 + \theta_6) = 0 \qquad \text{(A-23b)}$$

Assuming small displacements, equations (A-23) can be solved for force *F*:

$$F = W\left(\frac{u_4}{R_{eff\,4}} + \frac{u_5}{R_{eff\,5}} + \frac{u_6}{R_{eff\,6}}\right) + F_{f\,4} \qquad \text{(A-24)}$$

Inspection of free body diagrams of parts B and C in Figure A-7(b) shows that parts B and C experience in regime IV only an increase in angle θ_2 by comparison to regime III. Thus, the force-displacement relationships for parts B and C are still governed by equations (A-16) and (A-17). Therefore, the force and total displacement relationship in sliding regime IV can be obtained by combining equations (A-16), (A-17), (A-21), (A-22), and (A-24) and using $u = u_2 + u_3 + u_4 + u_5 + u_6$:

$$F = \frac{W}{R_{eff\,2} + R_{eff\,6}} u + \frac{F_{f\,2}\left(R_{eff\,2} - R_{eff\,3}\right) + F_{f\,3} R_{eff\,3} + F_{f\,4} R_{eff\,4} + F_{f\,5}\left(R_{eff\,5} - R_{eff\,4}\right) + F_{f\,6}\left(R_{eff\,6} - R_{eff\,5}\right)}{R_{eff\,2} + R_{eff\,6}}$$

(A-25)

This relationship is shown in Figure A-8 together with those for the previous regimes. This regime is valid until a displacement $u=u^{IV}$ is reached.

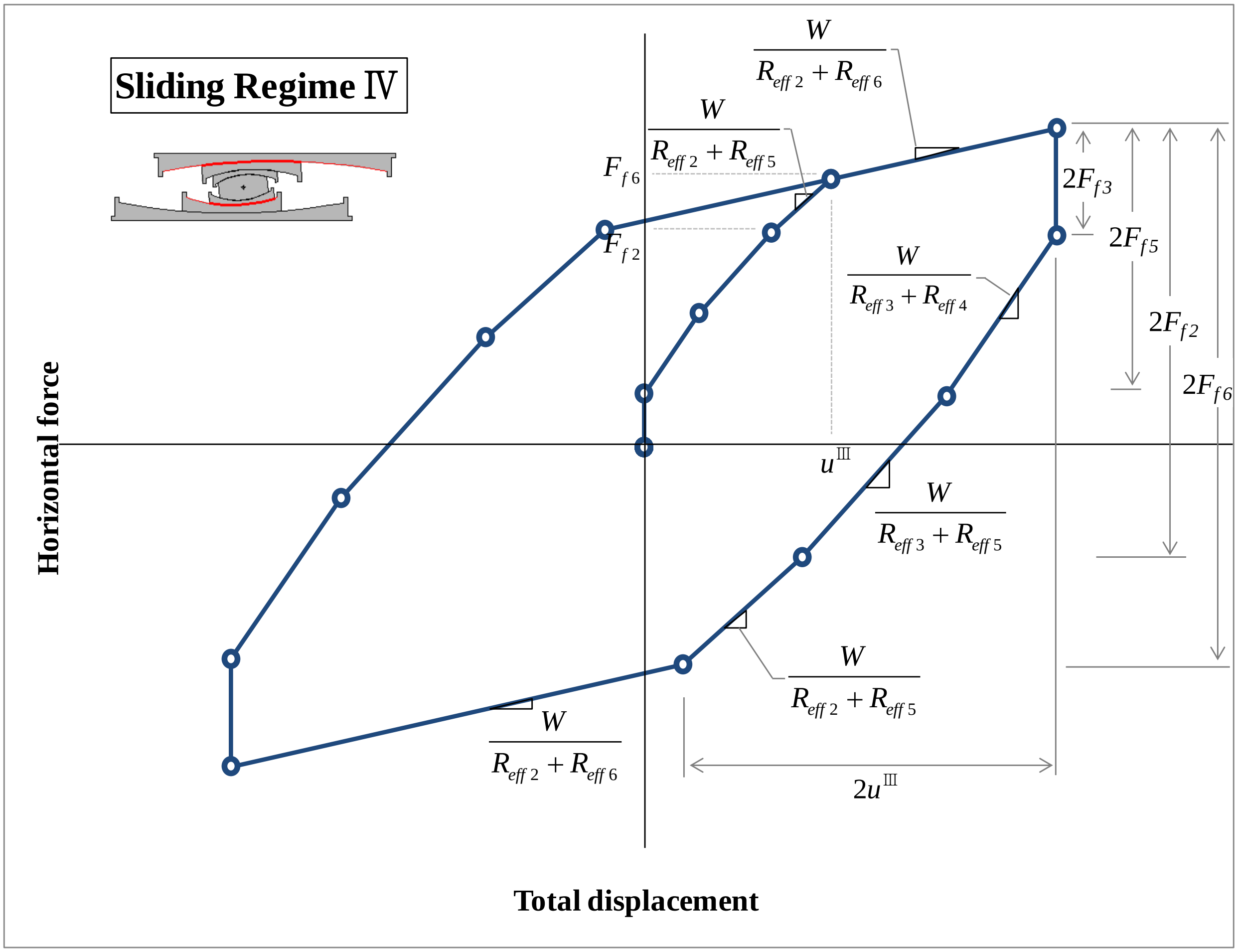

FIGURE A-8 Force-Displacement Relationship in Sliding Regime IV

A-5 Sliding Regime V

The sliding regime V initiates when the lateral force $F = F_{f1}$, motion stops on surface 2, motion begins on surface 1 and motion continues on surface 6 as shown in Figure A-9(a). The transition occurs at a displacement u^{IV} obtained by solving equation (A-25) for displacement u when $F = F_{f1}$:

$$u^{\text{IV}} = u^{\text{III}} + \left(F_{f1} - F_{f6}\right) \times \left[\left(R_{eff\,2} + R_{eff\,6}\right) / W\right] \tag{A-26}$$

Based on the FBD of Figure A-9(b) and geometric considerations in similarity to the presentation for regimes I to IV, the following is obtained:

$$u_1 = R_{eff\,1} \sin\theta_1 \tag{A-27}$$

$$F = \frac{W}{R_{eff\,1}} u_1 + F_{f1} \tag{A-28}$$

$$F = W\left(\frac{u_1}{R_{eff\,1}} + \frac{u_2}{R_{eff\,2}}\right) + F_{f\,2} \tag{A-29}$$

$$F = W\left(\frac{u_1}{R_{eff\,1}} + \frac{u_2}{R_{eff\,2}} + \frac{u_3}{R_{eff\,3}}\right) + F_{f\,3} \tag{A-30}$$

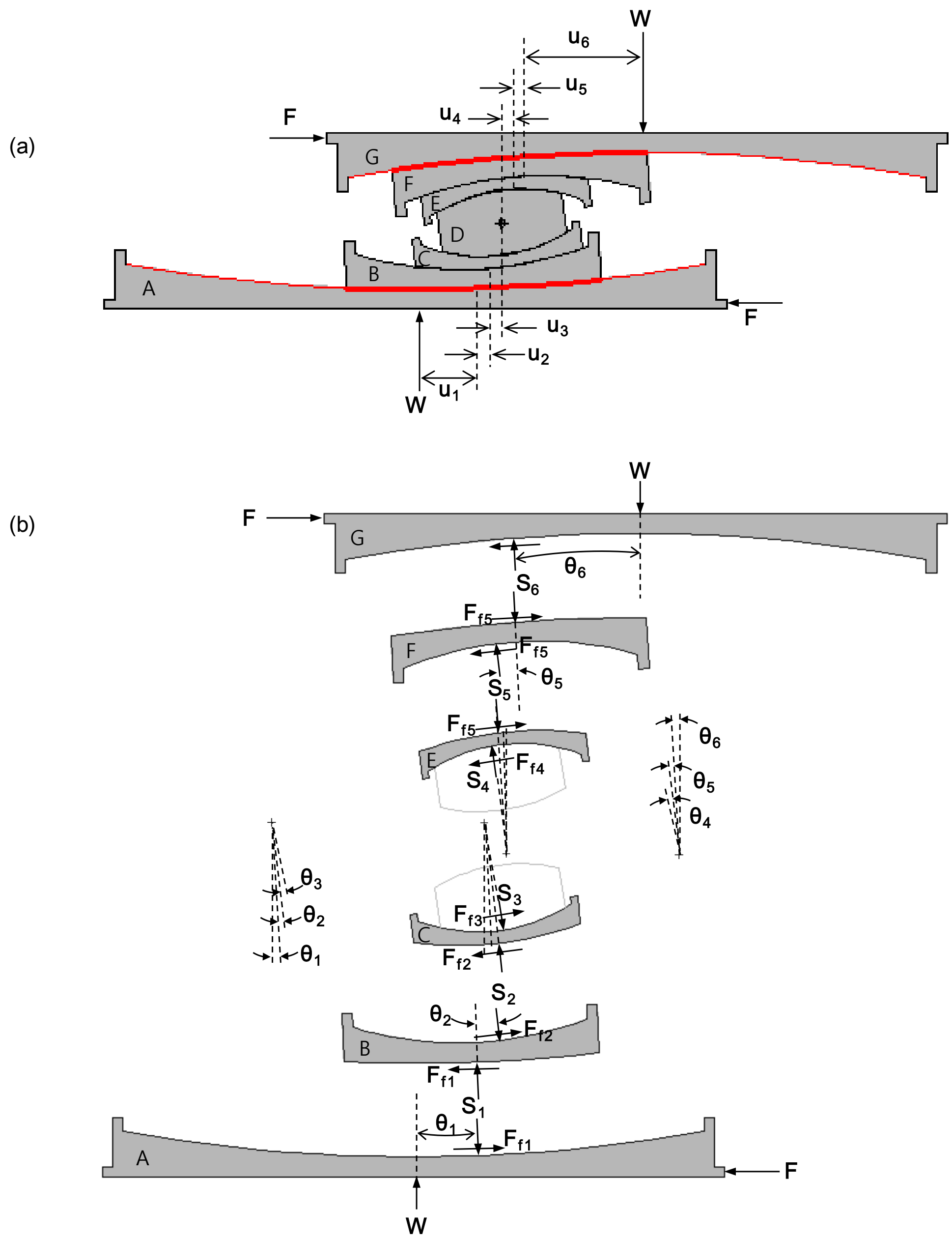

FIGURE A-9 Displaced Shape (a) and Free Body Diagrams (b) of the Quintuple FP Isolator in Sliding Regime V

The force-displacement relation in regime V is obtained by combining equations (A-21), (A-22), (A-24), (A-28), (A-29) and (A-30) and using $u = u_1 + u_2 + u_3 + u_4 + u_5 + u_6$:

$$F = \frac{W}{R_{eff1} + R_{eff6}} u + \frac{F_{f1}\left(R_{eff1} - R_{eff2}\right) + F_{f2}\left(R_{eff2} - R_{eff3}\right) + F_{f3} R_{eff3} + F_{f4} R_{eff4} + F_{f5}\left(R_{eff5} - R_{eff4}\right) + F_{f6}\left(R_{eff6} - R_{eff5}\right)}{R_{eff1} + R_{eff6}} \quad \text{(A-31)}$$

This relationship is shown in Figure A-10 together with those for the previous regimes. This regime is valid until a displacement $u = u_{dr6}$ is reached.

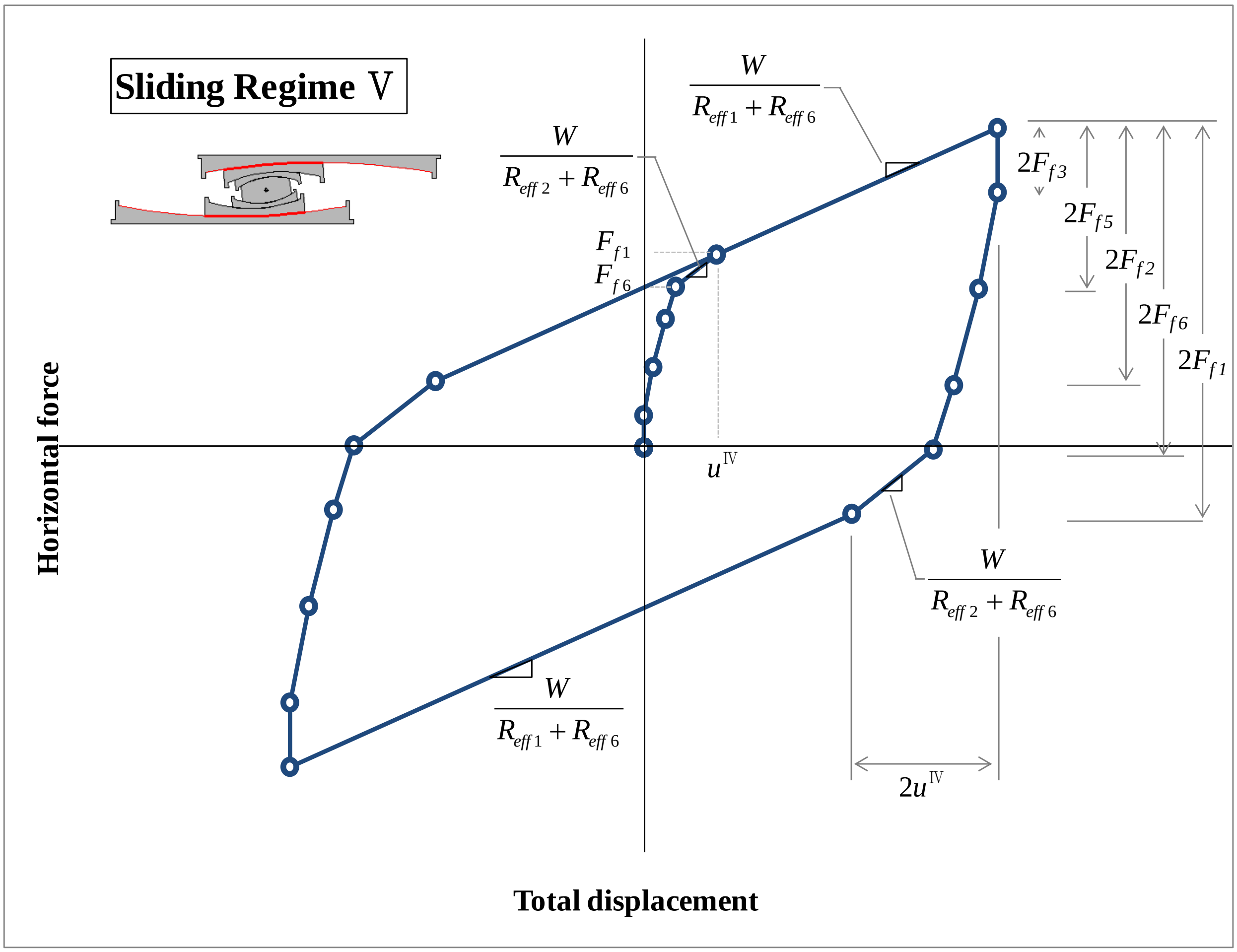

FIGURE A-10 Force-Displacement Relationship in Sliding Regime V

A-6 Sliding Regime VI

The sliding regime VI initiates when part F of the isolator contacts the restrainer of part G so that motion on surface 6 stops, motion starts on surface 5 and motion continues on surface 1 as shown in Figure A-11(a). This occurs at a displacement equal to u_{dr6}.

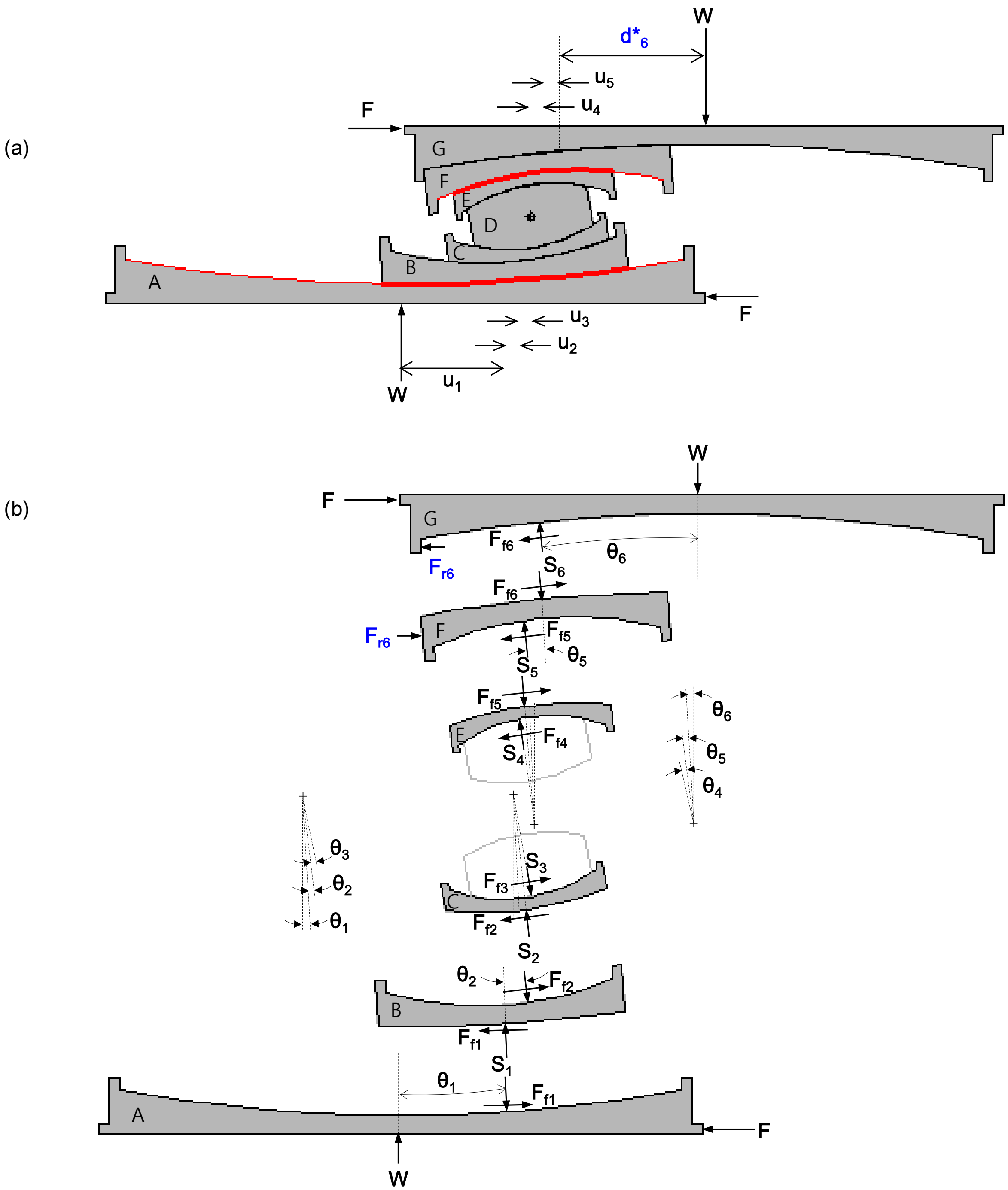

FIGURE A-11 Displaced Shape (a) and Free Body Diagrams (b) of the Quintuple FP Isolator in Sliding Regime VI

At the point of transition, the displacement on surface 6 is $u_6 = d_6^*$ and the horizontal force F is given by the following equation and termed F_{dr6}

$$F_{dr6} = \frac{W}{R_{eff6}} d_6^* + F_{f6} \tag{A-32}$$

Displacement u_{dr6} is obtained by solving equation (A-31) for the displacement and using $F = F_{dr6}$:

$$u_{dr6} = u^{\mathrm{IV}} + \left(F_{dr6} - F_{f1}\right) \times \left[\left(R_{eff1} + R_{eff6}\right)/W\right] \tag{A-33}$$

Based on the FBD of Figure A-11(b) and geometric considerations in similarity to the presentation for regimes I to V, the following equations are obtained:

$$F = \frac{W}{R_{eff6}} d_6^* + F_{f6} + F_{r6} \tag{A-34}$$

$$F = W\left(\frac{u_5}{R_{eff5}} + \frac{d_6^*}{R_{eff6}}\right) + F_{f5} \tag{A-35}$$

$$F = W\left(\frac{u_4}{R_{eff4}} + \frac{u_5}{R_{eff5}} + \frac{d_6^*}{R_{eff6}}\right) + F_{f4} \tag{A-36}$$

The force-displacement relation in regime VI is obtained by combining equations (A-28), (A-29), (A-30), (A-35) and (A-36) and using $u = d_1^* + u_2 + u_3 + u_4 + u_5 + u_6$:

$$F = \frac{W}{R_{eff1} + R_{eff5}}\left(u - u_{dr6}\right) + F_{dr6} \tag{A-37}$$

This relationship is shown in Figure A-12 together with those for the previous regimes. This regime is valid until a displacement $u=u_{dr1}$ is reached. The unloading process is same as regime V until the lateral force drops by amount $2F_{f2}$. Motion then starts on surface 6 when the horizontal force drops by $F_{r6} + 2F_{f6}$, that is, when the horizontal force is equal to

$$F = F_{dr6} - 2F_{f6} \tag{A-38}$$

For this to occur, the condition $F_{dr6} - 2F_{f6} > F - 2F_{f1}$ must be valid or, otherwise, motion will start on surface 1 instead of 6. Accordingly, motion occurs on surface 1 when the displacement satisfies the following condition

$$u > u_{dr6} + 2(\mu_1 - \mu_6)(R_{eff1} + R_{eff5}) \tag{A-39}$$

However, based on equation (A-41b) that follows, for typical configurations with $d_1^* = d_6^*$ and $R_{eff1} = R_{eff6}$, equation (A-39) will not be satisfied prior to the start of sliding regime VII. Thus for typical configurations, motion will start on surface 6 prior to surface 1, as shown in Figure A-12.

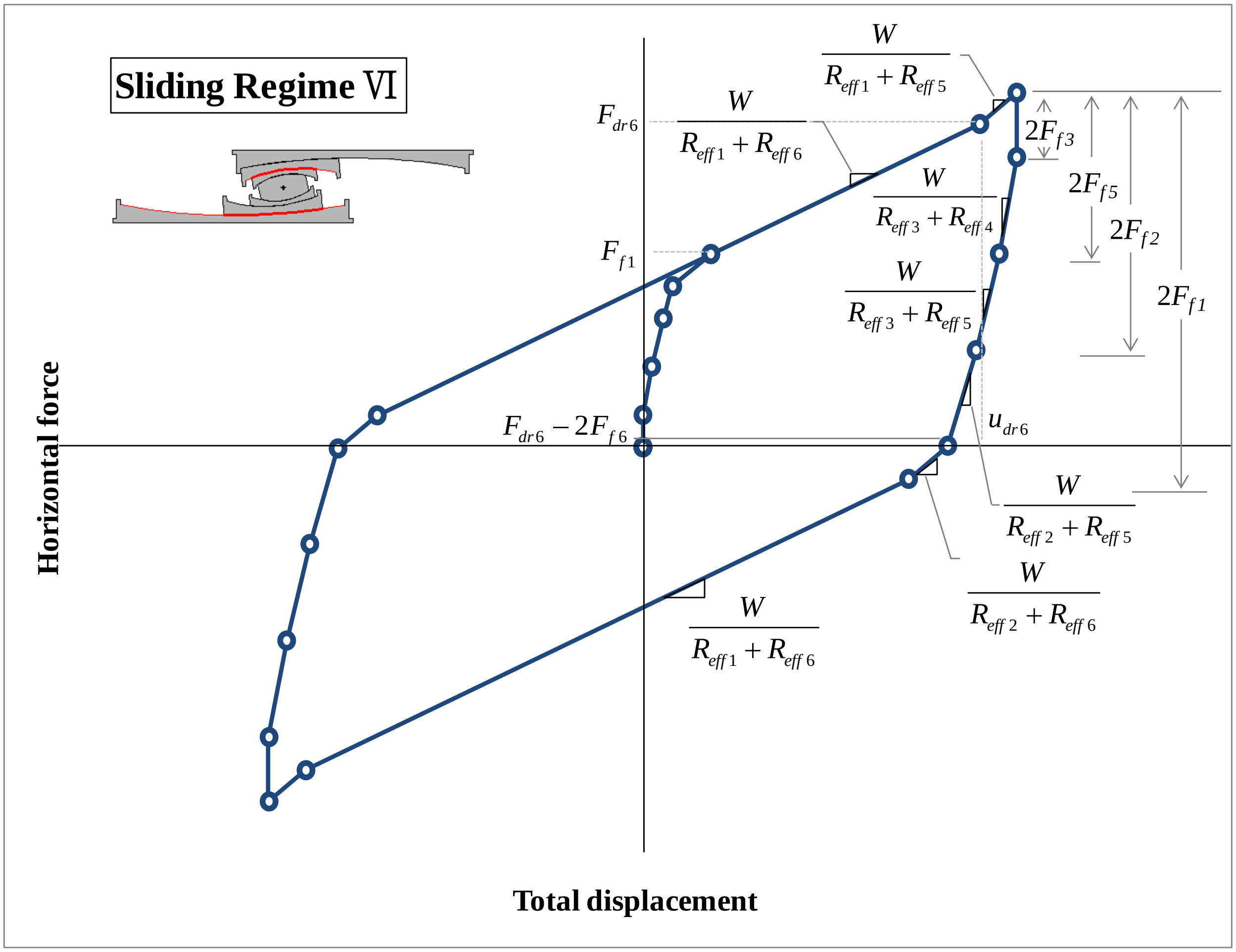

FIGURE A-12 Force-Displacement Relationship During Sliding Regime VI

A-7 Sliding Regime VII

The sliding regime VII initiates when part B of the isolator contacts the restrainer of part A so that motion on surface 1 stops, motion starts on surface 2 and motion continues on surface 5 as shown in Figure A-13(a). This occurs at a displacement equal to u_{dr1}.

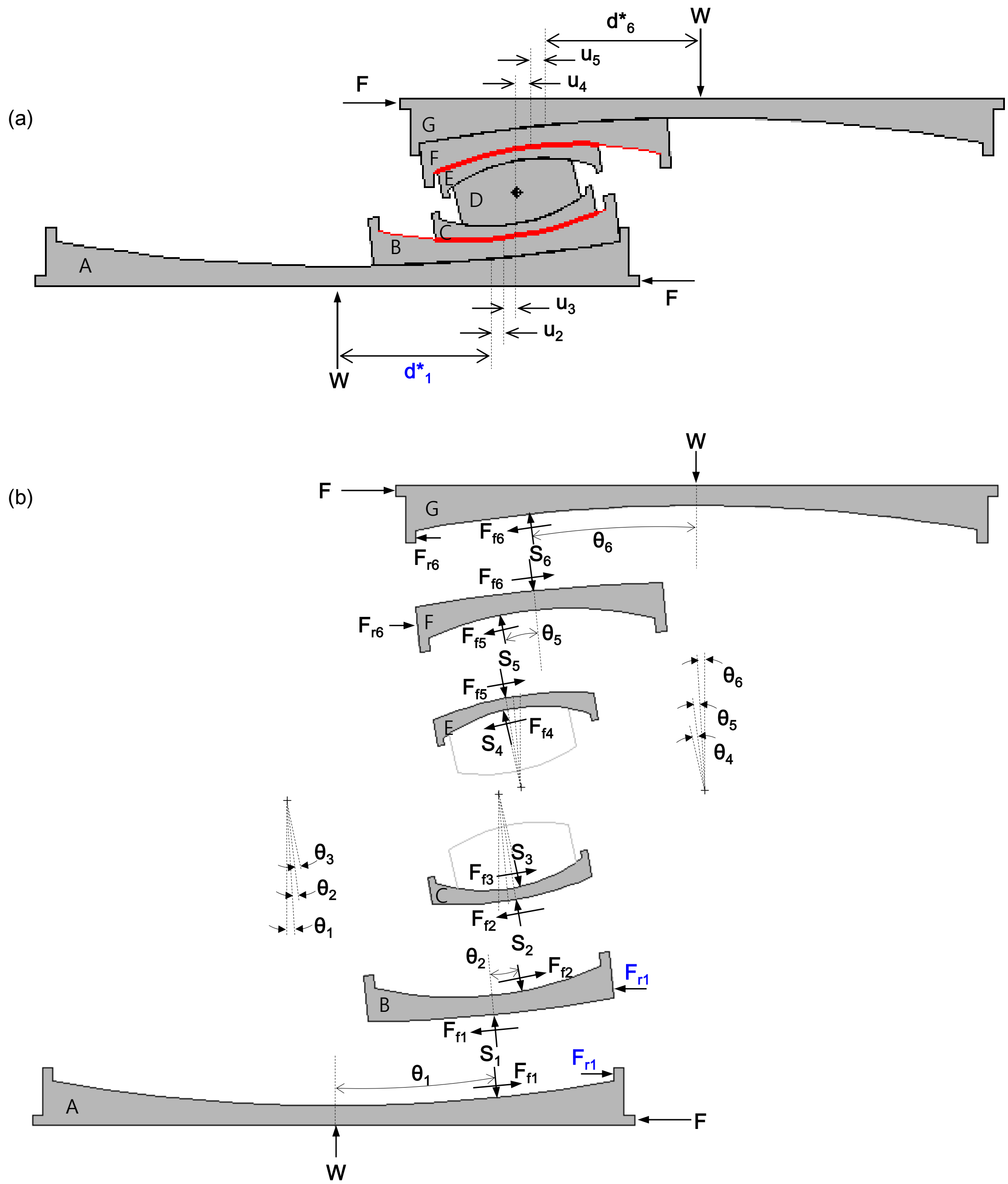

FIGURE A-13 Displaced Shape (a) and Free Body Diagrams (b) of the Quintuple FP Isolator During Sliding Regime VII

At the transition point, the displacement on surface 1 is $u_1 = d_1^*$ and the horizontal force F is given by the following equation and termed F_{dr1}

$$F_{dr1} = \frac{W}{R_{eff1}} d_1^* + F_{f1} \tag{A-40}$$

Displacement u_{dr1} is obtained by solving equation (A-37) for the displacement and using $F=F_{dr1}$:

$$u_{dr1} = u_{dr6} + \left(F_{dr1} - F_{dr6}\right) \times \left[\left(R_{eff1} + R_{eff5}\right) / W\right] \tag{A-41a}$$

or

$$u_{dr1} = u_{dr6} + \left[\left(\frac{d_1^*}{R_{eff1}} + \mu_1\right) - \left(\frac{d_6^*}{R_{eff6}} + \mu_6\right)\right]\left(R_{eff1} + R_{eff5}\right) \tag{A-41b}$$

Based on the FBD in Figure A-13(b) and geometric considerations in similarity to the presentation for regimes I to VI, the followings is obtained:

$$F = \frac{W}{R_{eff1}} d_1^* + F_{f1} + F_{r1} \tag{A-42}$$

$$F = W\left(\frac{d_1^*}{R_{eff1}} + \frac{u_2}{R_{eff2}}\right) + F_{f2} \tag{A-43}$$

$$F = W\left(\frac{d_1^*}{R_{eff1}} + \frac{u_2}{R_{eff2}} + \frac{u_3}{R_{eff3}}\right) + F_{f3} \tag{A-44}$$

The force-displacement relation in regime VII is obtained by combining equations (A-34), (A-35), (A-36), (A-43) and (A-44) and using $u = d_1^* + u_2 + u_3 + u_4 + u_5 + d_6^*$:

$$F = \frac{W}{R_{eff2} + R_{eff5}}\left(u - u_{dr1}\right) + F_{dr1} \tag{A-45}$$

This relationship is shown in Figure A-14 together with those for the previous regimes. This regime is valid until a displacement u_{dr5} is reached. The unloading process is the same as that of regime VI until the lateral force drops by $2F_{f2}$. Motion then starts on surface 6 to be followed by motion on surface 1. For this to occur, the condition $F_{dr6} - 2F_{f6} > F_{dr1} - 2F_{f1}$ must be valid or, otherwise, motion will start on surface 1 and will be followed by motion on surface 6. For typical configurations ($d_1^* = d_6^*$ and $R_{eff1} = R_{eff6}$), motion will start on surface 6 prior to surface 1, as shown in Figure A-14.

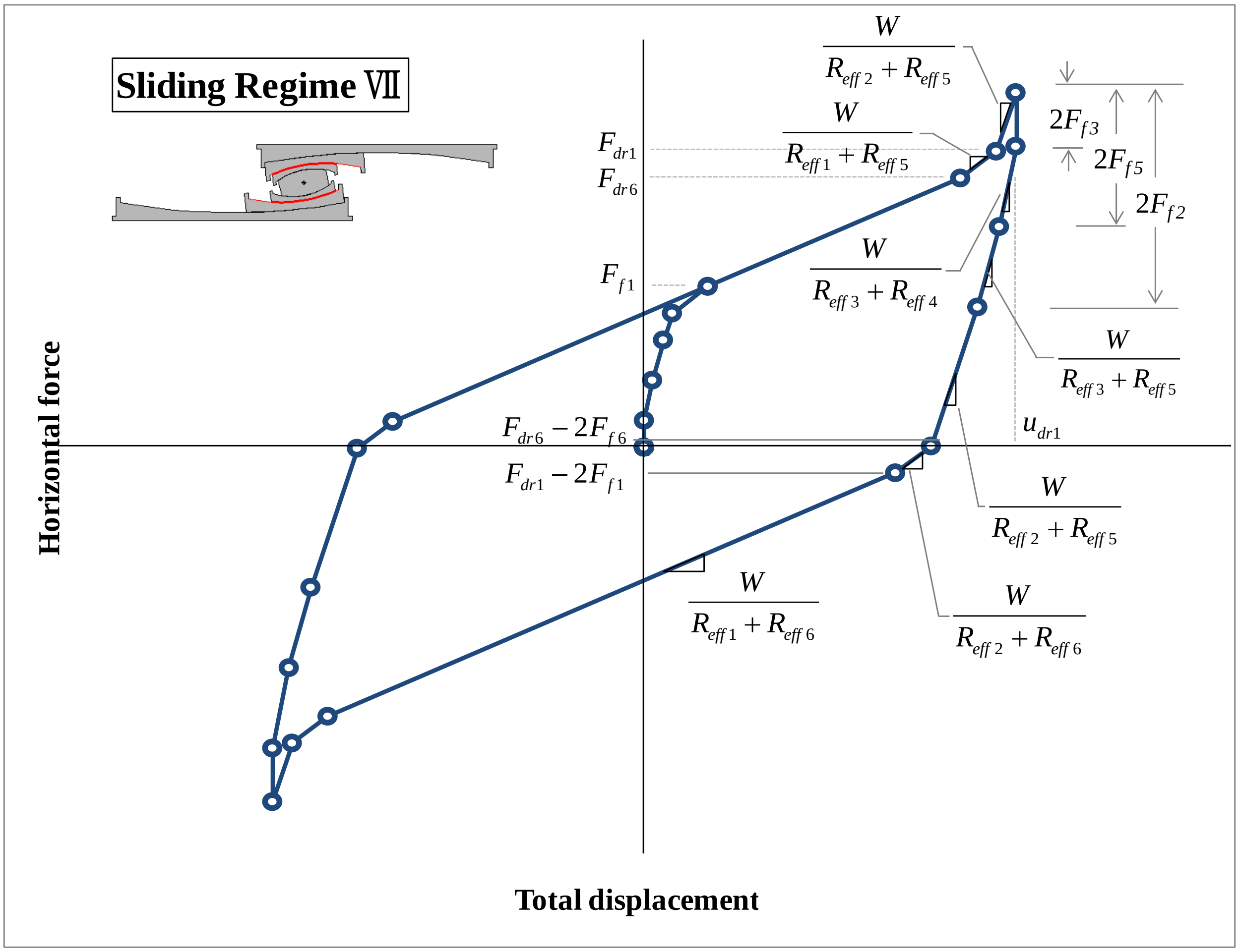

FIGURE A-14 Force-Displacement Relationship During Sliding Regime VII

A-8 Sliding Regime VIII

The sliding regime VIII initiates when part E of the isolator contact to the restrainer of slider F so that motion on surface 5 stops, motion resumes on surface 4 and motion continues on surface 2 as shown in Figure 15(a). This occurs at a displacement equal to u_{dr5}.

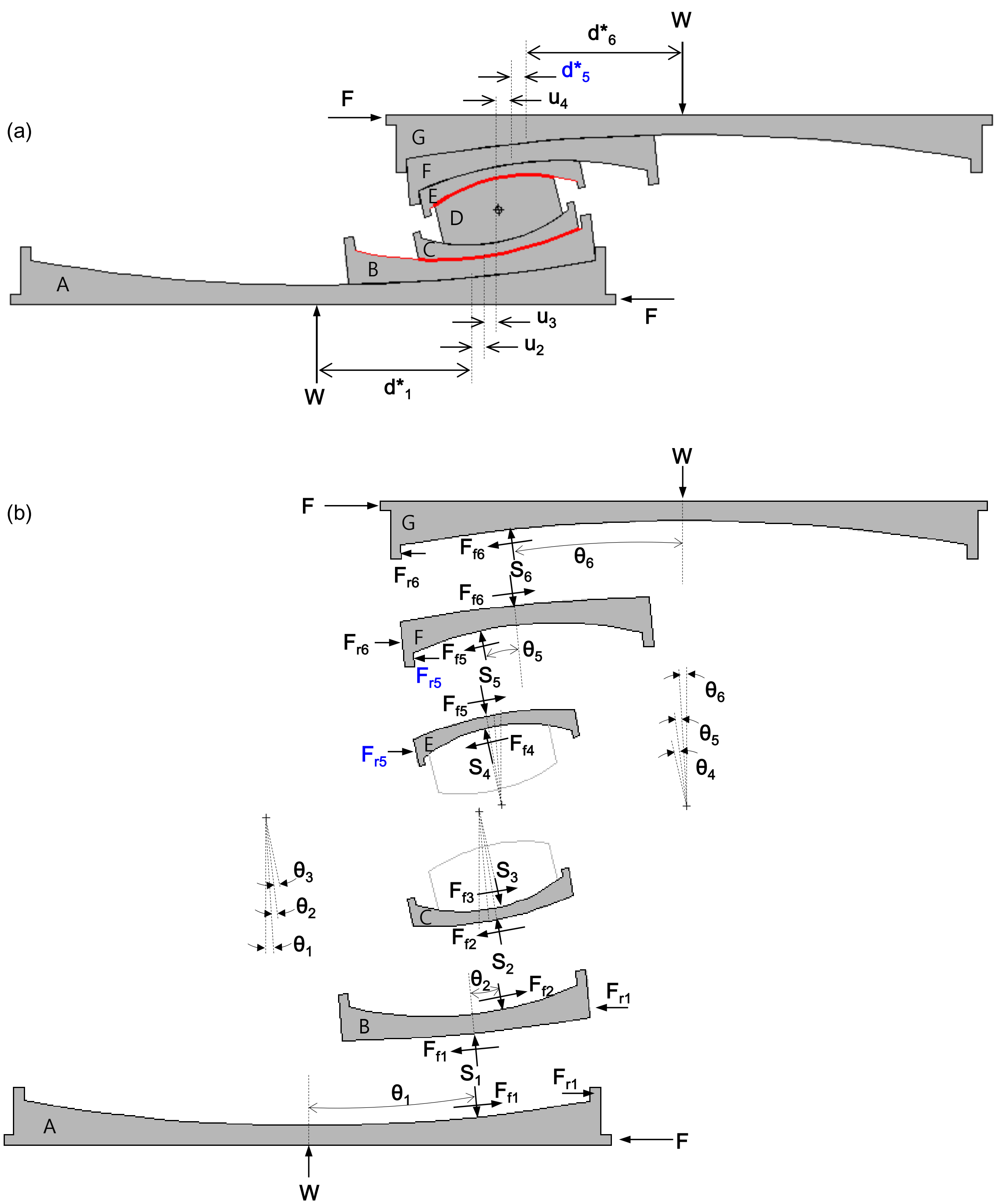

FIGURE A-15 Displaced Shape (a) and Free Body Diagrams (b) of the Quintuple FP Isolator During Sliding Regime VIII

At the transition point, the displacement on surface 5 is $u_5 = d_5^*$ and the horizontal force F is given by the following equation and termed F_{dr5}

$$F_{dr5} = W\left(\frac{d_5^*}{R_{eff\,5}} + \frac{d_6^*}{R_{eff\,6}}\right) + F_{f\,5} \qquad \text{(A-46)}$$

Displacement u_{dr5} is determined by solving equation (A-46) for the displacement and using F= F_{dr5}:

$$u_{dr5} = u_{dr1} + \left(F_{dr5} - F_{dr1}\right) \times \left[\left(R_{eff\,2} + R_{eff\,5}\right)/W\right] \qquad \text{(A-47)}$$

From the FBD in Figure A-15(b) and geometric considerations in similarity to the presentation for regimes I to VII, the followings is obtained:

$$F = \frac{W}{R_{eff\,6}} d_6^* + F_{f\,6} + F_{r6} \qquad \text{(A-48)}$$

$$F = W\left(\frac{d_5^*}{R_{eff\,5}} + \frac{d_6^*}{R_{eff\,6}}\right) + F_{f\,5} + F_{r5} \qquad \text{(A-49)}$$

$$F = W\left(\frac{u_4}{R_{eff\,4}} + \frac{d_5^*}{R_{eff\,5}} + \frac{d_6^*}{R_{eff\,6}}\right) + F_{f\,4} \qquad \text{(A-50)}$$

The force-displacement relation in regime VIII is obtained combining equations (A-43), (A-44) and (A-50) and using $u = d_1^* + u_2 + u_3 + u_4 + d_5^* + d_6^*$:

$$F = \frac{W}{R_{eff\,2} + R_{eff\,4}}\left(u - u_{dr5}\right) + F_{dr5} \qquad \text{(A-51)}$$

This relationship is shown in Figure A-16 together with those for the previous regimes. This regime is valid until a displacement u_{dr2} is reached. Upon reversal of motion, the lateral force drops by $2F_{f\,3}\left(=2F_{f\,4}\right)$. Motion then starts on surface 5 when the horizontal force is equal to $F_{dr5} - 2F_{f\,5}$. For this to occur, the condition $F_{dr5} - 2F_{f\,5} > F - 2F_{f\,2}$ must be valid or, otherwise, motion will start on surface 2 instead of 5. Based on the similar analysis in regime VI, motion will start on surface 5 prior to surface 2 for typical configurations ($R_{eff2} = R_{eff5}$ and $d_2^* = d_5^*$), as shown in Figure A-16. Motion then follows on the surfaces 1 and 6, as presented in regime VII.

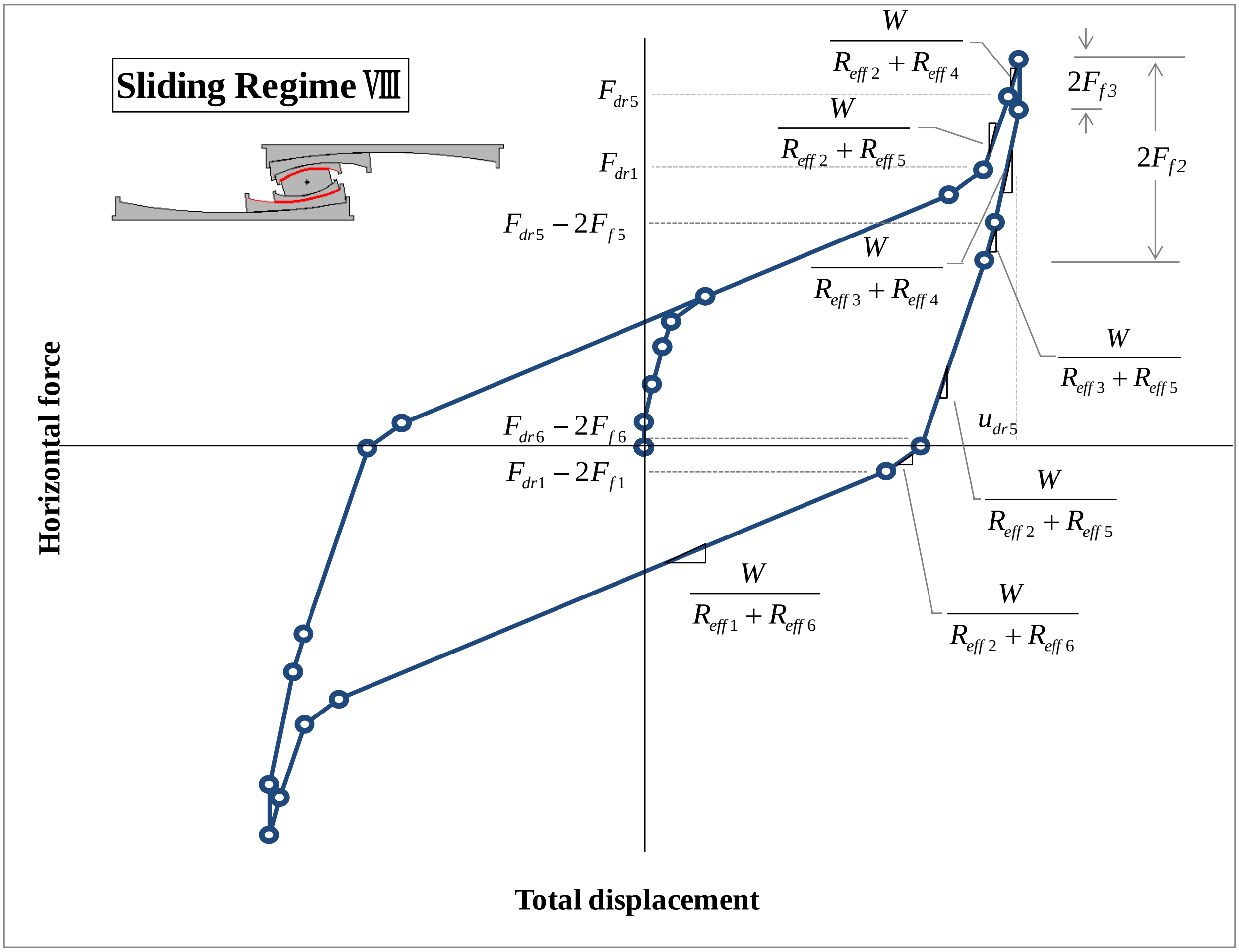

FIGURE A-16 Force-Displacement Relationship During Sliding Regime VIII

A-9 Sliding Regime IX

The sliding regime IX begins when part C of the isolator contacts the restrainer of part B, so that motion stops on surface 2, motion resumes on surface 3 and motion continues on surface 4, as shown in Figure A-17(a). This occurs at a displacement equal to u_{dr2}.

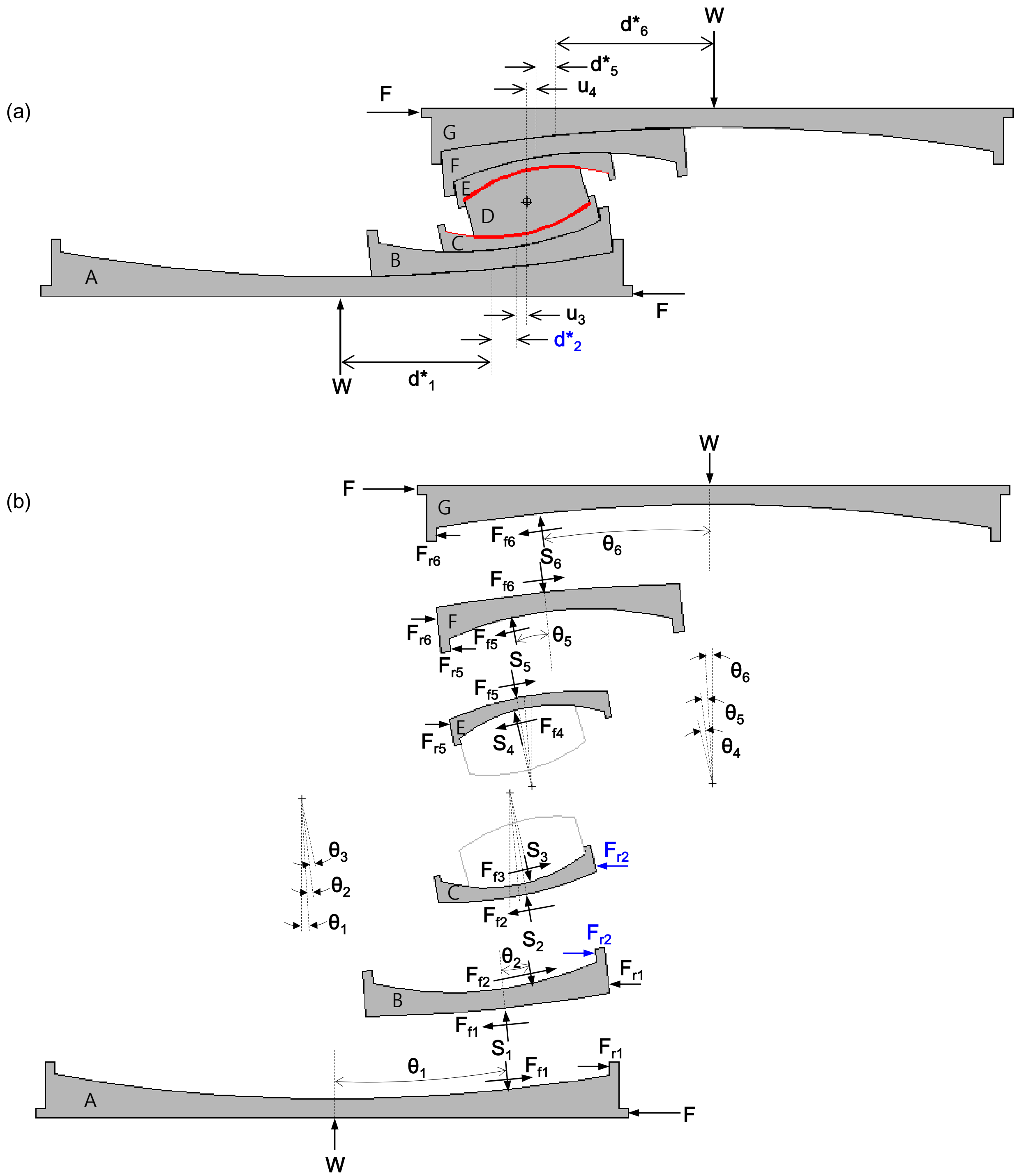

FIGURE A-17 Displaced Shape (a) and Free Body Diagrams (b) of the Quintuple FP Isolator During Sliding Regime IX

At the transition point, the displacement on surface 2 is $u_2 = d_2^*$ and the horizontal force F is given by the following equation and termed F_{dr2}

$$F_{dr2} = W\left(\frac{d_1^*}{R_{eff1}} + \frac{d_2^*}{R_{eff2}}\right) + F_{f2} \quad \text{(A-52)}$$

Displacement u_{dr2} is obtained by solving equation (A-51) for the displacement and using $F = F_{dr2}$:

$$u_{dr2} = u_{dr5} + \left(F_{dr2} - F_{dr5}\right) \times \left[\left(R_{eff2} + R_{eff4}\right) / W\right] \quad \text{(A-53)}$$

Based on FBD in Figure A-17 (b) and geometric considerations in similarity to the presentation for regimes I to VIII, the followings are obtained:

$$F = \frac{W}{R_{eff1}} d_1^* + F_{f1} + F_{r1} \quad \text{(A-54)}$$

$$F = W\left(\frac{d_1^*}{R_{eff1}} + \frac{d_2^*}{R_{eff2}}\right) + F_{f2} + F_{r2} \quad \text{(A-55)}$$

$$F = W\left(\frac{d_1^*}{R_{eff1}} + \frac{d_2^*}{R_{eff2}} + \frac{u_3}{R_{eff3}}\right) + F_{f3} \quad \text{(A-56)}$$

The force-displacement relation in regime IX is obtained by combining equations (A-50) and (A-56) and using $u = d_1^* + d_2^* + u_3 + u_4 + d_5^* + d_6^*$:

$$F = \frac{W}{R_{eff3} + R_{eff4}}\left(u - u_{dr5}\right) + F_{dr2} \quad \text{(A-57)}$$

This relationship is shown in Figure A-18 together with those for the previous regimes. This regime is valid until total displacement capacity is reached. Upon reversal of motion, the lateral force drops by $2F_{f3}\left(= 2F_{f4}\right)$. Motion then starts on surface 5 instead of surface 2. For this to occur, the condition F_{dr5}-$2F_{f5}$ > F_{dr2}-$2F_{f2}$ must be valid or, otherwise, motion will start on surface 2 instead of surface 5 prior to surface 2. For typical configurations ($R_{eff2} = R_{eff5}$ and $d_2^* = d_5^*$), motion will start on surface. Motion then follows on the surfaces 1 and 6, as presented in regime VII.

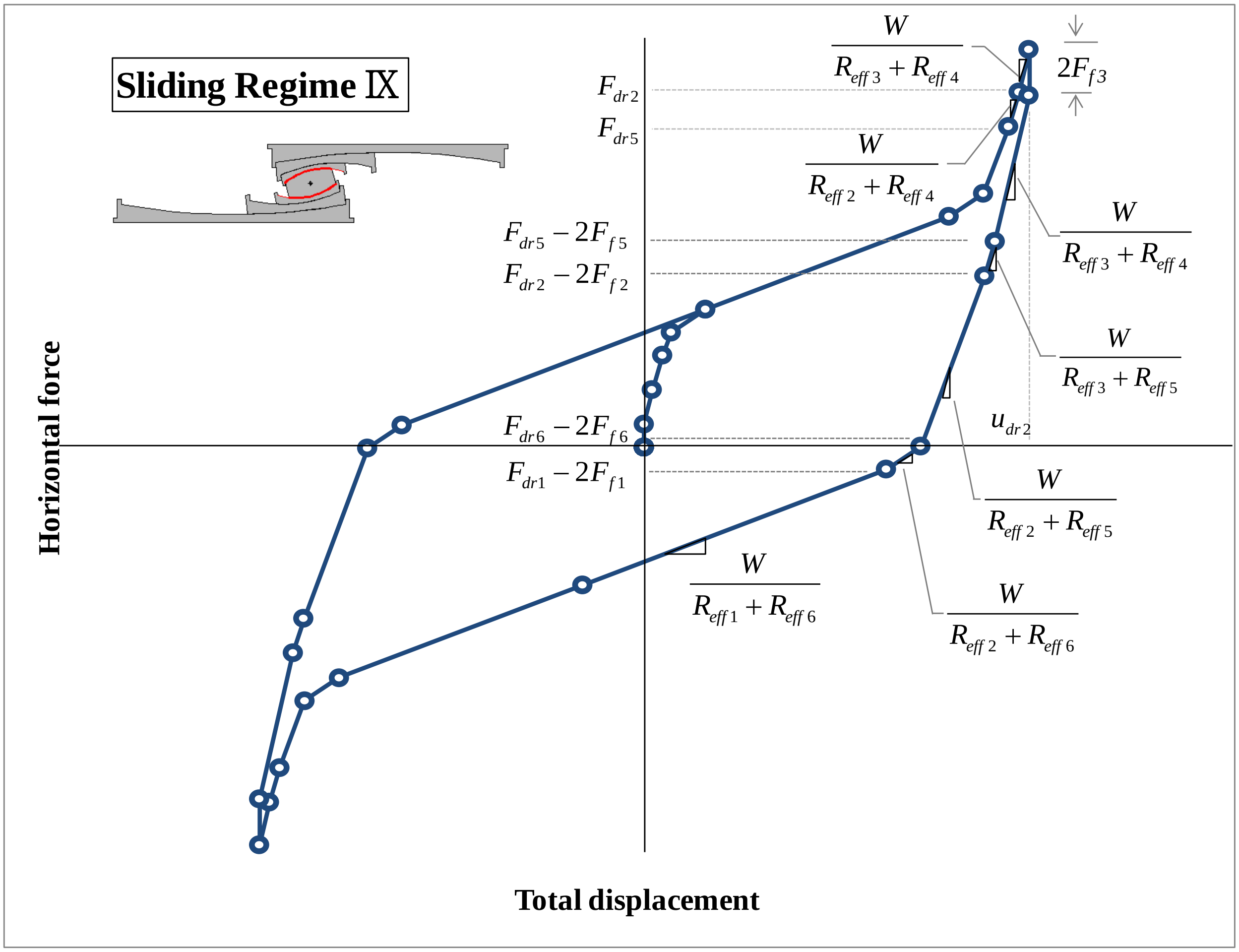

FIGURE A-18 Force-Displacement Relationship During Sliding Regime IX

APPENDIX B
DETAILS OF COMPUTATIONAL MODEL IN PROGRAM SAP2000

B-1 Computational Model for the Isolator in Table 3-3

Figure B-1 presents a section of the analyzed isolator that shows the dimensional and the frictional parameters (friction is constant in this analysis). This is the isolator of Configuration 1 with the properties presented in Table 3-3 and with force-displacement loops shown in Figure 3-5.

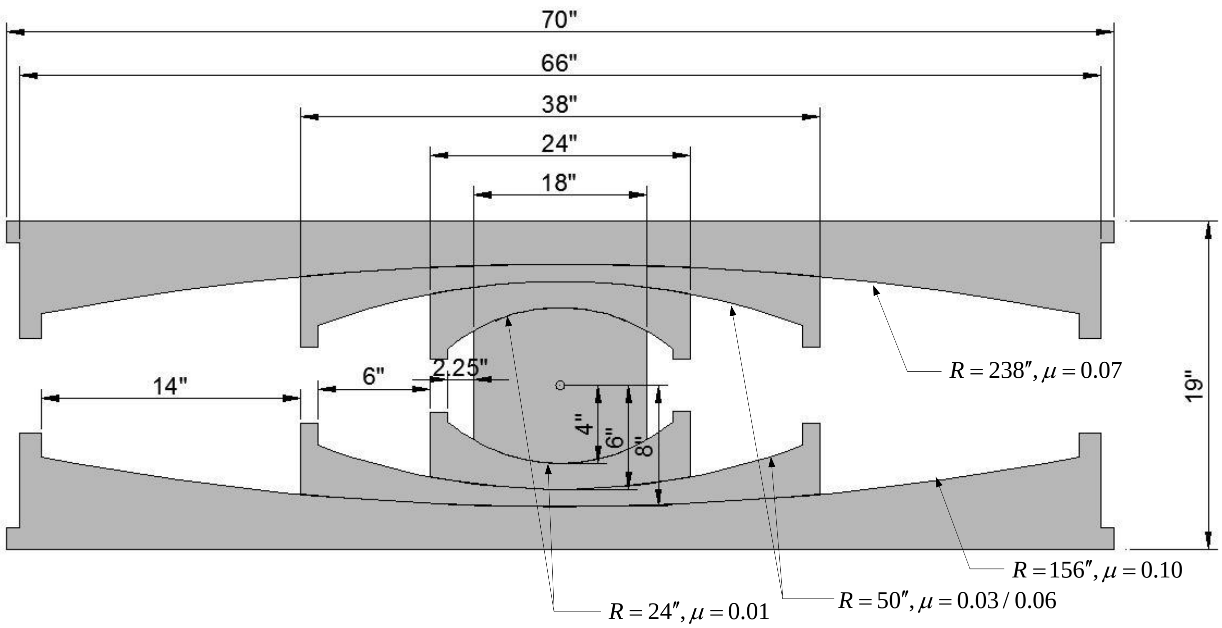

FIGURE B-1 Geometrical and Frictional Properties of Analyzed Quintuple FP Isolator

Figure B-2 illustrates the model of the isolator used in program SAP2000 for simulating the behavior of a single isolator under imposed gravity load *W* and lateral history of prescribed displacement. A rigid massless bar was used to connect two identical isolators and impose motion through a control point. Each of the two isolators in the model represented the analyzed isolator carrying the load *W*. The model depicted in Figure B-2 is for the case of using the Triple FP element of SAP2000. Table B-1a presents the effective properties of the analyzed isolator that were used to calculate the properties of elements used in the computational model.

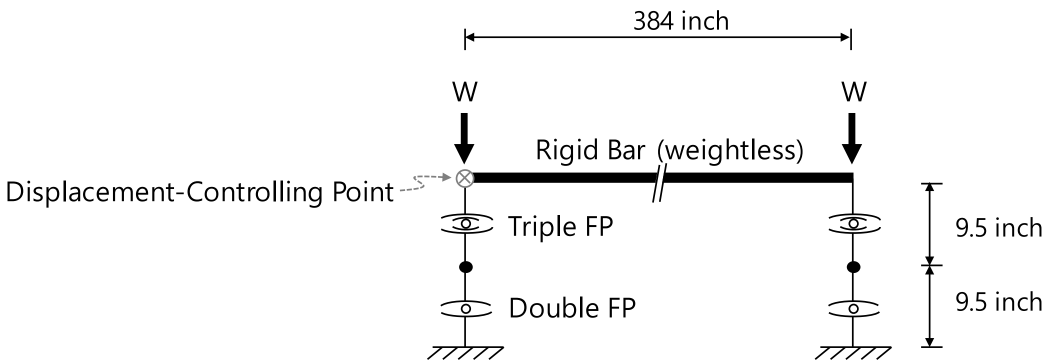

FIGURE B-2 Model of Quintuple FP Isolator for Analysis in Program SAP2000

The input parameters for each of the Triple FP and the Double FP elements in program SAP2000 utilized in the simulation are presented in Table B-1b. These parameters include the radii of curvature, the friction coefficient values, and the displacement capacities (defined as stop distances in SAP2000). It is noted that the "fast" and "slow" values of the coefficient of friction were specified equal and the rate parameter in the SAP2000 elements was defined as zero (or an arbitrary value) so that there is no velocity dependence of the coefficient of friction. Other parameters such as element mass, effective stiffness and rotational moment of inertia did not have any noticeable effect in the analysis results as long as they were selected to reasonably represent properties of the isolator. The values for element mass and rotational moment of inertia were properly estimated considering the isolator geometry. The effective stiffness in SAP2000 was selected to be half of that of the isolator at a displacement equal to half of the isolator displacement capacity. This stiffness was then assigned to the triple FP and double FP elements in a series. The vertical stiffness was calculated as the stiffness of a column having the height of the isolator (19 inch) and diameter equal to the diameter of part D of the isolator (18 inch) and distributed on the basis of the details provided in the document of Sarlis and Constantinou (2010). The rotational and torsional stiffness were specified to be zero.

TABLE B-1a Effective Properties of Quintuple FP Isolator and Properties in Computational Model in SAP2000 per Table 3-3 (Top Table Reports Properties of Isolator; Bottom Table Reports Parameters of SAP2000 Model)

<table>
<tr><td colspan="2">Sliding surface</td><td>Radius of curvature (in)</td><td>Coefficient of friction</td><td>Displacement capacity (in)</td></tr>
<tr><td colspan="2">Surface 1</td><td>$R_{eff\,1} = 230$</td><td>$\mu_1 = 0.10$</td><td>$d_1^* = 13.53$</td></tr>
<tr><td colspan="2">Surface 2</td><td>$R_{eff\,2} = 44$</td><td>$\mu_2 = 0.06$</td><td>$d_2^* = 5.28$</td></tr>
<tr><td colspan="2">Surface 3</td><td>$R_{eff\,3} = 20$</td><td>$\mu_3 = 0.01$</td><td>$d_3^* = 1.875$</td></tr>
<tr><td colspan="2">Surface 4</td><td>$R_{eff\,4} = 20$</td><td>$\mu_4 = 0.01$</td><td>$d_4^* = 1.875$</td></tr>
<tr><td colspan="2">Surface 5</td><td>$R_{eff\,5} = 44$</td><td>$\mu_5 = 0.03$</td><td>$d_5^* = 5.28$</td></tr>
<tr><td colspan="2">Surface 6</td><td>$R_{eff\,6} = 148$</td><td>$\mu_6 = 0.07$</td><td>$d_6^* = 13.28$</td></tr>
<tr><td colspan="2">Sliding surface</td><td>Radius of curvature (in)</td><td>Coefficient of friction</td><td>Displacement capacity (in)</td></tr>
<tr><td rowspan="3">Triple FP Element</td><td>Lower surface</td><td>$\tilde{R}_{eff1} = 44$</td><td>$\tilde{\mu}_1 = 0.06$</td><td>$\tilde{d}_1 = 7.868$</td></tr>
<tr><td>Inner surfaces</td><td>$\tilde{R}_{eff\,2,3} = 20$</td><td>$\tilde{\mu}_{2,3} = 0.01$</td><td>$\tilde{d}_2$, $\tilde{d}_3 = 1.875$</td></tr>
<tr><td>Upper surface</td><td>$\tilde{R}_{eff\,4} = 44$</td><td>$\tilde{\mu}_4 = 0.03$</td><td>$\tilde{d}_4 = 9.229$</td></tr>
<tr><td rowspan="2">Double FP Element</td><td>Upper surface</td><td>$\tilde{R}_{eff\,5} = 104$</td><td>$\tilde{\mu}_5 = 0.07$</td><td>$\tilde{d}_5 = 9.333$</td></tr>
<tr><td>Lower surface</td><td>$\tilde{R}_{eff\,6} = 186$</td><td>$\tilde{\mu}_6 = 0.10$</td><td>$\tilde{d}_6 = 10.941$</td></tr>
</table>

TABLE B-1b Values of Parameters of Elements in Program SAP2000 in Case without Velocity-Dependence of Friction per Table 3-3

Models	Triple FP			Double FP		
Sliding surface	Lower	Inner Surfaces	Upper	Upper	[1]Inner Surfaces	Lower
Radius of sliding surface (inch)	44	20	44	104	0	186
Friction coefficient (FAST and SLOW)	0.03	0.01	0.06	0.07	1	0.10
Rate parameter (sec/in)	0	0	0	0	0	0
Stop distance (inch)	9.229	1.875	7.868	9.333	0	10.941
Supported weight (kip)	900	900	900	900	900	900
Yield displacement (inch)	0.01	0.01	0.01	0.01	0.01	0.01
Stiffness (elastic) (kip/in)	1350	450	2700	3150	[2] 3825	4500
Effective stiffness (kip/in)	5.6			5.6		
Rotational moment of inertia (kip-in-sec^2)	0.057			0		
Element height (inch)	9.5			9.5		
Shear deformation location (in)-(distance from top joint of FP element)	4.75			4.75		
Element mass (kip-s^2/in)	0.001			0.001		
Vertical stiffness (kip/in)	323,667			485,500		
Rotational / torsional stiffness (R1,R2,R3)	0			fixed		

[1]Values of parameters specified for inner surfaces in Double FP element are artificial and intend to impede motion at the inner sliding surfaces, specifically (a) zero for radius and stop distance and (b) unity for friction.

[2] Value arbitrarily selected to be average of values for upper and lower parts. Very large values should not be used as they result in convergence problems.

B-2 Computational Model for the Isolator in Table 4-1

Figure B-3 presents a section of the tested isolator that shows the dimensional and frictional parameters (friction values are for quasi-static conditions). This is the isolator with the properties presented in Table 4-1 and with force-displacement loops shown in Figure 4-2.

A computational model of the tested isolator was also constructed based on the approach described above. The properties for the tested isolator used in computational model are presented in Tables B-2a (actual properties) and B-2b (input parameters for each of the Triple FP and Double FP elements).

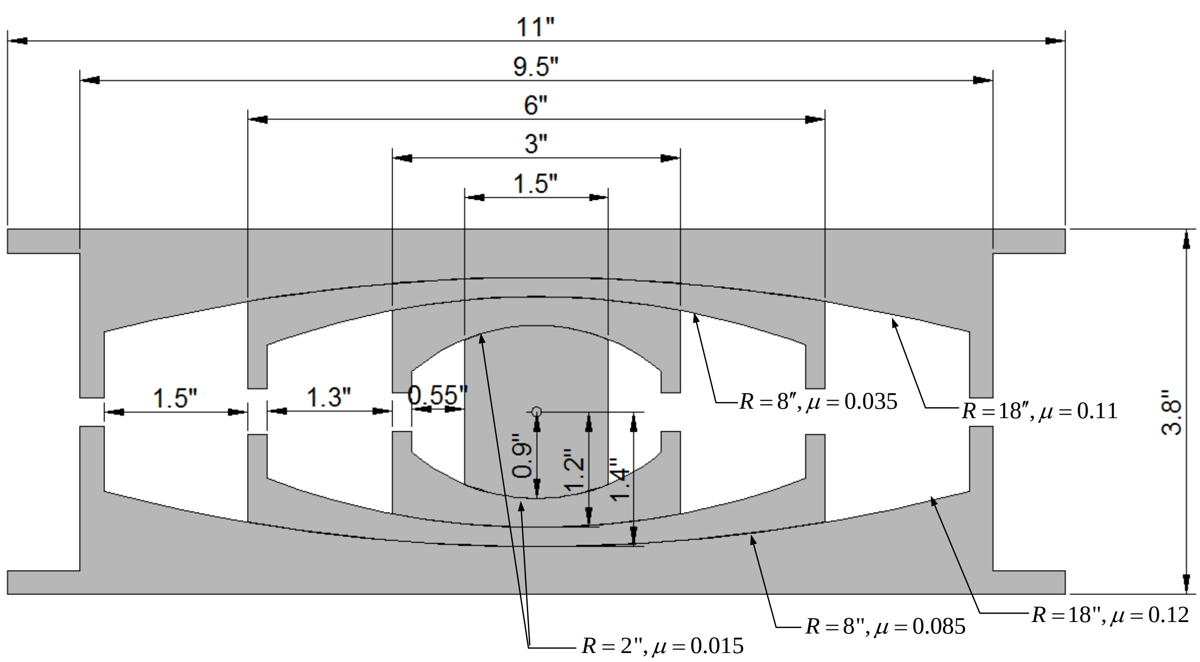

FIGURE B-3 Geometrical and Frictional Properties of Tested Quintuple FP Isolator

TABLE B-2a Effective Properties of the Tested Isolator and Properties in Computational Model in SAP2000 per Table 4-1 (Top Table Reports Properties of Isolator; Bottom Table Reports Parameters of SAP2000 Model)

Sliding surface	Radius of curvature (in)	Coefficient of friction	Displacement capacity (in)
Surface 1	$R_{eff\,1} = 16.6$	$\mu_1 = 0.12$	$d_1^* = 1.383$
Surface 2	$R_{eff\,2} = 6.8$	$\mu_2 = 0.085$	$d_2^* = 1.105$
Surface 3	$R_{eff\,3} = 1.1$	$\mu_3 = 0.015$	$d_3^* = 0.303$
Surface 4	$R_{eff\,4} = 1.1$	$\mu_4 = 0.015$	$d_4^* = 0.303$
Surface 5	$R_{eff\,5} = 6.8$	$\mu_5 = 0.035$	$d_5^* = 1.105$
Surface 6	$R_{eff\,6} = 16.6$	$\mu_6 = 0.11$	$d_6^* = 1.383$

Sliding surface		Radius of curvature (in)	Coefficient of friction	Displacement capacity (in)
Triple FP Element	Lower surface	$\tilde{R}_{eff\,1} = 6.8$	$\tilde{\mu}_1 = 0.085\,(0.11)$	$\tilde{d}_1 = 1.672$
	Inner surfaces	$\tilde{R}_{eff\,2,3} = 1.1$	$\tilde{\mu}_{2,3} = 0.015\,(0.04)$	$\tilde{d}_2$, $\tilde{d}_3 = 0.303$
	Upper surface	$\tilde{R}_{eff\,4} = 6.8$	$\tilde{\mu}_4 = 0.035\,(0.09)$	$\tilde{d}_1 = 1.672$
Double FP Element	Upper surface	$\tilde{R}_{eff\,5} = 9.8$	$\tilde{\mu}_5 = 0.11\,(0.15)$	$\tilde{d}_5 = 0.816$
	Lower surface	$\tilde{R}_{eff\,6} = 9.8$	$\tilde{\mu}_6 = 0.12\,(0.16)$	$\tilde{d}_6 = 0.816$

TABLE B-2b Values of Parameters of Elements in Program SAP2000 in Case without Velocity-Dependence of Friction per Table 4-1 (Values in Parenthesis are for Case with Velocity-Dependence of Friction)

Models	Triple FP			Double FP		
Sliding surface	Lower	Inner Surfaces	Upper	Upper	Inner Surfaces	Lower
Radius of sliding surface (inch)	6.8	1.1	6.8	9.8	0	9.8
Friction coefficient SLOW	0.085	0.015	0.035	0.11	1	0.12
Friction coefficient FAST	0.085 (0.11)	0.015 (0.04)	0.035 (0.09)	0.11 (0.15)	1 (1)	0.12 (0.16)
Rate parameter (sec/in)	0 (3.0)	0 (1.5)	0 (3.0)	0 (2.0)	0 (0)	0 (2.0)
Stop distance (inch)	1.672	0.303	1.672	0.816	0	0.816
Supported weight (kip)	20	20	20	20	20	20
Yield displacement (inch)	0.01	0.01	0.01	0.01	0.01	0.01
Stiffness (elastic) (kip/in)	110	40	90	150	155	160
Effective stiffness (kip/in)	1.25			1.25		
Rotational moment of inertia (kip-in-sec^2)	1.455×10^{-4}			0		
Element height (inch)	1.95			1.95		
Shear deformation location (in)-(distance from top joint of FP element)	0.975			0.975		
Element mass (kip-s^2/in)	0.0001			0.0001		
Vertical stiffness (kip/in)	10,945			16,417		
Rotational / torsional stiffness (R1,R2,R3)	0			fixed		

MCEER Technical Reports

MCEER publishes technical reports on a variety of subjects written by authors funded through MCEER. These reports are available from both MCEER Publications and the National Technical Information Service (NTIS). Requests for reports should be directed to MCEER Publications, MCEER, University at Buffalo, State University of New York, 133A Ketter Hall, Buffalo, New York 14260. Reports can also be requested through NTIS, P.O. Box 1425, Springfield, Virginia 22151. NTIS accession numbers are shown in parenthesis, if available.

NCEER-87-0001 "First-Year Program in Research, Education and Technology Transfer," 3/5/87, (PB88-134275, A04, MF-A01).

NCEER-87-0002 "Experimental Evaluation of Instantaneous Optimal Algorithms for Structural Control," by R.C. Lin, T.T. Soong and A.M. Reinhorn, 4/20/87, (PB88-134341, A04, MF-A01).

NCEER-87-0003 "Experimentation Using the Earthquake Simulation Facilities at University at Buffalo," by A.M. Reinhorn and R.L. Ketter, not available.

NCEER-87-0004 "The System Characteristics and Performance of a Shaking Table," by J.S. Hwang, K.C. Chang and G.C. Lee, 6/1/87, (PB88-134259, A03, MF-A01). This report is available only through NTIS (see address given above).

NCEER-87-0005 "A Finite Element Formulation for Nonlinear Viscoplastic Material Using a Q Model," by O. Gyebi and G. Dasgupta, 11/2/87, (PB88-213764, A08, MF-A01).

NCEER-87-0006 "Symbolic Manipulation Program (SMP) - Algebraic Codes for Two and Three Dimensional Finite Element Formulations," by X. Lee and G. Dasgupta, 11/9/87, (PB88-218522, A05, MF-A01).

NCEER-87-0007 "Instantaneous Optimal Control Laws for Tall Buildings Under Seismic Excitations," by J.N. Yang, A. Akbarpour and P. Ghaemmaghami, 6/10/87, (PB88-134333, A06, MF-A01). This report is only available through NTIS (see address given above).

NCEER-87-0008 "IDARC: Inelastic Damage Analysis of Reinforced Concrete Frame - Shear-Wall Structures," by Y.J. Park, A.M. Reinhorn and S.K. Kunnath, 7/20/87, (PB88-134325, A09, MF-A01). This report is only available through NTIS (see address given above).

NCEER-87-0009 "Liquefaction Potential for New York State: A Preliminary Report on Sites in Manhattan and Buffalo," by M. Budhu, V. Vijayakumar, R.F. Giese and L. Baumgras, 8/31/87, (PB88-163704, A03, MF-A01). This report is available only through NTIS (see address given above).

NCEER-87-0010 "Vertical and Torsional Vibration of Foundations in Inhomogeneous Media," by A.S. Veletsos and K.W. Dotson, 6/1/87, (PB88-134291, A03, MF-A01). This report is only available through NTIS (see address given above).

NCEER-87-0011 "Seismic Probabilistic Risk Assessment and Seismic Margins Studies for Nuclear Power Plants," by Howard H.M. Hwang, 6/15/87, (PB88-134267, A03, MF-A01). This report is only available through NTIS (see address given above).

NCEER-87-0012 "Parametric Studies of Frequency Response of Secondary Systems Under Ground-Acceleration Excitations," by Y. Yong and Y.K. Lin, 6/10/87, (PB88-134309, A03, MF-A01). This report is only available through NTIS (see address given above).

NCEER-87-0013 "Frequency Response of Secondary Systems Under Seismic Excitation," by J.A. HoLung, J. Cai and Y.K. Lin, 7/31/87, (PB88-134317, A05, MF-A01). This report is only available through NTIS (see address given above).

NCEER-87-0014 "Modelling Earthquake Ground Motions in Seismically Active Regions Using Parametric Time Series Methods," by G.W. Ellis and A.S. Cakmak, 8/25/87, (PB88-134283, A08, MF-A01). This report is only available through NTIS (see address given above).

NCEER-87-0015 "Detection and Assessment of Seismic Structural Damage," by E. DiPasquale and A.S. Cakmak, 8/25/87, (PB88-163712, A05, MF-A01). This report is only available through NTIS (see address given above).

NCEER-87-0016 "Pipeline Experiment at Parkfield, California," by J. Isenberg and E. Richardson, 9/15/87, (PB88-163720, A03, MF-A01). This report is available only through NTIS (see address given above).

NCEER-87-0017 "Digital Simulation of Seismic Ground Motion," by M. Shinozuka, G. Deodatis and T. Harada, 8/31/87, (PB88-155197, A04, MF-A01). This report is available only through NTIS (see address given above).

NCEER-87-0018 "Practical Considerations for Structural Control: System Uncertainty, System Time Delay and Truncation of Small Control Forces," J.N. Yang and A. Akbarpour, 8/10/87, (PB88-163738, A08, MF-A01). This report is only available through NTIS (see address given above).

NCEER-87-0019 "Modal Analysis of Nonclassically Damped Structural Systems Using Canonical Transformation," by J.N. Yang, S. Sarkani and F.X. Long, 9/27/87, (PB88-187851, A04, MF-A01).

NCEER-87-0020 "A Nonstationary Solution in Random Vibration Theory," by J.R. Red-Horse and P.D. Spanos, 11/3/87, (PB88-163746, A03, MF-A01).

NCEER-87-0021 "Horizontal Impedances for Radially Inhomogeneous Viscoelastic Soil Layers," by A.S. Veletsos and K.W. Dotson, 10/15/87, (PB88-150859, A04, MF-A01).

NCEER-87-0022 "Seismic Damage Assessment of Reinforced Concrete Members," by Y.S. Chung, C. Meyer and M. Shinozuka, 10/9/87, (PB88-150867, A05, MF-A01). This report is available only through NTIS (see address given above).

NCEER-87-0023 "Active Structural Control in Civil Engineering," by T.T. Soong, 11/11/87, (PB88-187778, A03, MF-A01).

NCEER-87-0024 "Vertical and Torsional Impedances for Radially Inhomogeneous Viscoelastic Soil Layers," by K.W. Dotson and A.S. Veletsos, 12/87, (PB88-187786, A03, MF-A01).

NCEER-87-0025 "Proceedings from the Symposium on Seismic Hazards, Ground Motions, Soil-Liquefaction and Engineering Practice in Eastern North America," October 20-22, 1987, edited by K.H. Jacob, 12/87, (PB88-188115, A23, MF-A01). This report is available only through NTIS (see address given above).

NCEER-87-0026 "Report on the Whittier-Narrows, California, Earthquake of October 1, 1987," by J. Pantelic and A. Reinhorn, 11/87, (PB88-187752, A03, MF-A01). This report is available only through NTIS (see address given above).

NCEER-87-0027 "Design of a Modular Program for Transient Nonlinear Analysis of Large 3-D Building Structures," by S. Srivastav and J.F. Abel, 12/30/87, (PB88-187950, A05, MF-A01). This report is only available through NTIS (see address given above).

NCEER-87-0028 "Second-Year Program in Research, Education and Technology Transfer," 3/8/88, (PB88-219480, A04, MF-A01).

NCEER-88-0001 "Workshop on Seismic Computer Analysis and Design of Buildings With Interactive Graphics," by W. McGuire, J.F. Abel and C.H. Conley, 1/18/88, (PB88-187760, A03, MF-A01). This report is only available through NTIS (see address given above).

NCEER-88-0002 "Optimal Control of Nonlinear Flexible Structures," by J.N. Yang, F.X. Long and D. Wong, 1/22/88, (PB88-213772, A06, MF-A01).

NCEER-88-0003 "Substructuring Techniques in the Time Domain for Primary-Secondary Structural Systems," by G.D. Manolis and G. Juhn, 2/10/88, (PB88-213780, A04, MF-A01).

NCEER-88-0004 "Iterative Seismic Analysis of Primary-Secondary Systems," by A. Singhal, L.D. Lutes and P.D. Spanos, 2/23/88, (PB88-213798, A04, MF-A01).

NCEER-88-0005 "Stochastic Finite Element Expansion for Random Media," by P.D. Spanos and R. Ghanem, 3/14/88, (PB88-213806, A03, MF-A01).

NCEER-88-0006 "Combining Structural Optimization and Structural Control," by F.Y. Cheng and C.P. Pantelides, 1/10/88, (PB88-213814, A05, MF-A01).

NCEER-88-0007 "Seismic Performance Assessment of Code-Designed Structures," by H.H-M. Hwang, J-W. Jaw and H-J. Shau, 3/20/88, (PB88-219423, A04, MF-A01). This report is only available through NTIS (see address given above).

NCEER-88-0008 "Reliability Analysis of Code-Designed Structures Under Natural Hazards," by H.H-M. Hwang, H. Ushiba and M. Shinozuka, 2/29/88, (PB88-229471, A07, MF-A01). This report is only available through NTIS (see address given above).

NCEER-88-0009 "Seismic Fragility Analysis of Shear Wall Structures," by J-W Jaw and H.H-M. Hwang, 4/30/88, (PB89-102867, A04, MF-A01).

NCEER-88-0010 "Base Isolation of a Multi-Story Building Under a Harmonic Ground Motion - A Comparison of Performances of Various Systems," by F-G Fan, G. Ahmadi and I.G. Tadjbakhsh, 5/18/88, (PB89-122238, A06, MF-A01). This report is only available through NTIS (see address given above).

NCEER-88-0011 "Seismic Floor Response Spectra for a Combined System by Green's Functions," by F.M. Lavelle, L.A. Bergman and P.D. Spanos, 5/1/88, (PB89-102875, A03, MF-A01).

NCEER-88-0012 "A New Solution Technique for Randomly Excited Hysteretic Structures," by G.Q. Cai and Y.K. Lin, 5/16/88, (PB89-102883, A03, MF-A01).

NCEER-88-0013 "A Study of Radiation Damping and Soil-Structure Interaction Effects in the Centrifuge," by K. Weissman, supervised by J.H. Prevost, 5/24/88, (PB89-144703, A06, MF-A01).

NCEER-88-0014 "Parameter Identification and Implementation of a Kinematic Plasticity Model for Frictional Soils," by J.H. Prevost and D.V. Griffiths, not available.

NCEER-88-0015 "Two- and Three- Dimensional Dynamic Finite Element Analyses of the Long Valley Dam," by D.V. Griffiths and J.H. Prevost, 6/17/88, (PB89-144711, A04, MF-A01).

NCEER-88-0016 "Damage Assessment of Reinforced Concrete Structures in Eastern United States," by A.M. Reinhorn, M.J. Seidel, S.K. Kunnath and Y.J. Park, 6/15/88, (PB89-122220, A04, MF-A01). This report is only available through NTIS (see address given above).

NCEER-88-0017 "Dynamic Compliance of Vertically Loaded Strip Foundations in Multilayered Viscoelastic Soils," by S. Ahmad and A.S.M. Israil, 6/17/88, (PB89-102891, A04, MF-A01).

NCEER-88-0018 "An Experimental Study of Seismic Structural Response With Added Viscoelastic Dampers," by R.C. Lin, Z. Liang, T.T. Soong and R.H. Zhang, 6/30/88, (PB89-122212, A05, MF-A01). This report is available only through NTIS (see address given above).

NCEER-88-0019 "Experimental Investigation of Primary - Secondary System Interaction," by G.D. Manolis, G. Juhn and A.M. Reinhorn, 5/27/88, (PB89-122204, A04, MF-A01).

NCEER-88-0020 "A Response Spectrum Approach For Analysis of Nonclassically Damped Structures," by J.N. Yang, S. Sarkani and F.X. Long, 4/22/88, (PB89-102909, A04, MF-A01).

NCEER-88-0021 "Seismic Interaction of Structures and Soils: Stochastic Approach," by A.S. Veletsos and A.M. Prasad, 7/21/88, (PB89-122196, A04, MF-A01). This report is only available through NTIS (see address given above).

NCEER-88-0022 "Identification of the Serviceability Limit State and Detection of Seismic Structural Damage," by E. DiPasquale and A.S. Cakmak, 6/15/88, (PB89-122188, A05, MF-A01). This report is available only through NTIS (see address given above).

NCEER-88-0023 "Multi-Hazard Risk Analysis: Case of a Simple Offshore Structure," by B.K. Bhartia and E.H. Vanmarcke, 7/21/88, (PB89-145213, A05, MF-A01).

NCEER-88-0024 "Automated Seismic Design of Reinforced Concrete Buildings," by Y.S. Chung, C. Meyer and M. Shinozuka, 7/5/88, (PB89-122170, A06, MF-A01). This report is available only through NTIS (see address given above).

NCEER-88-0025 "Experimental Study of Active Control of MDOF Structures Under Seismic Excitations," by L.L. Chung, R.C. Lin, T.T. Soong and A.M. Reinhorn, 7/10/88, (PB89-122600, A04, MF-A01).

NCEER-88-0026 "Earthquake Simulation Tests of a Low-Rise Metal Structure," by J.S. Hwang, K.C. Chang, G.C. Lee and R.L. Ketter, 8/1/88, (PB89-102917, A04, MF-A01).

NCEER-88-0027 "Systems Study of Urban Response and Reconstruction Due to Catastrophic Earthquakes," by F. Kozin and H.K. Zhou, 9/22/88, (PB90-162348, A04, MF-A01).

NCEER-88-0028 "Seismic Fragility Analysis of Plane Frame Structures," by H.H-M. Hwang and Y.K. Low, 7/31/88, (PB89-131445, A06, MF-A01).

NCEER-88-0029 "Response Analysis of Stochastic Structures," by A. Kardara, C. Bucher and M. Shinozuka, 9/22/88, (PB89-174429, A04, MF-A01).

NCEER-88-0030 "Nonnormal Accelerations Due to Yielding in a Primary Structure," by D.C.K. Chen and L.D. Lutes, 9/19/88, (PB89-131437, A04, MF-A01).

NCEER-88-0031 "Design Approaches for Soil-Structure Interaction," by A.S. Veletsos, A.M. Prasad and Y. Tang, 12/30/88, (PB89-174437, A03, MF-A01). This report is available only through NTIS (see address given above).

NCEER-88-0032 "A Re-evaluation of Design Spectra for Seismic Damage Control," by C.J. Turkstra and A.G. Tallin, 11/7/88, (PB89-145221, A05, MF-A01).

NCEER-88-0033 "The Behavior and Design of Noncontact Lap Splices Subjected to Repeated Inelastic Tensile Loading," by V.E. Sagan, P. Gergely and R.N. White, 12/8/88, (PB89-163737, A08, MF-A01).

NCEER-88-0034 "Seismic Response of Pile Foundations," by S.M. Mamoon, P.K. Banerjee and S. Ahmad, 11/1/88, (PB89-145239, A04, MF-A01).

NCEER-88-0035 "Modeling of R/C Building Structures With Flexible Floor Diaphragms (IDARC2)," by A.M. Reinhorn, S.K. Kunnath and N. Panahshahi, 9/7/88, (PB89-207153, A07, MF-A01).

NCEER-88-0036 "Solution of the Dam-Reservoir Interaction Problem Using a Combination of FEM, BEM with Particular Integrals, Modal Analysis, and Substructuring," by C-S. Tsai, G.C. Lee and R.L. Ketter, 12/31/88, (PB89-207146, A04, MF-A01).

NCEER-88-0037 "Optimal Placement of Actuators for Structural Control," by F.Y. Cheng and C.P. Pantelides, 8/15/88, (PB89-162846, A05, MF-A01).

NCEER-88-0038 "Teflon Bearings in Aseismic Base Isolation: Experimental Studies and Mathematical Modeling," by A. Mokha, M.C. Constantinou and A.M. Reinhorn, 12/5/88, (PB89-218457, A10, MF-A01). This report is available only through NTIS (see address given above).

NCEER-88-0039 "Seismic Behavior of Flat Slab High-Rise Buildings in the New York City Area," by P. Weidlinger and M. Ettouney, 10/15/88, (PB90-145681, A04, MF-A01).

NCEER-88-0040 "Evaluation of the Earthquake Resistance of Existing Buildings in New York City," by P. Weidlinger and M. Ettouney, 10/15/88, not available.

NCEER-88-0041 "Small-Scale Modeling Techniques for Reinforced Concrete Structures Subjected to Seismic Loads," by W. Kim, A. El-Attar and R.N. White, 11/22/88, (PB89-189625, A05, MF-A01).

NCEER-88-0042 "Modeling Strong Ground Motion from Multiple Event Earthquakes," by G.W. Ellis and A.S. Cakmak, 10/15/88, (PB89-174445, A03, MF-A01).

NCEER-88-0043 "Nonstationary Models of Seismic Ground Acceleration," by M. Grigoriu, S.E. Ruiz and E. Rosenblueth, 7/15/88, (PB89-189617, A04, MF-A01).

NCEER-88-0044 "SARCF User's Guide: Seismic Analysis of Reinforced Concrete Frames," by Y.S. Chung, C. Meyer and M. Shinozuka, 11/9/88, (PB89-174452, A08, MF-A01).

NCEER-88-0045 "First Expert Panel Meeting on Disaster Research and Planning," edited by J. Pantelic and J. Stoyle, 9/15/88, (PB89-174460, A05, MF-A01).

NCEER-88-0046 "Preliminary Studies of the Effect of Degrading Infill Walls on the Nonlinear Seismic Response of Steel Frames," by C.Z. Chrysostomou, P. Gergely and J.F. Abel, 12/19/88, (PB89-208383, A05, MF-A01).

NCEER-88-0047 "Reinforced Concrete Frame Component Testing Facility - Design, Construction, Instrumentation and Operation," by S.P. Pessiki, C. Conley, T. Bond, P. Gergely and R.N. White, 12/16/88, (PB89-174478, A04, MF-A01).

NCEER-89-0001 "Effects of Protective Cushion and Soil Compliancy on the Response of Equipment Within a Seismically Excited Building," by J.A. HoLung, 2/16/89, (PB89-207179, A04, MF-A01).

NCEER-89-0002 "Statistical Evaluation of Response Modification Factors for Reinforced Concrete Structures," by H.H-M. Hwang and J-W. Jaw, 2/17/89, (PB89-207187, A05, MF-A01).

NCEER-89-0003 "Hysteretic Columns Under Random Excitation," by G-Q. Cai and Y.K. Lin, 1/9/89, (PB89-196513, A03, MF-A01).

NCEER-89-0004 "Experimental Study of `Elephant Foot Bulge' Instability of Thin-Walled Metal Tanks," by Z-H. Jia and R.L. Ketter, 2/22/89, (PB89-207195, A03, MF-A01).

NCEER-89-0005 "Experiment on Performance of Buried Pipelines Across San Andreas Fault," by J. Isenberg, E. Richardson and T.D. O'Rourke, 3/10/89, (PB89-218440, A04, MF-A01). This report is available only through NTIS (see address given above).

NCEER-89-0006 "A Knowledge-Based Approach to Structural Design of Earthquake-Resistant Buildings," by M. Subramani, P. Gergely, C.H. Conley, J.F. Abel and A.H. Zaghw, 1/15/89, (PB89-218465, A06, MF-A01).

NCEER-89-0007 "Liquefaction Hazards and Their Effects on Buried Pipelines," by T.D. O'Rourke and P.A. Lane, 2/1/89, (PB89-218481, A09, MF-A01).

NCEER-89-0008 "Fundamentals of System Identification in Structural Dynamics," by H. Imai, C-B. Yun, O. Maruyama and M. Shinozuka, 1/26/89, (PB89-207211, A04, MF-A01).

NCEER-89-0009 "Effects of the 1985 Michoacan Earthquake on Water Systems and Other Buried Lifelines in Mexico," by A.G. Ayala and M.J. O'Rourke, 3/8/89, (PB89-207229, A06, MF-A01).

NCEER-89-R010 "NCEER Bibliography of Earthquake Education Materials," by K.E.K. Ross, Second Revision, 9/1/89, (PB90-125352, A05, MF-A01). This report is replaced by NCEER-92-0018.

NCEER-89-0011 "Inelastic Three-Dimensional Response Analysis of Reinforced Concrete Building Structures (IDARC-3D), Part I - Modeling," by S.K. Kunnath and A.M. Reinhorn, 4/17/89, (PB90-114612, A07, MF-A01). This report is available only through NTIS (see address given above).

NCEER-89-0012 "Recommended Modifications to ATC-14," by C.D. Poland and J.O. Malley, 4/12/89, (PB90-108648, A15, MF-A01).

NCEER-89-0013 "Repair and Strengthening of Beam-to-Column Connections Subjected to Earthquake Loading," by M. Corazao and A.J. Durrani, 2/28/89, (PB90-109885, A06, MF-A01).

NCEER-89-0014 "Program EXKAL2 for Identification of Structural Dynamic Systems," by O. Maruyama, C-B. Yun, M. Hoshiya and M. Shinozuka, 5/19/89, (PB90-109877, A09, MF-A01).

NCEER-89-0015 "Response of Frames With Bolted Semi-Rigid Connections, Part I - Experimental Study and Analytical Predictions," by P.J. DiCorso, A.M. Reinhorn, J.R. Dickerson, J.B. Radziminski and W.L. Harper, 6/1/89, not available.

NCEER-89-0016 "ARMA Monte Carlo Simulation in Probabilistic Structural Analysis," by P.D. Spanos and M.P. Mignolet, 7/10/89, (PB90-109893, A03, MF-A01).

NCEER-89-P017 "Preliminary Proceedings from the Conference on Disaster Preparedness - The Place of Earthquake Education in Our Schools," Edited by K.E.K. Ross, 6/23/89, (PB90-108606, A03, MF-A01).

NCEER-89-0017 "Proceedings from the Conference on Disaster Preparedness - The Place of Earthquake Education in Our Schools," Edited by K.E.K. Ross, 12/31/89, (PB90-207895, A012, MF-A02). This report is available only through NTIS (see address given above).

NCEER-89-0018 "Multidimensional Models of Hysteretic Material Behavior for Vibration Analysis of Shape Memory Energy Absorbing Devices, by E.J. Graesser and F.A. Cozzarelli, 6/7/89, (PB90-164146, A04, MF-A01).

NCEER-89-0019 "Nonlinear Dynamic Analysis of Three-Dimensional Base Isolated Structures (3D-BASIS)," by S. Nagarajaiah, A.M. Reinhorn and M.C. Constantinou, 8/3/89, (PB90-161936, A06, MF-A01). This report has been replaced by NCEER-93-0011.

NCEER-89-0020 "Structural Control Considering Time-Rate of Control Forces and Control Rate Constraints," by F.Y. Cheng and C.P. Pantelides, 8/3/89, (PB90-120445, A04, MF-A01).

NCEER-89-0021 "Subsurface Conditions of Memphis and Shelby County," by K.W. Ng, T-S. Chang and H-H.M. Hwang, 7/26/89, (PB90-120437, A03, MF-A01).

NCEER-89-0022 "Seismic Wave Propagation Effects on Straight Jointed Buried Pipelines," by K. Elhmadi and M.J. O'Rourke, 8/24/89, (PB90-162322, A10, MF-A02).

NCEER-89-0023 "Workshop on Serviceability Analysis of Water Delivery Systems," edited by M. Grigoriu, 3/6/89, (PB90-127424, A03, MF-A01).

NCEER-89-0024 "Shaking Table Study of a 1/5 Scale Steel Frame Composed of Tapered Members," by K.C. Chang, J.S. Hwang and G.C. Lee, 9/18/89, (PB90-160169, A04, MF-A01).

NCEER-89-0025 "DYNA1D: A Computer Program for Nonlinear Seismic Site Response Analysis - Technical Documentation," by Jean H. Prevost, 9/14/89, (PB90-161944, A07, MF-A01). This report is available only through NTIS (see address given above).

NCEER-89-0026 "1:4 Scale Model Studies of Active Tendon Systems and Active Mass Dampers for Aseismic Protection," by A.M. Reinhorn, T.T. Soong, R.C. Lin, Y.P. Yang, Y. Fukao, H. Abe and M. Nakai, 9/15/89, (PB90-173246, A10, MF-A02). This report is available only through NTIS (see address given above).

NCEER-89-0027 "Scattering of Waves by Inclusions in a Nonhomogeneous Elastic Half Space Solved by Boundary Element Methods," by P.K. Hadley, A. Askar and A.S. Cakmak, 6/15/89, (PB90-145699, A07, MF-A01).

NCEER-89-0028 "Statistical Evaluation of Deflection Amplification Factors for Reinforced Concrete Structures," by H.H.M. Hwang, J-W. Jaw and A.L. Ch'ng, 8/31/89, (PB90-164633, A05, MF-A01).

NCEER-89-0029 "Bedrock Accelerations in Memphis Area Due to Large New Madrid Earthquakes," by H.H.M. Hwang, C.H.S. Chen and G. Yu, 11/7/89, (PB90-162330, A04, MF-A01).

NCEER-89-0030 "Seismic Behavior and Response Sensitivity of Secondary Structural Systems," by Y.Q. Chen and T.T. Soong, 10/23/89, (PB90-164658, A08, MF-A01).

NCEER-89-0031 "Random Vibration and Reliability Analysis of Primary-Secondary Structural Systems," by Y. Ibrahim, M. Grigoriu and T.T. Soong, 11/10/89, (PB90-161951, A04, MF-A01).

NCEER-89-0032 "Proceedings from the Second U.S. - Japan Workshop on Liquefaction, Large Ground Deformation and Their Effects on Lifelines, September 26-29, 1989," Edited by T.D. O'Rourke and M. Hamada, 12/1/89, (PB90-209388, A22, MF-A03).

NCEER-89-0033 "Deterministic Model for Seismic Damage Evaluation of Reinforced Concrete Structures," by J.M. Bracci, A.M. Reinhorn, J.B. Mander and S.K. Kunnath, 9/27/89, (PB91-108803, A06, MF-A01).

NCEER-89-0034 "On the Relation Between Local and Global Damage Indices," by E. DiPasquale and A.S. Cakmak, 8/15/89, (PB90-173865, A05, MF-A01).

NCEER-89-0035 "Cyclic Undrained Behavior of Nonplastic and Low Plasticity Silts," by A.J. Walker and H.E. Stewart, 7/26/89, (PB90-183518, A10, MF-A01).

NCEER-89-0036 "Liquefaction Potential of Surficial Deposits in the City of Buffalo, New York," by M. Budhu, R. Giese and L. Baumgrass, 1/17/89, (PB90-208455, A04, MF-A01).

NCEER-89-0037 "A Deterministic Assessment of Effects of Ground Motion Incoherence," by A.S. Veletsos and Y. Tang, 7/15/89, (PB90-164294, A03, MF-A01).

NCEER-89-0038 "Workshop on Ground Motion Parameters for Seismic Hazard Mapping," July 17-18, 1989, edited by R.V. Whitman, 12/1/89, (PB90-173923, A04, MF-A01).

NCEER-89-0039 "Seismic Effects on Elevated Transit Lines of the New York City Transit Authority," by C.J. Costantino, C.A. Miller and E. Heymsfield, 12/26/89, (PB90-207887, A06, MF-A01).

NCEER-89-0040 "Centrifugal Modeling of Dynamic Soil-Structure Interaction," by K. Weissman, Supervised by J.H. Prevost, 5/10/89, (PB90-207879, A07, MF-A01).

NCEER-89-0041 "Linearized Identification of Buildings With Cores for Seismic Vulnerability Assessment," by I-K. Ho and A.E. Aktan, 11/1/89, (PB90-251943, A07, MF-A01).

NCEER-90-0001 "Geotechnical and Lifeline Aspects of the October 17, 1989 Loma Prieta Earthquake in San Francisco," by T.D. O'Rourke, H.E. Stewart, F.T. Blackburn and T.S. Dickerman, 1/90, (PB90-208596, A05, MF-A01).

NCEER-90-0002 "Nonnormal Secondary Response Due to Yielding in a Primary Structure," by D.C.K. Chen and L.D. Lutes, 2/28/90, (PB90-251976, A07, MF-A01).

NCEER-90-0003 "Earthquake Education Materials for Grades K-12," by K.E.K. Ross, 4/16/90, (PB91-251984, A05, MF-A05). This report has been replaced by NCEER-92-0018.

NCEER-90-0004 "Catalog of Strong Motion Stations in Eastern North America," by R.W. Busby, 4/3/90, (PB90-251984, A05, MF-A01).

NCEER-90-0005 "NCEER Strong-Motion Data Base: A User Manual for the GeoBase Release (Version 1.0 for the Sun3)," by P. Friberg and K. Jacob, 3/31/90 (PB90-258062, A04, MF-A01).

NCEER-90-0006 "Seismic Hazard Along a Crude Oil Pipeline in the Event of an 1811-1812 Type New Madrid Earthquake," by H.H.M. Hwang and C-H.S. Chen, 4/16/90, (PB90-258054, A04, MF-A01).

NCEER-90-0007 "Site-Specific Response Spectra for Memphis Sheahan Pumping Station," by H.H.M. Hwang and C.S. Lee, 5/15/90, (PB91-108811, A05, MF-A01).

NCEER-90-0008 "Pilot Study on Seismic Vulnerability of Crude Oil Transmission Systems," by T. Ariman, R. Dobry, M. Grigoriu, F. Kozin, M. O'Rourke, T. O'Rourke and M. Shinozuka, 5/25/90, (PB91-108837, A06, MF-A01).

NCEER-90-0009 "A Program to Generate Site Dependent Time Histories: EQGEN," by G.W. Ellis, M. Srinivasan and A.S. Cakmak, 1/30/90, (PB91-108829, A04, MF-A01).

NCEER-90-0010 "Active Isolation for Seismic Protection of Operating Rooms," by M.E. Talbott, Supervised by M. Shinozuka, 6/8/9, (PB91-110205, A05, MF-A01).

NCEER-90-0011 "Program LINEARID for Identification of Linear Structural Dynamic Systems," by C-B. Yun and M. Shinozuka, 6/25/90, (PB91-110312, A08, MF-A01).

NCEER-90-0012 "Two-Dimensional Two-Phase Elasto-Plastic Seismic Response of Earth Dams," by A.N. Yiagos, Supervised by J.H. Prevost, 6/20/90, (PB91-110197, A13, MF-A02).

NCEER-90-0013 "Secondary Systems in Base-Isolated Structures: Experimental Investigation, Stochastic Response and Stochastic Sensitivity," by G.D. Manolis, G. Juhn, M.C. Constantinou and A.M. Reinhorn, 7/1/90, (PB91-110320, A08, MF-A01).

NCEER-90-0014 "Seismic Behavior of Lightly-Reinforced Concrete Column and Beam-Column Joint Details," by S.P. Pessiki, C.H. Conley, P. Gergely and R.N. White, 8/22/90, (PB91-108795, A11, MF-A02).

NCEER-90-0015 "Two Hybrid Control Systems for Building Structures Under Strong Earthquakes," by J.N. Yang and A. Danielians, 6/29/90, (PB91-125393, A04, MF-A01).

NCEER-90-0016 "Instantaneous Optimal Control with Acceleration and Velocity Feedback," by J.N. Yang and Z. Li, 6/29/90, (PB91-125401, A03, MF-A01).

NCEER-90-0017 "Reconnaissance Report on the Northern Iran Earthquake of June 21, 1990," by M. Mehrain, 10/4/90, (PB91-125377, A03, MF-A01).

NCEER-90-0018 "Evaluation of Liquefaction Potential in Memphis and Shelby County," by T.S. Chang, P.S. Tang, C.S. Lee and H. Hwang, 8/10/90, (PB91-125427, A09, MF-A01).

NCEER-90-0019 "Experimental and Analytical Study of a Combined Sliding Disc Bearing and Helical Steel Spring Isolation System," by M.C. Constantinou, A.S. Mokha and A.M. Reinhorn, 10/4/90, (PB91-125385, A06, MF-A01). This report is available only through NTIS (see address given above).

NCEER-90-0020 "Experimental Study and Analytical Prediction of Earthquake Response of a Sliding Isolation System with a Spherical Surface," by A.S. Mokha, M.C. Constantinou and A.M. Reinhorn, 10/11/90, (PB91-125419, A05, MF-A01).

NCEER-90-0021 "Dynamic Interaction Factors for Floating Pile Groups," by G. Gazetas, K. Fan, A. Kaynia and E. Kausel, 9/10/90, (PB91-170381, A05, MF-A01).

NCEER-90-0022 "Evaluation of Seismic Damage Indices for Reinforced Concrete Structures," by S. Rodriguez-Gomez and A.S. Cakmak, 9/30/90, PB91-171322, A06, MF-A01).

NCEER-90-0023 "Study of Site Response at a Selected Memphis Site," by H. Desai, S. Ahmad, E.S. Gazetas and M.R. Oh, 10/11/90, (PB91-196857, A03, MF-A01).

NCEER-90-0024 "A User's Guide to Strongmo: Version 1.0 of NCEER's Strong-Motion Data Access Tool for PCs and Terminals," by P.A. Friberg and C.A.T. Susch, 11/15/90, (PB91-171272, A03, MF-A01).

NCEER-90-0025 "A Three-Dimensional Analytical Study of Spatial Variability of Seismic Ground Motions," by L-L. Hong and A.H.-S. Ang, 10/30/90, (PB91-170399, A09, MF-A01).

NCEER-90-0026 "MUMOID User's Guide - A Program for the Identification of Modal Parameters," by S. Rodriguez-Gomez and E. DiPasquale, 9/30/90, (PB91-171298, A04, MF-A01).

NCEER-90-0027 "SARCF-II User's Guide - Seismic Analysis of Reinforced Concrete Frames," by S. Rodriguez-Gomez, Y.S. Chung and C. Meyer, 9/30/90, (PB91-171280, A05, MF-A01).

NCEER-90-0028 "Viscous Dampers: Testing, Modeling and Application in Vibration and Seismic Isolation," by N. Makris and M.C. Constantinou, 12/20/90 (PB91-190561, A06, MF-A01).

NCEER-90-0029 "Soil Effects on Earthquake Ground Motions in the Memphis Area," by H. Hwang, C.S. Lee, K.W. Ng and T.S. Chang, 8/2/90, (PB91-190751, A05, MF-A01).

NCEER-91-0001 "Proceedings from the Third Japan-U.S. Workshop on Earthquake Resistant Design of Lifeline Facilities and Countermeasures for Soil Liquefaction, December 17-19, 1990," edited by T.D. O'Rourke and M. Hamada, 2/1/91, (PB91-179259, A99, MF-A04).

NCEER-91-0002 "Physical Space Solutions of Non-Proportionally Damped Systems," by M. Tong, Z. Liang and G.C. Lee, 1/15/91, (PB91-179242, A04, MF-A01).

NCEER-91-0003 "Seismic Response of Single Piles and Pile Groups," by K. Fan and G. Gazetas, 1/10/91, (PB92-174994, A04, MF-A01).

NCEER-91-0004 "Damping of Structures: Part 1 - Theory of Complex Damping," by Z. Liang and G. Lee, 10/10/91, (PB92-197235, A12, MF-A03).

NCEER-91-0005 "3D-BASIS - Nonlinear Dynamic Analysis of Three Dimensional Base Isolated Structures: Part II," by S. Nagarajaiah, A.M. Reinhorn and M.C. Constantinou, 2/28/91, (PB91-190553, A07, MF-A01). This report has been replaced by NCEER-93-0011.

NCEER-91-0006 "A Multidimensional Hysteretic Model for Plasticity Deforming Metals in Energy Absorbing Devices," by E.J. Graesser and F.A. Cozzarelli, 4/9/91, (PB92-108364, A04, MF-A01).

NCEER-91-0007 "A Framework for Customizable Knowledge-Based Expert Systems with an Application to a KBES for Evaluating the Seismic Resistance of Existing Buildings," by E.G. Ibarra-Anaya and S.J. Fenves, 4/9/91, (PB91-210930, A08, MF-A01).

NCEER-91-0008 "Nonlinear Analysis of Steel Frames with Semi-Rigid Connections Using the Capacity Spectrum Method," by G.G. Deierlein, S-H. Hsieh, Y-J. Shen and J.F. Abel, 7/2/91, (PB92-113828, A05, MF-A01).

NCEER-91-0009 "Earthquake Education Materials for Grades K-12," by K.E.K. Ross, 4/30/91, (PB91-212142, A06, MF-A01). This report has been replaced by NCEER-92-0018.

NCEER-91-0010 "Phase Wave Velocities and Displacement Phase Differences in a Harmonically Oscillating Pile," by N. Makris and G. Gazetas, 7/8/91, (PB92-108356, A04, MF-A01).

NCEER-91-0011 "Dynamic Characteristics of a Full-Size Five-Story Steel Structure and a 2/5 Scale Model," by K.C. Chang, G.C. Yao, G.C. Lee, D.S. Hao and Y.C. Yeh," 7/2/91, (PB93-116648, A06, MF-A02).

NCEER-91-0012 "Seismic Response of a 2/5 Scale Steel Structure with Added Viscoelastic Dampers," by K.C. Chang, T.T. Soong, S-T. Oh and M.L. Lai, 5/17/91, (PB92-110816, A05, MF-A01).

NCEER-91-0013 "Earthquake Response of Retaining Walls; Full-Scale Testing and Computational Modeling," by S. Alampalli and A-W.M. Elgamal, 6/20/91, not available.

NCEER-91-0014 "3D-BASIS-M: Nonlinear Dynamic Analysis of Multiple Building Base Isolated Structures," by P.C. Tsopelas, S. Nagarajaiah, M.C. Constantinou and A.M. Reinhorn, 5/28/91, (PB92-113885, A09, MF-A02).

NCEER-91-0015 "Evaluation of SEAOC Design Requirements for Sliding Isolated Structures," by D. Theodossiou and M.C. Constantinou, 6/10/91, (PB92-114602, A11, MF-A03).

NCEER-91-0016 "Closed-Loop Modal Testing of a 27-Story Reinforced Concrete Flat Plate-Core Building," by H.R. Somaprasad, T. Toksoy, H. Yoshiyuki and A.E. Aktan, 7/15/91, (PB92-129980, A07, MF-A02).

NCEER-91-0017 "Shake Table Test of a 1/6 Scale Two-Story Lightly Reinforced Concrete Building," by A.G. El-Attar, R.N. White and P. Gergely, 2/28/91, (PB92-222447, A06, MF-A02).

NCEER-91-0018 "Shake Table Test of a 1/8 Scale Three-Story Lightly Reinforced Concrete Building," by A.G. El-Attar, R.N. White and P. Gergely, 2/28/91, (PB93-116630, A08, MF-A02).

NCEER-91-0019 "Transfer Functions for Rigid Rectangular Foundations," by A.S. Veletsos, A.M. Prasad and W.H. Wu, 7/31/91, not available.

NCEER-91-0020 "Hybrid Control of Seismic-Excited Nonlinear and Inelastic Structural Systems," by J.N. Yang, Z. Li and A. Danielians, 8/1/91, (PB92-143171, A06, MF-A02).

NCEER-91-0021 "The NCEER-91 Earthquake Catalog: Improved Intensity-Based Magnitudes and Recurrence Relations for U.S. Earthquakes East of New Madrid," by L. Seeber and J.G. Armbruster, 8/28/91, (PB92-176742, A06, MF-A02).

NCEER-91-0022 "Proceedings from the Implementation of Earthquake Planning and Education in Schools: The Need for Change - The Roles of the Changemakers," by K.E.K. Ross and F. Winslow, 7/23/91, (PB92-129998, A12, MF-A03).

NCEER-91-0023 "A Study of Reliability-Based Criteria for Seismic Design of Reinforced Concrete Frame Buildings," by H.H.M. Hwang and H-M. Hsu, 8/10/91, (PB92-140235, A09, MF-A02).

NCEER-91-0024 "Experimental Verification of a Number of Structural System Identification Algorithms," by R.G. Ghanem, H. Gavin and M. Shinozuka, 9/18/91, (PB92-176577, A18, MF-A04).

NCEER-91-0025 "Probabilistic Evaluation of Liquefaction Potential," by H.H.M. Hwang and C.S. Lee," 11/25/91, (PB92-143429, A05, MF-A01).

NCEER-91-0026 "Instantaneous Optimal Control for Linear, Nonlinear and Hysteretic Structures - Stable Controllers," by J.N. Yang and Z. Li, 11/15/91, (PB92-163807, A04, MF-A01).

NCEER-91-0027 "Experimental and Theoretical Study of a Sliding Isolation System for Bridges," by M.C. Constantinou, A. Kartoum, A.M. Reinhorn and P. Bradford, 11/15/91, (PB92-176973, A10, MF-A03).

NCEER-92-0001 "Case Studies of Liquefaction and Lifeline Performance During Past Earthquakes, Volume 1: Japanese Case Studies," Edited by M. Hamada and T. O'Rourke, 2/17/92, (PB92-197243, A18, MF-A04).

NCEER-92-0002 "Case Studies of Liquefaction and Lifeline Performance During Past Earthquakes, Volume 2: United States Case Studies," Edited by T. O'Rourke and M. Hamada, 2/17/92, (PB92-197250, A20, MF-A04).

NCEER-92-0003 "Issues in Earthquake Education," Edited by K. Ross, 2/3/92, (PB92-222389, A07, MF-A02).

NCEER-92-0004 "Proceedings from the First U.S. - Japan Workshop on Earthquake Protective Systems for Bridges," Edited by I.G. Buckle, 2/4/92, (PB94-142239, A99, MF-A06).

NCEER-92-0005 "Seismic Ground Motion from a Haskell-Type Source in a Multiple-Layered Half-Space," A.P. Theoharis, G. Deodatis and M. Shinozuka, 1/2/92, not available.

NCEER-92-0006 "Proceedings from the Site Effects Workshop," Edited by R. Whitman, 2/29/92, (PB92-197201, A04, MF-A01).

NCEER-92-0007 "Engineering Evaluation of Permanent Ground Deformations Due to Seismically-Induced Liquefaction," by M.H. Baziar, R. Dobry and A-W.M. Elgamal, 3/24/92, (PB92-222421, A13, MF-A03).

NCEER-92-0008 "A Procedure for the Seismic Evaluation of Buildings in the Central and Eastern United States," by C.D. Poland and J.O. Malley, 4/2/92, (PB92-222439, A20, MF-A04).

NCEER-92-0009 "Experimental and Analytical Study of a Hybrid Isolation System Using Friction Controllable Sliding Bearings," by M.Q. Feng, S. Fujii and M. Shinozuka, 5/15/92, (PB93-150282, A06, MF-A02).

NCEER-92-0010 "Seismic Resistance of Slab-Column Connections in Existing Non-Ductile Flat-Plate Buildings," by A.J. Durrani and Y. Du, 5/18/92, (PB93-116812, A06, MF-A02).

NCEER-92-0011 "The Hysteretic and Dynamic Behavior of Brick Masonry Walls Upgraded by Ferrocement Coatings Under Cyclic Loading and Strong Simulated Ground Motion," by H. Lee and S.P. Prawel, 5/11/92, not available.

NCEER-92-0012 "Study of Wire Rope Systems for Seismic Protection of Equipment in Buildings," by G.F. Demetriades, M.C. Constantinou and A.M. Reinhorn, 5/20/92, (PB93-116655, A08, MF-A02).

NCEER-92-0013 "Shape Memory Structural Dampers: Material Properties, Design and Seismic Testing," by P.R. Witting and F.A. Cozzarelli, 5/26/92, (PB93-116663, A05, MF-A01).

NCEER-92-0014 "Longitudinal Permanent Ground Deformation Effects on Buried Continuous Pipelines," by M.J. O'Rourke, and C. Nordberg, 6/15/92, (PB93-116671, A08, MF-A02).

NCEER-92-0015 "A Simulation Method for Stationary Gaussian Random Functions Based on the Sampling Theorem," by M. Grigoriu and S. Balopoulou, 6/11/92, (PB93-127496, A05, MF-A01).

NCEER-92-0016 "Gravity-Load-Designed Reinforced Concrete Buildings: Seismic Evaluation of Existing Construction and Detailing Strategies for Improved Seismic Resistance," by G.W. Hoffmann, S.K. Kunnath, A.M. Reinhorn and J.B. Mander, 7/15/92, (PB94-142007, A08, MF-A02).

NCEER-92-0017 "Observations on Water System and Pipeline Performance in the Limón Area of Costa Rica Due to the April 22, 1991 Earthquake," by M. O'Rourke and D. Ballantyne, 6/30/92, (PB93-126811, A06, MF-A02).

NCEER-92-0018 "Fourth Edition of Earthquake Education Materials for Grades K-12," Edited by K.E.K. Ross, 8/10/92, (PB93-114023, A07, MF-A02).

NCEER-92-0019 "Proceedings from the Fourth Japan-U.S. Workshop on Earthquake Resistant Design of Lifeline Facilities and Countermeasures for Soil Liquefaction," Edited by M. Hamada and T.D. O'Rourke, 8/12/92, (PB93-163939, A99, MF-E11).

NCEER-92-0020 "Active Bracing System: A Full Scale Implementation of Active Control," by A.M. Reinhorn, T.T. Soong, R.C. Lin, M.A. Riley, Y.P. Wang, S. Aizawa and M. Higashino, 8/14/92, (PB93-127512, A06, MF-A02).

NCEER-92-0021 "Empirical Analysis of Horizontal Ground Displacement Generated by Liquefaction-Induced Lateral Spreads," by S.F. Bartlett and T.L. Youd, 8/17/92, (PB93-188241, A06, MF-A02).

NCEER-92-0022 "IDARC Version 3.0: Inelastic Damage Analysis of Reinforced Concrete Structures," by S.K. Kunnath, A.M. Reinhorn and R.F. Lobo, 8/31/92, (PB93-227502, A07, MF-A02).

NCEER-92-0023 "A Semi-Empirical Analysis of Strong-Motion Peaks in Terms of Seismic Source, Propagation Path and Local Site Conditions, by M. Kamiyama, M.J. O'Rourke and R. Flores-Berrones, 9/9/92, (PB93-150266, A08, MF-A02).

NCEER-92-0024 "Seismic Behavior of Reinforced Concrete Frame Structures with Nonductile Details, Part I: Summary of Experimental Findings of Full Scale Beam-Column Joint Tests," by A. Beres, R.N. White and P. Gergely, 9/30/92, (PB93-227783, A05, MF-A01).

NCEER-92-0025 "Experimental Results of Repaired and Retrofitted Beam-Column Joint Tests in Lightly Reinforced Concrete Frame Buildings," by A. Beres, S. El-Borgi, R.N. White and P. Gergely, 10/29/92, (PB93-227791, A05, MF-A01).

NCEER-92-0026 "A Generalization of Optimal Control Theory: Linear and Nonlinear Structures," by J.N. Yang, Z. Li and S. Vongchavalitkul, 11/2/92, (PB93-188621, A05, MF-A01).

NCEER-92-0027 "Seismic Resistance of Reinforced Concrete Frame Structures Designed Only for Gravity Loads: Part I - Design and Properties of a One-Third Scale Model Structure," by J.M. Bracci, A.M. Reinhorn and J.B. Mander, 12/1/92, (PB94-104502, A08, MF-A02).

NCEER-92-0028 "Seismic Resistance of Reinforced Concrete Frame Structures Designed Only for Gravity Loads: Part II - Experimental Performance of Subassemblages," by L.E. Aycardi, J.B. Mander and A.M. Reinhorn, 12/1/92, (PB94-104510, A08, MF-A02).

NCEER-92-0029 "Seismic Resistance of Reinforced Concrete Frame Structures Designed Only for Gravity Loads: Part III - Experimental Performance and Analytical Study of a Structural Model," by J.M. Bracci, A.M. Reinhorn and J.B. Mander, 12/1/92, (PB93-227528, A09, MF-A01).

NCEER-92-0030 "Evaluation of Seismic Retrofit of Reinforced Concrete Frame Structures: Part I - Experimental Performance of Retrofitted Subassemblages," by D. Choudhuri, J.B. Mander and A.M. Reinhorn, 12/8/92, (PB93-198307, A07, MF-A02).

NCEER-92-0031 "Evaluation of Seismic Retrofit of Reinforced Concrete Frame Structures: Part II - Experimental Performance and Analytical Study of a Retrofitted Structural Model," by J.M. Bracci, A.M. Reinhorn and J.B. Mander, 12/8/92, (PB93-198315, A09, MF-A03).

NCEER-92-0032 "Experimental and Analytical Investigation of Seismic Response of Structures with Supplemental Fluid Viscous Dampers," by M.C. Constantinou and M.D. Symans, 12/21/92, (PB93-191435, A10, MF-A03). This report is available only through NTIS (see address given above).

NCEER-92-0033 "Reconnaissance Report on the Cairo, Egypt Earthquake of October 12, 1992," by M. Khater, 12/23/92, (PB93-188621, A03, MF-A01).

NCEER-92-0034 "Low-Level Dynamic Characteristics of Four Tall Flat-Plate Buildings in New York City," by H. Gavin, S. Yuan, J. Grossman, E. Pekelis and K. Jacob, 12/28/92, (PB93-188217, A07, MF-A02).

NCEER-93-0001 "An Experimental Study on the Seismic Performance of Brick-Infilled Steel Frames With and Without Retrofit," by J.B. Mander, B. Nair, K. Wojtkowski and J. Ma, 1/29/93, (PB93-227510, A07, MF-A02).

NCEER-93-0002 "Social Accounting for Disaster Preparedness and Recovery Planning," by S. Cole, E. Pantoja and V. Razak, 2/22/93, (PB94-142114, A12, MF-A03).

NCEER-93-0003 "Assessment of 1991 NEHRP Provisions for Nonstructural Components and Recommended Revisions," by T.T. Soong, G. Chen, Z. Wu, R-H. Zhang and M. Grigoriu, 3/1/93, (PB93-188639, A06, MF-A02).

NCEER-93-0004 "Evaluation of Static and Response Spectrum Analysis Procedures of SEAOC/UBC for Seismic Isolated Structures," by C.W. Winters and M.C. Constantinou, 3/23/93, (PB93-198299, A10, MF-A03).

NCEER-93-0005 "Earthquakes in the Northeast - Are We Ignoring the Hazard? A Workshop on Earthquake Science and Safety for Educators," edited by K.E.K. Ross, 4/2/93, (PB94-103066, A09, MF-A02).

NCEER-93-0006 "Inelastic Response of Reinforced Concrete Structures with Viscoelastic Braces," by R.F. Lobo, J.M. Bracci, K.L. Shen, A.M. Reinhorn and T.T. Soong, 4/5/93, (PB93-227486, A05, MF-A02).

NCEER-93-0007 "Seismic Testing of Installation Methods for Computers and Data Processing Equipment," by K. Kosar, T.T. Soong, K.L. Shen, J.A. HoLung and Y.K. Lin, 4/12/93, (PB93-198299, A07, MF-A02).

NCEER-93-0008 "Retrofit of Reinforced Concrete Frames Using Added Dampers," by A. Reinhorn, M. Constantinou and C. Li, not available.

NCEER-93-0009 "Seismic Behavior and Design Guidelines for Steel Frame Structures with Added Viscoelastic Dampers," by K.C. Chang, M.L. Lai, T.T. Soong, D.S. Hao and Y.C. Yeh, 5/1/93, (PB94-141959, A07, MF-A02).

NCEER-93-0010 "Seismic Performance of Shear-Critical Reinforced Concrete Bridge Piers," by J.B. Mander, S.M. Waheed, M.T.A. Chaudhary and S.S. Chen, 5/12/93, (PB93-227494, A08, MF-A02).

NCEER-93-0011 "3D-BASIS-TABS: Computer Program for Nonlinear Dynamic Analysis of Three Dimensional Base Isolated Structures," by S. Nagarajaiah, C. Li, A.M. Reinhorn and M.C. Constantinou, 8/2/93, (PB94-141819, A09, MF-A02).

NCEER-93-0012 "Effects of Hydrocarbon Spills from an Oil Pipeline Break on Ground Water," by O.J. Helweg and H.H.M. Hwang, 8/3/93, (PB94-141942, A06, MF-A02).

NCEER-93-0013 "Simplified Procedures for Seismic Design of Nonstructural Components and Assessment of Current Code Provisions," by M.P. Singh, L.E. Suarez, E.E. Matheu and G.O. Maldonado, 8/4/93, (PB94-141827, A09, MF-A02).

NCEER-93-0014 "An Energy Approach to Seismic Analysis and Design of Secondary Systems," by G. Chen and T.T. Soong, 8/6/93, (PB94-142767, A11, MF-A03).

NCEER-93-0015 "Proceedings from School Sites: Becoming Prepared for Earthquakes - Commemorating the Third Anniversary of the Loma Prieta Earthquake," Edited by F.E. Winslow and K.E.K. Ross, 8/16/93, (PB94-154275, A16, MF-A02).

NCEER-93-0016 "Reconnaissance Report of Damage to Historic Monuments in Cairo, Egypt Following the October 12, 1992 Dahshur Earthquake," by D. Sykora, D. Look, G. Croci, E. Karaesmen and E. Karaesmen, 8/19/93, (PB94-142221, A08, MF-A02).

NCEER-93-0017 "The Island of Guam Earthquake of August 8, 1993," by S.W. Swan and S.K. Harris, 9/30/93, (PB94-141843, A04, MF-A01).

NCEER-93-0018 "Engineering Aspects of the October 12, 1992 Egyptian Earthquake," by A.W. Elgamal, M. Amer, K. Adalier and A. Abul-Fadl, 10/7/93, (PB94-141983, A05, MF-A01).

NCEER-93-0019 "Development of an Earthquake Motion Simulator and its Application in Dynamic Centrifuge Testing," by I. Krstelj, Supervised by J.H. Prevost, 10/23/93, (PB94-181773, A-10, MF-A03).

NCEER-93-0020 "NCEER-Taisei Corporation Research Program on Sliding Seismic Isolation Systems for Bridges: Experimental and Analytical Study of a Friction Pendulum System (FPS)," by M.C. Constantinou, P. Tsopelas, Y-S. Kim and S. Okamoto, 11/1/93, (PB94-142775, A08, MF-A02).

NCEER-93-0021 "Finite Element Modeling of Elastomeric Seismic Isolation Bearings," by L.J. Billings, Supervised by R. Shepherd, 11/8/93, not available.

NCEER-93-0022 "Seismic Vulnerability of Equipment in Critical Facilities: Life-Safety and Operational Consequences," by K. Porter, G.S. Johnson, M.M. Zadeh, C. Scawthorn and S. Eder, 11/24/93, (PB94-181765, A16, MF-A03).

NCEER-93-0023 "Hokkaido Nansei-oki, Japan Earthquake of July 12, 1993, by P.I. Yanev and C.R. Scawthorn, 12/23/93, (PB94-181500, A07, MF-A01).

NCEER-94-0001 "An Evaluation of Seismic Serviceability of Water Supply Networks with Application to the San Francisco Auxiliary Water Supply System," by I. Markov, Supervised by M. Grigoriu and T. O'Rourke, 1/21/94, (PB94-204013, A07, MF-A02).

NCEER-94-0002 "NCEER-Taisei Corporation Research Program on Sliding Seismic Isolation Systems for Bridges: Experimental and Analytical Study of Systems Consisting of Sliding Bearings, Rubber Restoring Force Devices and Fluid Dampers," Volumes I and II, by P. Tsopelas, S. Okamoto, M.C. Constantinou, D. Ozaki and S. Fujii, 2/4/94, (PB94-181740, A09, MF-A02 and PB94-181757, A12, MF-A03).

NCEER-94-0003 "A Markov Model for Local and Global Damage Indices in Seismic Analysis," by S. Rahman and M. Grigoriu, 2/18/94, (PB94-206000, A12, MF-A03).

NCEER-94-0004 "Proceedings from the NCEER Workshop on Seismic Response of Masonry Infills," edited by D.P. Abrams, 3/1/94, (PB94-180783, A07, MF-A02).

NCEER-94-0005 "The Northridge, California Earthquake of January 17, 1994: General Reconnaissance Report," edited by J.D. Goltz, 3/11/94, (PB94-193943, A10, MF-A03).

NCEER-94-0006 "Seismic Energy Based Fatigue Damage Analysis of Bridge Columns: Part I - Evaluation of Seismic Capacity," by G.A. Chang and J.B. Mander, 3/14/94, (PB94-219185, A11, MF-A03).

NCEER-94-0007 "Seismic Isolation of Multi-Story Frame Structures Using Spherical Sliding Isolation Systems," by T.M. Al-Hussaini, V.A. Zayas and M.C. Constantinou, 3/17/94, (PB94-193745, A09, MF-A02).

NCEER-94-0008 "The Northridge, California Earthquake of January 17, 1994: Performance of Highway Bridges," edited by I.G. Buckle, 3/24/94, (PB94-193851, A06, MF-A02).

NCEER-94-0009 "Proceedings of the Third U.S.-Japan Workshop on Earthquake Protective Systems for Bridges," edited by I.G. Buckle and I. Friedland, 3/31/94, (PB94-195815, A99, MF-A06).

NCEER-94-0010 "3D-BASIS-ME: Computer Program for Nonlinear Dynamic Analysis of Seismically Isolated Single and Multiple Structures and Liquid Storage Tanks," by P.C. Tsopelas, M.C. Constantinou and A.M. Reinhorn, 4/12/94, (PB94-204922, A09, MF-A02).

NCEER-94-0011 "The Northridge, California Earthquake of January 17, 1994: Performance of Gas Transmission Pipelines," by T.D. O'Rourke and M.C. Palmer, 5/16/94, (PB94-204989, A05, MF-A01).

NCEER-94-0012 "Feasibility Study of Replacement Procedures and Earthquake Performance Related to Gas Transmission Pipelines," by T.D. O'Rourke and M.C. Palmer, 5/25/94, (PB94-206638, A09, MF-A02).

NCEER-94-0013 "Seismic Energy Based Fatigue Damage Analysis of Bridge Columns: Part II - Evaluation of Seismic Demand," by G.A. Chang and J.B. Mander, 6/1/94, (PB95-18106, A08, MF-A02).

NCEER-94-0014 "NCEER-Taisei Corporation Research Program on Sliding Seismic Isolation Systems for Bridges: Experimental and Analytical Study of a System Consisting of Sliding Bearings and Fluid Restoring Force/Damping Devices," by P. Tsopelas and M.C. Constantinou, 6/13/94, (PB94-219144, A10, MF-A03).

NCEER-94-0015 "Generation of Hazard-Consistent Fragility Curves for Seismic Loss Estimation Studies," by H. Hwang and J-R. Huo, 6/14/94, (PB95-181996, A09, MF-A02).

NCEER-94-0016 "Seismic Study of Building Frames with Added Energy-Absorbing Devices," by W.S. Pong, C.S. Tsai and G.C. Lee, 6/20/94, (PB94-219136, A10, A03).

NCEER-94-0017 "Sliding Mode Control for Seismic-Excited Linear and Nonlinear Civil Engineering Structures," by J. Yang, J. Wu, A. Agrawal and Z. Li, 6/21/94, (PB95-138483, A06, MF-A02).

NCEER-94-0018 "3D-BASIS-TABS Version 2.0: Computer Program for Nonlinear Dynamic Analysis of Three Dimensional Base Isolated Structures," by A.M. Reinhorn, S. Nagarajaiah, M.C. Constantinou, P. Tsopelas and R. Li, 6/22/94, (PB95-182176, A08, MF-A02).

NCEER-94-0019 "Proceedings of the International Workshop on Civil Infrastructure Systems: Application of Intelligent Systems and Advanced Materials on Bridge Systems," Edited by G.C. Lee and K.C. Chang, 7/18/94, (PB95-252474, A20, MF-A04).

NCEER-94-0020 "Study of Seismic Isolation Systems for Computer Floors," by V. Lambrou and M.C. Constantinou, 7/19/94, (PB95-138533, A10, MF-A03).

NCEER-94-0021 "Proceedings of the U.S.-Italian Workshop on Guidelines for Seismic Evaluation and Rehabilitation of Unreinforced Masonry Buildings," Edited by D.P. Abrams and G.M. Calvi, 7/20/94, (PB95-138749, A13, MF-A03).

NCEER-94-0022 "NCEER-Taisei Corporation Research Program on Sliding Seismic Isolation Systems for Bridges: Experimental and Analytical Study of a System Consisting of Lubricated PTFE Sliding Bearings and Mild Steel Dampers," by P. Tsopelas and M.C. Constantinou, 7/22/94, (PB95-182184, A08, MF-A02).

NCEER-94-0023 “Development of Reliability-Based Design Criteria for Buildings Under Seismic Load,” by Y.K. Wen, H. Hwang and M. Shinozuka, 8/1/94, (PB95-211934, A08, MF-A02).

NCEER-94-0024 “Experimental Verification of Acceleration Feedback Control Strategies for an Active Tendon System,” by S.J. Dyke, B.F. Spencer, Jr., P. Quast, M.K. Sain, D.C. Kaspari, Jr. and T.T. Soong, 8/29/94, (PB95-212320, A05, MF-A01).

NCEER-94-0025 “Seismic Retrofitting Manual for Highway Bridges,” Edited by I.G. Buckle and I.F. Friedland, published by the Federal Highway Administration (PB95-212676, A15, MF-A03).

NCEER-94-0026 “Proceedings from the Fifth U.S.-Japan Workshop on Earthquake Resistant Design of Lifeline Facilities and Countermeasures Against Soil Liquefaction,” Edited by T.D. O’Rourke and M. Hamada, 11/7/94, (PB95-220802, A99, MF-E08).

NCEER-95-0001 "Experimental and Analytical Investigation of Seismic Retrofit of Structures with Supplemental Damping: Part 1 - Fluid Viscous Damping Devices," by A.M. Reinhorn, C. Li and M.C. Constantinou, 1/3/95, (PB95-266599, A09, MF-A02).

NCEER-95-0002 "Experimental and Analytical Study of Low-Cycle Fatigue Behavior of Semi-Rigid Top-And-Seat Angle Connections," by G. Pekcan, J.B. Mander and S.S. Chen, 1/5/95, (PB95-220042, A07, MF-A02).

NCEER-95-0003 "NCEER-ATC Joint Study on Fragility of Buildings," by T. Anagnos, C. Rojahn and A.S. Kiremidjian, 1/20/95, (PB95-220026, A06, MF-A02).

NCEER-95-0004 "Nonlinear Control Algorithms for Peak Response Reduction," by Z. Wu, T.T. Soong, V. Gattulli and R.C. Lin, 2/16/95, (PB95-220349, A05, MF-A01).

NCEER-95-0005 "Pipeline Replacement Feasibility Study: A Methodology for Minimizing Seismic and Corrosion Risks to Underground Natural Gas Pipelines," by R.T. Eguchi, H.A. Seligson and D.G. Honegger, 3/2/95, (PB95-252326, A06, MF-A02).

NCEER-95-0006 "Evaluation of Seismic Performance of an 11-Story Frame Building During the 1994 Northridge Earthquake," by F. Naeim, R. DiSulio, K. Benuska, A. Reinhorn and C. Li, not available.

NCEER-95-0007 "Prioritization of Bridges for Seismic Retrofitting," by N. Basöz and A.S. Kiremidjian, 4/24/95, (PB95-252300, A08, MF-A02).

NCEER-95-0008 "Method for Developing Motion Damage Relationships for Reinforced Concrete Frames," by A. Singhal and A.S. Kiremidjian, 5/11/95, (PB95-266607, A06, MF-A02).

NCEER-95-0009 "Experimental and Analytical Investigation of Seismic Retrofit of Structures with Supplemental Damping: Part II - Friction Devices," by C. Li and A.M. Reinhorn, 7/6/95, (PB96-128087, A11, MF-A03).

NCEER-95-0010 "Experimental Performance and Analytical Study of a Non-Ductile Reinforced Concrete Frame Structure Retrofitted with Elastomeric Spring Dampers," by G. Pekcan, J.B. Mander and S.S. Chen, 7/14/95, (PB96-137161, A08, MF-A02).

NCEER-95-0011 "Development and Experimental Study of Semi-Active Fluid Damping Devices for Seismic Protection of Structures," by M.D. Symans and M.C. Constantinou, 8/3/95, (PB96-136940, A23, MF-A04).

NCEER-95-0012 "Real-Time Structural Parameter Modification (RSPM): Development of Innervated Structures," by Z. Liang, M. Tong and G.C. Lee, 4/11/95, (PB96-137153, A06, MF-A01).

NCEER-95-0013 "Experimental and Analytical Investigation of Seismic Retrofit of Structures with Supplemental Damping: Part III - Viscous Damping Walls," by A.M. Reinhorn and C. Li, 10/1/95, (PB96-176409, A11, MF-A03).

NCEER-95-0014 "Seismic Fragility Analysis of Equipment and Structures in a Memphis Electric Substation," by J-R. Huo and H.H.M. Hwang, 8/10/95, (PB96-128087, A09, MF-A02).

NCEER-95-0015 "The Hanshin-Awaji Earthquake of January 17, 1995: Performance of Lifelines," Edited by M. Shinozuka, 11/3/95, (PB96-176383, A15, MF-A03).

NCEER-95-0016 "Highway Culvert Performance During Earthquakes," by T.L. Youd and C.J. Beckman, available as NCEER-96-0015.

NCEER-95-0017 "The Hanshin-Awaji Earthquake of January 17, 1995: Performance of Highway Bridges," Edited by I.G. Buckle, 12/1/95, not available.

NCEER-95-0018 "Modeling of Masonry Infill Panels for Structural Analysis," by A.M. Reinhorn, A. Madan, R.E. Valles, Y. Reichmann and J.B. Mander, 12/8/95, (PB97-110886, MF-A01, A06).

NCEER-95-0019 "Optimal Polynomial Control for Linear and Nonlinear Structures," by A.K. Agrawal and J.N. Yang, 12/11/95, (PB96-168737, A07, MF-A02).

NCEER-95-0020 "Retrofit of Non-Ductile Reinforced Concrete Frames Using Friction Dampers," by R.S. Rao, P. Gergely and R.N. White, 12/22/95, (PB97-133508, A10, MF-A02).

NCEER-95-0021 "Parametric Results for Seismic Response of Pile-Supported Bridge Bents," by G. Mylonakis, A. Nikolaou and G. Gazetas, 12/22/95, (PB97-100242, A12, MF-A03).

NCEER-95-0022 "Kinematic Bending Moments in Seismically Stressed Piles," by A. Nikolaou, G. Mylonakis and G. Gazetas, 12/23/95, (PB97-113914, MF-A03, A13).

NCEER-96-0001 "Dynamic Response of Unreinforced Masonry Buildings with Flexible Diaphragms," by A.C. Costley and D.P. Abrams," 10/10/96, (PB97-133573, MF-A03, A15).

NCEER-96-0002 "State of the Art Review: Foundations and Retaining Structures," by I. Po Lam, not available.

NCEER-96-0003 "Ductility of Rectangular Reinforced Concrete Bridge Columns with Moderate Confinement," by N. Wehbe, M. Saiidi, D. Sanders and B. Douglas, 11/7/96, (PB97-133557, A06, MF-A02).

NCEER-96-0004 "Proceedings of the Long-Span Bridge Seismic Research Workshop," edited by I.G. Buckle and I.M. Friedland, not available.

NCEER-96-0005 "Establish Representative Pier Types for Comprehensive Study: Eastern United States," by J. Kulicki and Z. Prucz, 5/28/96, (PB98-119217, A07, MF-A02).

NCEER-96-0006 "Establish Representative Pier Types for Comprehensive Study: Western United States," by R. Imbsen, R.A. Schamber and T.A. Osterkamp, 5/28/96, (PB98-118607, A07, MF-A02).

NCEER-96-0007 "Nonlinear Control Techniques for Dynamical Systems with Uncertain Parameters," by R.G. Ghanem and M.I. Bujakov, 5/27/96, (PB97-100259, A17, MF-A03).

NCEER-96-0008 "Seismic Evaluation of a 30-Year Old Non-Ductile Highway Bridge Pier and Its Retrofit," by J.B. Mander, B. Mahmoodzadegan, S. Bhadra and S.S. Chen, 5/31/96, (PB97-110902, MF-A03, A10).

NCEER-96-0009 "Seismic Performance of a Model Reinforced Concrete Bridge Pier Before and After Retrofit," by J.B. Mander, J.H. Kim and C.A. Ligozio, 5/31/96, (PB97-110910, MF-A02, A10).

NCEER-96-0010 "IDARC2D Version 4.0: A Computer Program for the Inelastic Damage Analysis of Buildings," by R.E. Valles, A.M. Reinhorn, S.K. Kunnath, C. Li and A. Madan, 6/3/96, (PB97-100234, A17, MF-A03).

NCEER-96-0011 "Estimation of the Economic Impact of Multiple Lifeline Disruption: Memphis Light, Gas and Water Division Case Study," by S.E. Chang, H.A. Seligson and R.T. Eguchi, 8/16/96, (PB97-133490, A11, MF-A03).

NCEER-96-0012 "Proceedings from the Sixth Japan-U.S. Workshop on Earthquake Resistant Design of Lifeline Facilities and Countermeasures Against Soil Liquefaction, Edited by M. Hamada and T. O'Rourke, 9/11/96, (PB97-133581, A99, MF-A06).

NCEER-96-0013 "Chemical Hazards, Mitigation and Preparedness in Areas of High Seismic Risk: A Methodology for Estimating the Risk of Post-Earthquake Hazardous Materials Release," by H.A. Seligson, R.T. Eguchi, K.J. Tierney and K. Richmond, 11/7/96, (PB97-133565, MF-A02, A08).

NCEER-96-0014 "Response of Steel Bridge Bearings to Reversed Cyclic Loading," by J.B. Mander, D-K. Kim, S.S. Chen and G.J. Premus, 11/13/96, (PB97-140735, A12, MF-A03).

NCEER-96-0015 "Highway Culvert Performance During Past Earthquakes," by T.L. Youd and C.J. Beckman, 11/25/96, (PB97-133532, A06, MF-A01).

NCEER-97-0001 "Evaluation, Prevention and Mitigation of Pounding Effects in Building Structures," by R.E. Valles and A.M. Reinhorn, 2/20/97, (PB97-159552, A14, MF-A03).

NCEER-97-0002 "Seismic Design Criteria for Bridges and Other Highway Structures," by C. Rojahn, R. Mayes, D.G. Anderson, J. Clark, J.H. Hom, R.V. Nutt and M.J. O'Rourke, 4/30/97, (PB97-194658, A06, MF-A03).

NCEER-97-0003 "Proceedings of the U.S.-Italian Workshop on Seismic Evaluation and Retrofit," Edited by D.P. Abrams and G.M. Calvi, 3/19/97, (PB97-194666, A13, MF-A03).

NCEER-97-0004 "Investigation of Seismic Response of Buildings with Linear and Nonlinear Fluid Viscous Dampers," by A.A. Seleemah and M.C. Constantinou, 5/21/97, (PB98-109002, A15, MF-A03).

NCEER-97-0005 "Proceedings of the Workshop on Earthquake Engineering Frontiers in Transportation Facilities," edited by G.C. Lee and I.M. Friedland, 8/29/97, (PB98-128911, A25, MR-A04).

NCEER-97-0006 "Cumulative Seismic Damage of Reinforced Concrete Bridge Piers," by S.K. Kunnath, A. El-Bahy, A. Taylor and W. Stone, 9/2/97, (PB98-108814, A11, MF-A03).

NCEER-97-0007 "Structural Details to Accommodate Seismic Movements of Highway Bridges and Retaining Walls," by R.A. Imbsen, R.A. Schamber, E. Thorkildsen, A. Kartoum, B.T. Martin, T.N. Rosser and J.M. Kulicki, 9/3/97, (PB98-108996, A09, MF-A02).

NCEER-97-0008 "A Method for Earthquake Motion-Damage Relationships with Application to Reinforced Concrete Frames," by A. Singhal and A.S. Kiremidjian, 9/10/97, (PB98-108988, A13, MF-A03).

NCEER-97-0009 "Seismic Analysis and Design of Bridge Abutments Considering Sliding and Rotation," by K. Fishman and R. Richards, Jr., 9/15/97, (PB98-108897, A06, MF-A02).

NCEER-97-0010 "Proceedings of the FHWA/NCEER Workshop on the National Representation of Seismic Ground Motion for New and Existing Highway Facilities," edited by I.M. Friedland, M.S. Power and R.L. Mayes, 9/22/97, (PB98-128903, A21, MF-A04).

NCEER-97-0011 "Seismic Analysis for Design or Retrofit of Gravity Bridge Abutments," by K.L. Fishman, R. Richards, Jr. and R.C. Divito, 10/2/97, (PB98-128937, A08, MF-A02).

NCEER-97-0012 "Evaluation of Simplified Methods of Analysis for Yielding Structures," by P. Tsopelas, M.C. Constantinou, C.A. Kircher and A.S. Whittaker, 10/31/97, (PB98-128929, A10, MF-A03).

NCEER-97-0013 "Seismic Design of Bridge Columns Based on Control and Repairability of Damage," by C-T. Cheng and J.B. Mander, 12/8/97, (PB98-144249, A11, MF-A03).

NCEER-97-0014 "Seismic Resistance of Bridge Piers Based on Damage Avoidance Design," by J.B. Mander and C-T. Cheng, 12/10/97, (PB98-144223, A09, MF-A02).

NCEER-97-0015 "Seismic Response of Nominally Symmetric Systems with Strength Uncertainty," by S. Balopoulou and M. Grigoriu, 12/23/97, (PB98-153422, A11, MF-A03).

NCEER-97-0016 "Evaluation of Seismic Retrofit Methods for Reinforced Concrete Bridge Columns," by T.J. Wipf, F.W. Klaiber and F.M. Russo, 12/28/97, (PB98-144215, A12, MF-A03).

NCEER-97-0017 "Seismic Fragility of Existing Conventional Reinforced Concrete Highway Bridges," by C.L. Mullen and A.S. Cakmak, 12/30/97, (PB98-153406, A08, MF-A02).

NCEER-97-0018 "Loss Asssessment of Memphis Buildings," edited by D.P. Abrams and M. Shinozuka, 12/31/97, (PB98-144231, A13, MF-A03).

NCEER-97-0019 "Seismic Evaluation of Frames with Infill Walls Using Quasi-static Experiments," by K.M. Mosalam, R.N. White and P. Gergely, 12/31/97, (PB98-153455, A07, MF-A02).

NCEER-97-0020 "Seismic Evaluation of Frames with Infill Walls Using Pseudo-dynamic Experiments," by K.M. Mosalam, R.N. White and P. Gergely, 12/31/97, (PB98-153430, A07, MF-A02).

NCEER-97-0021 "Computational Strategies for Frames with Infill Walls: Discrete and Smeared Crack Analyses and Seismic Fragility," by K.M. Mosalam, R.N. White and P. Gergely, 12/31/97, (PB98-153414, A10, MF-A02).

NCEER-97-0022 "Proceedings of the NCEER Workshop on Evaluation of Liquefaction Resistance of Soils," edited by T.L. Youd and I.M. Idriss, 12/31/97, (PB98-155617, A15, MF-A03).

MCEER-98-0001 "Extraction of Nonlinear Hysteretic Properties of Seismically Isolated Bridges from Quick-Release Field Tests," by Q. Chen, B.M. Douglas, E.M. Maragakis and I.G. Buckle, 5/26/98, (PB99-118838, A06, MF-A01).

MCEER-98-0002 "Methodologies for Evaluating the Importance of Highway Bridges," by A. Thomas, S. Eshenaur and J. Kulicki, 5/29/98, (PB99-118846, A10, MF-A02).

MCEER-98-0003 "Capacity Design of Bridge Piers and the Analysis of Overstrength," by J.B. Mander, A. Dutta and P. Goel, 6/1/98, (PB99-118853, A09, MF-A02).

MCEER-98-0004 "Evaluation of Bridge Damage Data from the Loma Prieta and Northridge, California Earthquakes," by N. Basoz and A. Kiremidjian, 6/2/98, (PB99-118861, A15, MF-A03).

MCEER-98-0005 "Screening Guide for Rapid Assessment of Liquefaction Hazard at Highway Bridge Sites," by T. L. Youd, 6/16/98, (PB99-118879, A06, not available on microfiche).

MCEER-98-0006 "Structural Steel and Steel/Concrete Interface Details for Bridges," by P. Ritchie, N. Kauhl and J. Kulicki, 7/13/98, (PB99-118945, A06, MF-A01).

MCEER-98-0007 "Capacity Design and Fatigue Analysis of Confined Concrete Columns," by A. Dutta and J.B. Mander, 7/14/98, (PB99-118960, A14, MF-A03).

MCEER-98-0008 "Proceedings of the Workshop on Performance Criteria for Telecommunication Services Under Earthquake Conditions," edited by A.J. Schiff, 7/15/98, (PB99-118952, A08, MF-A02).

MCEER-98-0009 "Fatigue Analysis of Unconfined Concrete Columns," by J.B. Mander, A. Dutta and J.H. Kim, 9/12/98, (PB99-123655, A10, MF-A02).

MCEER-98-0010 "Centrifuge Modeling of Cyclic Lateral Response of Pile-Cap Systems and Seat-Type Abutments in Dry Sands," by A.D. Gadre and R. Dobry, 10/2/98, (PB99-123606, A13, MF-A03).

MCEER-98-0011 "IDARC-BRIDGE: A Computational Platform for Seismic Damage Assessment of Bridge Structures," by A.M. Reinhorn, V. Simeonov, G. Mylonakis and Y. Reichman, 10/2/98, (PB99-162919, A15, MF-A03).

MCEER-98-0012 "Experimental Investigation of the Dynamic Response of Two Bridges Before and After Retrofitting with Elastomeric Bearings," by D.A. Wendichansky, S.S. Chen and J.B. Mander, 10/2/98, (PB99-162927, A15, MF-A03).

MCEER-98-0013 "Design Procedures for Hinge Restrainers and Hinge Sear Width for Multiple-Frame Bridges," by R. Des Roches and G.L. Fenves, 11/3/98, (PB99-140477, A13, MF-A03).

MCEER-98-0014 "Response Modification Factors for Seismically Isolated Bridges," by M.C. Constantinou and J.K. Quarshie, 11/3/98, (PB99-140485, A14, MF-A03).

MCEER-98-0015 "Proceedings of the U.S.-Italy Workshop on Seismic Protective Systems for Bridges," edited by I.M. Friedland and M.C. Constantinou, 11/3/98, (PB2000-101711, A22, MF-A04).

MCEER-98-0016 "Appropriate Seismic Reliability for Critical Equipment Systems: Recommendations Based on Regional Analysis of Financial and Life Loss," by K. Porter, C. Scawthorn, C. Taylor and N. Blais, 11/10/98, (PB99-157265, A08, MF-A02).

MCEER-98-0017 "Proceedings of the U.S. Japan Joint Seminar on Civil Infrastructure Systems Research," edited by M. Shinozuka and A. Rose, 11/12/98, (PB99-156713, A16, MF-A03).

MCEER-98-0018 "Modeling of Pile Footings and Drilled Shafts for Seismic Design," by I. PoLam, M. Kapuskar and D. Chaudhuri, 12/21/98, (PB99-157257, A09, MF-A02).

MCEER-99-0001 "Seismic Evaluation of a Masonry Infilled Reinforced Concrete Frame by Pseudodynamic Testing," by S.G. Buonopane and R.N. White, 2/16/99, (PB99-162851, A09, MF-A02).

MCEER-99-0002 "Response History Analysis of Structures with Seismic Isolation and Energy Dissipation Systems: Verification Examples for Program SAP2000," by J. Scheller and M.C. Constantinou, 2/22/99, (PB99-162869, A08, MF-A02).

MCEER-99-0003 "Experimental Study on the Seismic Design and Retrofit of Bridge Columns Including Axial Load Effects," by A. Dutta, T. Kokorina and J.B. Mander, 2/22/99, (PB99-162877, A09, MF-A02).

MCEER-99-0004 "Experimental Study of Bridge Elastomeric and Other Isolation and Energy Dissipation Systems with Emphasis on Uplift Prevention and High Velocity Near-source Seismic Excitation," by A. Kasalanati and M. C. Constantinou, 2/26/99, (PB99-162885, A12, MF-A03).

MCEER-99-0005 "Truss Modeling of Reinforced Concrete Shear-flexure Behavior," by J.H. Kim and J.B. Mander, 3/8/99, (PB99-163693, A12, MF-A03).

MCEER-99-0006 "Experimental Investigation and Computational Modeling of Seismic Response of a 1:4 Scale Model Steel Structure with a Load Balancing Supplemental Damping System," by G. Pekcan, J.B. Mander and S.S. Chen, 4/2/99, (PB99-162893, A11, MF-A03).

MCEER-99-0007 "Effect of Vertical Ground Motions on the Structural Response of Highway Bridges," by M.R. Button, C.J. Cronin and R.L. Mayes, 4/10/99, (PB2000-101411, A10, MF-A03).

MCEER-99-0008 "Seismic Reliability Assessment of Critical Facilities: A Handbook, Supporting Documentation, and Model Code Provisions," by G.S. Johnson, R.E. Sheppard, M.D. Quilici, S.J. Eder and C.R. Scawthorn, 4/12/99, (PB2000-101701, A18, MF-A04).

MCEER-99-0009 "Impact Assessment of Selected MCEER Highway Project Research on the Seismic Design of Highway Structures," by C. Rojahn, R. Mayes, D.G. Anderson, J.H. Clark, D'Appolonia Engineering, S. Gloyd and R.V. Nutt, 4/14/99, (PB99-162901, A10, MF-A02).

MCEER-99-0010 "Site Factors and Site Categories in Seismic Codes," by R. Dobry, R. Ramos and M.S. Power, 7/19/99, (PB2000-101705, A08, MF-A02).

MCEER-99-0011 "Restrainer Design Procedures for Multi-Span Simply-Supported Bridges," by M.J. Randall, M. Saiidi, E. Maragakis and T. Isakovic, 7/20/99, (PB2000-101702, A10, MF-A02).

MCEER-99-0012 "Property Modification Factors for Seismic Isolation Bearings," by M.C. Constantinou, P. Tsopelas, A. Kasalanati and E. Wolff, 7/20/99, (PB2000-103387, A11, MF-A03).

MCEER-99-0013 "Critical Seismic Issues for Existing Steel Bridges," by P. Ritchie, N. Kauhl and J. Kulicki, 7/20/99, (PB2000-101697, A09, MF-A02).

MCEER-99-0014 "Nonstructural Damage Database," by A. Kao, T.T. Soong and A. Vender, 7/24/99, (PB2000-101407, A06, MF-A01).

MCEER-99-0015 "Guide to Remedial Measures for Liquefaction Mitigation at Existing Highway Bridge Sites," by H.G. Cooke and J. K. Mitchell, 7/26/99, (PB2000-101703, A11, MF-A03).

MCEER-99-0016 "Proceedings of the MCEER Workshop on Ground Motion Methodologies for the Eastern United States," edited by N. Abrahamson and A. Becker, 8/11/99, (PB2000-103385, A07, MF-A02).

MCEER-99-0017 "Quindío, Colombia Earthquake of January 25, 1999: Reconnaissance Report," by A.P. Asfura and P.J. Flores, 10/4/99, (PB2000-106893, A06, MF-A01).

MCEER-99-0018 "Hysteretic Models for Cyclic Behavior of Deteriorating Inelastic Structures," by M.V. Sivaselvan and A.M. Reinhorn, 11/5/99, (PB2000-103386, A08, MF-A02).

MCEER-99-0019 "Proceedings of the 7th U.S.- Japan Workshop on Earthquake Resistant Design of Lifeline Facilities and Countermeasures Against Soil Liquefaction," edited by T.D. O'Rourke, J.P. Bardet and M. Hamada, 11/19/99, (PB2000-103354, A99, MF-A06).

MCEER-99-0020 "Development of Measurement Capability for Micro-Vibration Evaluations with Application to Chip Fabrication Facilities," by G.C. Lee, Z. Liang, J.W. Song, J.D. Shen and W.C. Liu, 12/1/99, (PB2000-105993, A08, MF-A02).

MCEER-99-0021 "Design and Retrofit Methodology for Building Structures with Supplemental Energy Dissipating Systems," by G. Pekcan, J.B. Mander and S.S. Chen, 12/31/99, (PB2000-105994, A11, MF-A03).

MCEER-00-0001 "The Marmara, Turkey Earthquake of August 17, 1999: Reconnaissance Report," edited by C. Scawthorn; with major contributions by M. Bruneau, R. Eguchi, T. Holzer, G. Johnson, J. Mander, J. Mitchell, W. Mitchell, A. Papageorgiou, C. Scaethorn, and G. Webb, 3/23/00, (PB2000-106200, A11, MF-A03).

MCEER-00-0002 "Proceedings of the MCEER Workshop for Seismic Hazard Mitigation of Health Care Facilities," edited by G.C. Lee, M. Ettouney, M. Grigoriu, J. Hauer and J. Nigg, 3/29/00, (PB2000-106892, A08, MF-A02).

MCEER-00-0003 "The Chi-Chi, Taiwan Earthquake of September 21, 1999: Reconnaissance Report," edited by G.C. Lee and C.H. Loh, with major contributions by G.C. Lee, M. Bruneau, I.G. Buckle, S.E. Chang, P.J. Flores, T.D. O'Rourke, M. Shinozuka, T.T. Soong, C-H. Loh, K-C. Chang, Z-J. Chen, J-S. Hwang, M-L. Lin, G-Y. Liu, K-C. Tsai, G.C. Yao and C-L. Yen, 4/30/00, (PB2001-100980, A10, MF-A02).

MCEER-00-0004 "Seismic Retrofit of End-Sway Frames of Steel Deck-Truss Bridges with a Supplemental Tendon System: Experimental and Analytical Investigation," by G. Pekcan, J.B. Mander and S.S. Chen, 7/1/00, (PB2001-100982, A10, MF-A02).

MCEER-00-0005 "Sliding Fragility of Unrestrained Equipment in Critical Facilities," by W.H. Chong and T.T. Soong, 7/5/00, (PB2001-100983, A08, MF-A02).

MCEER-00-0006 "Seismic Response of Reinforced Concrete Bridge Pier Walls in the Weak Direction," by N. Abo-Shadi, M. Saiidi and D. Sanders, 7/17/00, (PB2001-100981, A17, MF-A03).

MCEER-00-0007 "Low-Cycle Fatigue Behavior of Longitudinal Reinforcement in Reinforced Concrete Bridge Columns," by J. Brown and S.K. Kunnath, 7/23/00, (PB2001-104392, A08, MF-A02).

MCEER-00-0008 "Soil Structure Interaction of Bridges for Seismic Analysis," I. PoLam and H. Law, 9/25/00, (PB2001-105397, A08, MF-A02).

MCEER-00-0009 "Proceedings of the First MCEER Workshop on Mitigation of Earthquake Disaster by Advanced Technologies (MEDAT-1), edited by M. Shinozuka, D.J. Inman and T.D. O'Rourke, 11/10/00, (PB2001-105399, A14, MF-A03).

MCEER-00-0010 "Development and Evaluation of Simplified Procedures for Analysis and Design of Buildings with Passive Energy Dissipation Systems, Revision 01," by O.M. Ramirez, M.C. Constantinou, C.A. Kircher, A.S. Whittaker, M.W. Johnson, J.D. Gomez and C. Chrysostomou, 11/16/01, (PB2001-105523, A23, MF-A04).

MCEER-00-0011 "Dynamic Soil-Foundation-Structure Interaction Analyses of Large Caissons," by C-Y. Chang, C-M. Mok, Z-L. Wang, R. Settgast, F. Waggoner, M.A. Ketchum, H.M. Gonnermann and C-C. Chin, 12/30/00, (PB2001-104373, A07, MF-A02).

MCEER-00-0012 "Experimental Evaluation of Seismic Performance of Bridge Restrainers," by A.G. Vlassis, E.M. Maragakis and M. Saiid Saiidi, 12/30/00, (PB2001-104354, A09, MF-A02).

MCEER-00-0013 "Effect of Spatial Variation of Ground Motion on Highway Structures," by M. Shinozuka, V. Saxena and G. Deodatis, 12/31/00, (PB2001-108755, A13, MF-A03).

MCEER-00-0014 "A Risk-Based Methodology for Assessing the Seismic Performance of Highway Systems," by S.D. Werner, C.E. Taylor, J.E. Moore, II, J.S. Walton and S. Cho, 12/31/00, (PB2001-108756, A14, MF-A03).

MCEER-01-0001 "Experimental Investigation of P-Delta Effects to Collapse During Earthquakes," by D. Vian and M. Bruneau, 6/25/01, (PB2002-100534, A17, MF-A03).

MCEER-01-0002 "Proceedings of the Second MCEER Workshop on Mitigation of Earthquake Disaster by Advanced Technologies (MEDAT-2)," edited by M. Bruneau and D.J. Inman, 7/23/01, (PB2002-100434, A16, MF-A03).

MCEER-01-0003 "Sensitivity Analysis of Dynamic Systems Subjected to Seismic Loads," by C. Roth and M. Grigoriu, 9/18/01, (PB2003-100884, A12, MF-A03).

MCEER-01-0004 "Overcoming Obstacles to Implementing Earthquake Hazard Mitigation Policies: Stage 1 Report," by D.J. Alesch and W.J. Petak, 12/17/01, (PB2002-107949, A07, MF-A02).

MCEER-01-0005 "Updating Real-Time Earthquake Loss Estimates: Methods, Problems and Insights," by C.E. Taylor, S.E. Chang and R.T. Eguchi, 12/17/01, (PB2002-107948, A05, MF-A01).

MCEER-01-0006 "Experimental Investigation and Retrofit of Steel Pile Foundations and Pile Bents Under Cyclic Lateral Loadings," by A. Shama, J. Mander, B. Blabac and S. Chen, 12/31/01, (PB2002-107950, A13, MF-A03).

MCEER-02-0001 "Assessment of Performance of Bolu Viaduct in the 1999 Duzce Earthquake in Turkey" by P.C. Roussis, M.C. Constantinou, M. Erdik, E. Durukal and M. Dicleli, 5/8/02, (PB2003-100883, A08, MF-A02).

MCEER-02-0002 "Seismic Behavior of Rail Counterweight Systems of Elevators in Buildings," by M.P. Singh, Rildova and L.E. Suarez, 5/27/02. (PB2003-100882, A11, MF-A03).

MCEER-02-0003 "Development of Analysis and Design Procedures for Spread Footings," by G. Mylonakis, G. Gazetas, S. Nikolaou and A. Chauncey, 10/02/02, (PB2004-101636, A13, MF-A03, CD-A13).

MCEER-02-0004 "Bare-Earth Algorithms for Use with SAR and LIDAR Digital Elevation Models," by C.K. Huyck, R.T. Eguchi and B. Houshmand, 10/16/02, (PB2004-101637, A07, CD-A07).

MCEER-02-0005 "Review of Energy Dissipation of Compression Members in Concentrically Braced Frames," by K.Lee and M. Bruneau, 10/18/02, (PB2004-101638, A10, CD-A10).

MCEER-03-0001 "Experimental Investigation of Light-Gauge Steel Plate Shear Walls for the Seismic Retrofit of Buildings" by J. Berman and M. Bruneau, 5/2/03, (PB2004-101622, A10, MF-A03, CD-A10).

MCEER-03-0002 "Statistical Analysis of Fragility Curves," by M. Shinozuka, M.Q. Feng, H. Kim, T. Uzawa and T. Ueda, 6/16/03, (PB2004-101849, A09, CD-A09).

MCEER-03-0003 "Proceedings of the Eighth U.S.-Japan Workshop on Earthquake Resistant Design f Lifeline Facilities and Countermeasures Against Liquefaction," edited by M. Hamada, J.P. Bardet and T.D. O'Rourke, 6/30/03, (PB2004-104386, A99, CD-A99).

MCEER-03-0004 "Proceedings of the PRC-US Workshop on Seismic Analysis and Design of Special Bridges," edited by L.C. Fan and G.C. Lee, 7/15/03, (PB2004-104387, A14, CD-A14).

MCEER-03-0005 "Urban Disaster Recovery: A Framework and Simulation Model," by S.B. Miles and S.E. Chang, 7/25/03, (PB2004-104388, A07, CD-A07).

MCEER-03-0006 "Behavior of Underground Piping Joints Due to Static and Dynamic Loading," by R.D. Meis, M. Maragakis and R. Siddharthan, 11/17/03, (PB2005-102194, A13, MF-A03, CD-A00).

MCEER-04-0001 "Experimental Study of Seismic Isolation Systems with Emphasis on Secondary System Response and Verification of Accuracy of Dynamic Response History Analysis Methods," by E. Wolff and M. Constantinou, 1/16/04 (PB2005-102195, A99, MF-E08, CD-A00).

MCEER-04-0002 "Tension, Compression and Cyclic Testing of Engineered Cementitious Composite Materials," by K. Kesner and S.L. Billington, 3/1/04, (PB2005-102196, A08, CD-A08).

MCEER-04-0003 "Cyclic Testing of Braces Laterally Restrained by Steel Studs to Enhance Performance During Earthquakes," by O.C. Celik, J.W. Berman and M. Bruneau, 3/16/04, (PB2005-102197, A13, MF-A03, CD-A00).

MCEER-04-0004 "Methodologies for Post Earthquake Building Damage Detection Using SAR and Optical Remote Sensing: Application to the August 17, 1999 Marmara, Turkey Earthquake," by C.K. Huyck, B.J. Adams, S. Cho, R.T. Eguchi, B. Mansouri and B. Houshmand, 6/15/04, (PB2005-104888, A10, CD-A00).

MCEER-04-0005 "Nonlinear Structural Analysis Towards Collapse Simulation: A Dynamical Systems Approach," by M.V. Sivaselvan and A.M. Reinhorn, 6/16/04, (PB2005-104889, A11, MF-A03, CD-A00).

MCEER-04-0006 "Proceedings of the Second PRC-US Workshop on Seismic Analysis and Design of Special Bridges," edited by G.C. Lee and L.C. Fan, 6/25/04, (PB2005-104890, A16, CD-A00).

MCEER-04-0007 "Seismic Vulnerability Evaluation of Axially Loaded Steel Built-up Laced Members," by K. Lee and M. Bruneau, 6/30/04, (PB2005-104891, A16, CD-A00).

MCEER-04-0008 "Evaluation of Accuracy of Simplified Methods of Analysis and Design of Buildings with Damping Systems for Near-Fault and for Soft-Soil Seismic Motions," by E.A. Pavlou and M.C. Constantinou, 8/16/04, (PB2005-104892, A08, MF-A02, CD-A00).

MCEER-04-0009 "Assessment of Geotechnical Issues in Acute Care Facilities in California," by M. Lew, T.D. O'Rourke, R. Dobry and M. Koch, 9/15/04, (PB2005-104893, A08, CD-A00).

MCEER-04-0010 "Scissor-Jack-Damper Energy Dissipation System," by A.N. Sigaher-Boyle and M.C. Constantinou, 12/1/04 (PB2005-108221).

MCEER-04-0011 "Seismic Retrofit of Bridge Steel Truss Piers Using a Controlled Rocking Approach," by M. Pollino and M. Bruneau, 12/20/04 (PB2006-105795).

MCEER-05-0001 "Experimental and Analytical Studies of Structures Seismically Isolated with an Uplift-Restraint Isolation System," by P.C. Roussis and M.C. Constantinou, 1/10/05 (PB2005-108222).

MCEER-05-0002 "A Versatile Experimentation Model for Study of Structures Near Collapse Applied to Seismic Evaluation of Irregular Structures," by D. Kusumastuti, A.M. Reinhorn and A. Rutenberg, 3/31/05 (PB2006-101523).

MCEER-05-0003 "Proceedings of the Third PRC-US Workshop on Seismic Analysis and Design of Special Bridges," edited by L.C. Fan and G.C. Lee, 4/20/05, (PB2006-105796).

MCEER-05-0004 "Approaches for the Seismic Retrofit of Braced Steel Bridge Piers and Proof-of-Concept Testing of an Eccentrically Braced Frame with Tubular Link," by J.W. Berman and M. Bruneau, 4/21/05 (PB2006-101524).

MCEER-05-0005 "Simulation of Strong Ground Motions for Seismic Fragility Evaluation of Nonstructural Components in Hospitals," by A. Wanitkorkul and A. Filiatrault, 5/26/05 (PB2006-500027).

MCEER-05-0006 "Seismic Safety in California Hospitals: Assessing an Attempt to Accelerate the Replacement or Seismic Retrofit of Older Hospital Facilities," by D.J. Alesch, L.A. Arendt and W.J. Petak, 6/6/05 (PB2006-105794).

MCEER-05-0007 "Development of Seismic Strengthening and Retrofit Strategies for Critical Facilities Using Engineered Cementitious Composite Materials," by K. Kesner and S.L. Billington, 8/29/05 (PB2006-111701).

MCEER-05-0008 "Experimental and Analytical Studies of Base Isolation Systems for Seismic Protection of Power Transformers," by N. Murota, M.Q. Feng and G-Y. Liu, 9/30/05 (PB2006-111702).

MCEER-05-0009 "3D-BASIS-ME-MB: Computer Program for Nonlinear Dynamic Analysis of Seismically Isolated Structures," by P.C. Tsopelas, P.C. Roussis, M.C. Constantinou, R. Buchanan and A.M. Reinhorn, 10/3/05 (PB2006-111703).

MCEER-05-0010 "Steel Plate Shear Walls for Seismic Design and Retrofit of Building Structures," by D. Vian and M. Bruneau, 12/15/05 (PB2006-111704).

MCEER-05-0011 "The Performance-Based Design Paradigm," by M.J. Astrella and A. Whittaker, 12/15/05 (PB2006-111705).

MCEER-06-0001 "Seismic Fragility of Suspended Ceiling Systems," H. Badillo-Almaraz, A.S. Whittaker, A.M. Reinhorn and G.P. Cimellaro, 2/4/06 (PB2006-111706).

MCEER-06-0002 "Multi-Dimensional Fragility of Structures," by G.P. Cimellaro, A.M. Reinhorn and M. Bruneau, 3/1/06 (PB2007-106974, A09, MF-A02, CD A00).

MCEER-06-0003 "Built-Up Shear Links as Energy Dissipators for Seismic Protection of Bridges," by P. Dusicka, A.M. Itani and I.G. Buckle, 3/15/06 (PB2006-111708).

MCEER-06-0004 "Analytical Investigation of the Structural Fuse Concept," by R.E. Vargas and M. Bruneau, 3/16/06 (PB2006-111709).

MCEER-06-0005 "Experimental Investigation of the Structural Fuse Concept," by R.E. Vargas and M. Bruneau, 3/17/06 (PB2006-111710).

MCEER-06-0006 "Further Development of Tubular Eccentrically Braced Frame Links for the Seismic Retrofit of Braced Steel Truss Bridge Piers," by J.W. Berman and M. Bruneau, 3/27/06 (PB2007-105147).

MCEER-06-0007 "REDARS Validation Report," by S. Cho, C.K. Huyck, S. Ghosh and R.T. Eguchi, 8/8/06 (PB2007-106983).

MCEER-06-0008 "Review of Current NDE Technologies for Post-Earthquake Assessment of Retrofitted Bridge Columns," by J.W. Song, Z. Liang and G.C. Lee, 8/21/06 (PB2007-106984).

MCEER-06-0009 "Liquefaction Remediation in Silty Soils Using Dynamic Compaction and Stone Columns," by S. Thevanayagam, G.R. Martin, R. Nashed, T. Shenthan, T. Kanagalingam and N. Ecemis, 8/28/06 (PB2007-106985).

MCEER-06-0010 "Conceptual Design and Experimental Investigation of Polymer Matrix Composite Infill Panels for Seismic Retrofitting," by W. Jung, M. Chiewanichakorn and A.J. Aref, 9/21/06 (PB2007-106986).

MCEER-06-0011 "A Study of the Coupled Horizontal-Vertical Behavior of Elastomeric and Lead-Rubber Seismic Isolation Bearings," by G.P. Warn and A.S. Whittaker, 9/22/06 (PB2007-108679).

MCEER-06-0012 "Proceedings of the Fourth PRC-US Workshop on Seismic Analysis and Design of Special Bridges: Advancing Bridge Technologies in Research, Design, Construction and Preservation," Edited by L.C. Fan, G.C. Lee and L. Ziang, 10/12/06 (PB2007-109042).

MCEER-06-0013 "Cyclic Response and Low Cycle Fatigue Characteristics of Plate Steels," by P. Dusicka, A.M. Itani and I.G. Buckle, 11/1/06 06 (PB2007-106987).

MCEER-06-0014 "Proceedings of the Second US-Taiwan Bridge Engineering Workshop," edited by W.P. Yen, J. Shen, J-Y. Chen and M. Wang, 11/15/06 (PB2008-500041).

MCEER-06-0015 "User Manual and Technical Documentation for the REDARS^{TM} Import Wizard," by S. Cho, S. Ghosh, C.K. Huyck and S.D. Werner, 11/30/06 (PB2007-114766).

MCEER-06-0016 "Hazard Mitigation Strategy and Monitoring Technologies for Urban and Infrastructure Public Buildings: Proceedings of the China-US Workshops," edited by X.Y. Zhou, A.L. Zhang, G.C. Lee and M. Tong, 12/12/06 (PB2008-500018).

MCEER-07-0001 "Static and Kinetic Coefficients of Friction for Rigid Blocks," by C. Kafali, S. Fathali, M. Grigoriu and A.S. Whittaker, 3/20/07 (PB2007-114767).

MCEER-07-0002 "Hazard Mitigation Investment Decision Making: Organizational Response to Legislative Mandate," by L.A. Arendt, D.J. Alesch and W.J. Petak, 4/9/07 (PB2007-114768).

MCEER-07-0003 "Seismic Behavior of Bidirectional-Resistant Ductile End Diaphragms with Unbonded Braces in Straight or Skewed Steel Bridges," by O. Celik and M. Bruneau, 4/11/07 (PB2008-105141).

MCEER-07-0004 "Modeling Pile Behavior in Large Pile Groups Under Lateral Loading," by A.M. Dodds and G.R. Martin, 4/16/07(PB2008-105142).

MCEER-07-0005 "Experimental Investigation of Blast Performance of Seismically Resistant Concrete-Filled Steel Tube Bridge Piers," by S. Fujikura, M. Bruneau and D. Lopez-Garcia, 4/20/07 (PB2008-105143).

MCEER-07-0006 "Seismic Analysis of Conventional and Isolated Liquefied Natural Gas Tanks Using Mechanical Analogs," by I.P. Christovasilis and A.S. Whittaker, 5/1/07, not available.

MCEER-07-0007 "Experimental Seismic Performance Evaluation of Isolation/Restraint Systems for Mechanical Equipment – Part 1: Heavy Equipment Study," by S. Fathali and A. Filiatrault, 6/6/07 (PB2008-105144).

MCEER-07-0008 "Seismic Vulnerability of Timber Bridges and Timber Substructures," by A.A. Sharma, J.B. Mander, I.M. Friedland and D.R. Allicock, 6/7/07 (PB2008-105145).

MCEER-07-0009 "Experimental and Analytical Study of the XY-Friction Pendulum (XY-FP) Bearing for Bridge Applications," by C.C. Marin-Artieda, A.S. Whittaker and M.C. Constantinou, 6/7/07 (PB2008-105191).

MCEER-07-0010 "Proceedings of the PRC-US Earthquake Engineering Forum for Young Researchers," Edited by G.C. Lee and X.Z. Qi, 6/8/07 (PB2008-500058).

MCEER-07-0011 "Design Recommendations for Perforated Steel Plate Shear Walls," by R. Purba and M. Bruneau, 6/18/07, (PB2008-105192).

MCEER-07-0012 "Performance of Seismic Isolation Hardware Under Service and Seismic Loading," by M.C. Constantinou, A.S. Whittaker, Y. Kalpakidis, D.M. Fenz and G.P. Warn, 8/27/07, (PB2008-105193).

MCEER-07-0013 "Experimental Evaluation of the Seismic Performance of Hospital Piping Subassemblies," by E.R. Goodwin, E. Maragakis and A.M. Itani, 9/4/07, (PB2008-105194).

MCEER-07-0014 "A Simulation Model of Urban Disaster Recovery and Resilience: Implementation for the 1994 Northridge Earthquake," by S. Miles and S.E. Chang, 9/7/07, (PB2008-106426).

MCEER-07-0015 "Statistical and Mechanistic Fragility Analysis of Concrete Bridges," by M. Shinozuka, S. Banerjee and S-H. Kim, 9/10/07, (PB2008-106427).

MCEER-07-0016 "Three-Dimensional Modeling of Inelastic Buckling in Frame Structures," by M. Schachter and AM. Reinhorn, 9/13/07, (PB2008-108125).

MCEER-07-0017 "Modeling of Seismic Wave Scattering on Pile Groups and Caissons," by I. Po Lam, H. Law and C.T. Yang, 9/17/07 (PB2008-108150).

MCEER-07-0018 "Bridge Foundations: Modeling Large Pile Groups and Caissons for Seismic Design," by I. Po Lam, H. Law and G.R. Martin (Coordinating Author), 12/1/07 (PB2008-111190).

MCEER-07-0019 "Principles and Performance of Roller Seismic Isolation Bearings for Highway Bridges," by G.C. Lee, Y.C. Ou, Z. Liang, T.C. Niu and J. Song, 12/10/07 (PB2009-110466).

MCEER-07-0020 "Centrifuge Modeling of Permeability and Pinning Reinforcement Effects on Pile Response to Lateral Spreading," by L.L Gonzalez-Lagos, T. Abdoun and R. Dobry, 12/10/07 (PB2008-111191).

MCEER-07-0021 "Damage to the Highway System from the Pisco, Perú Earthquake of August 15, 2007," by J.S. O'Connor, L. Mesa and M. Nykamp, 12/10/07, (PB2008-108126).

MCEER-07-0022 "Experimental Seismic Performance Evaluation of Isolation/Restraint Systems for Mechanical Equipment – Part 2: Light Equipment Study," by S. Fathali and A. Filiatrault, 12/13/07 (PB2008-111192).

MCEER-07-0023 "Fragility Considerations in Highway Bridge Design," by M. Shinozuka, S. Banerjee and S.H. Kim, 12/14/07 (PB2008-111193).

MCEER-07-0024 "Performance Estimates for Seismically Isolated Bridges," by G.P. Warn and A.S. Whittaker, 12/30/07 (PB2008-112230).

MCEER-08-0001 "Seismic Performance of Steel Girder Bridge Superstructures with Conventional Cross Frames," by L.P. Carden, A.M. Itani and I.G. Buckle, 1/7/08, (PB2008-112231).

MCEER-08-0002 "Seismic Performance of Steel Girder Bridge Superstructures with Ductile End Cross Frames with Seismic Isolators," by L.P. Carden, A.M. Itani and I.G. Buckle, 1/7/08 (PB2008-112232).

MCEER-08-0003 "Analytical and Experimental Investigation of a Controlled Rocking Approach for Seismic Protection of Bridge Steel Truss Piers," by M. Pollino and M. Bruneau, 1/21/08 (PB2008-112233).

MCEER-08-0004 "Linking Lifeline Infrastructure Performance and Community Disaster Resilience: Models and Multi-Stakeholder Processes," by S.E. Chang, C. Pasion, K. Tatebe and R. Ahmad, 3/3/08 (PB2008-112234).

MCEER-08-0005 "Modal Analysis of Generally Damped Linear Structures Subjected to Seismic Excitations," by J. Song, Y-L. Chu, Z. Liang and G.C. Lee, 3/4/08 (PB2009-102311).

MCEER-08-0006 "System Performance Under Multi-Hazard Environments," by C. Kafali and M. Grigoriu, 3/4/08 (PB2008-112235).

MCEER-08-0007 "Mechanical Behavior of Multi-Spherical Sliding Bearings," by D.M. Fenz and M.C. Constantinou, 3/6/08 (PB2008-112236).

MCEER-08-0008 "Post-Earthquake Restoration of the Los Angeles Water Supply System," by T.H.P. Tabucchi and R.A. Davidson, 3/7/08 (PB2008-112237).

MCEER-08-0009 "Fragility Analysis of Water Supply Systems," by A. Jacobson and M. Grigoriu, 3/10/08 (PB2009-105545).

MCEER-08-0010 "Experimental Investigation of Full-Scale Two-Story Steel Plate Shear Walls with Reduced Beam Section Connections," by B. Qu, M. Bruneau, C-H. Lin and K-C. Tsai, 3/17/08 (PB2009-106368).

MCEER-08-0011 "Seismic Evaluation and Rehabilitation of Critical Components of Electrical Power Systems," S. Ersoy, B. Feizi, A. Ashrafi and M. Ala Saadeghvaziri, 3/17/08 (PB2009-105546).

MCEER-08-0012 "Seismic Behavior and Design of Boundary Frame Members of Steel Plate Shear Walls," by B. Qu and M. Bruneau, 4/26/08 . (PB2009-106744).

MCEER-08-0013 "Development and Appraisal of a Numerical Cyclic Loading Protocol for Quantifying Building System Performance," by A. Filiatrault, A. Wanitkorkul and M. Constantinou, 4/27/08 (PB2009-107906).

MCEER-08-0014 "Structural and Nonstructural Earthquake Design: The Challenge of Integrating Specialty Areas in Designing Complex, Critical Facilities," by W.J. Petak and D.J. Alesch, 4/30/08 (PB2009-107907).

MCEER-08-0015 "Seismic Performance Evaluation of Water Systems," by Y. Wang and T.D. O'Rourke, 5/5/08 (PB2009-107908).

MCEER-08-0016 "Seismic Response Modeling of Water Supply Systems," by P. Shi and T.D. O'Rourke, 5/5/08 (PB2009-107910).

MCEER-08-0017 "Numerical and Experimental Studies of Self-Centering Post-Tensioned Steel Frames," by D. Wang and A. Filiatrault, 5/12/08 (PB2009-110479).

MCEER-08-0018 "Development, Implementation and Verification of Dynamic Analysis Models for Multi-Spherical Sliding Bearings," by D.M. Fenz and M.C. Constantinou, 8/15/08 (PB2009-107911).

MCEER-08-0019 "Performance Assessment of Conventional and Base Isolated Nuclear Power Plants for Earthquake Blast Loadings," by Y.N. Huang, A.S. Whittaker and N. Luco, 10/28/08 (PB2009-107912).

MCEER-08-0020 "Remote Sensing for Resilient Multi-Hazard Disaster Response – Volume I: Introduction to Damage Assessment Methodologies," by B.J. Adams and R.T. Eguchi, 11/17/08 (PB2010-102695).

MCEER-08-0021 "Remote Sensing for Resilient Multi-Hazard Disaster Response – Volume II: Counting the Number of Collapsed Buildings Using an Object-Oriented Analysis: Case Study of the 2003 Bam Earthquake," by L. Gusella, C.K. Huyck and B.J. Adams, 11/17/08 (PB2010-100925).

MCEER-08-0022 "Remote Sensing for Resilient Multi-Hazard Disaster Response – Volume III: Multi-Sensor Image Fusion Techniques for Robust Neighborhood-Scale Urban Damage Assessment," by B.J. Adams and A. McMillan, 11/17/08 (PB2010-100926).

MCEER-08-0023 "Remote Sensing for Resilient Multi-Hazard Disaster Response – Volume IV: A Study of Multi-Temporal and Multi-Resolution SAR Imagery for Post-Katrina Flood Monitoring in New Orleans," by A. McMillan, J.G. Morley, B.J. Adams and S. Chesworth, 11/17/08 (PB2010-100927).

MCEER-08-0024 "Remote Sensing for Resilient Multi-Hazard Disaster Response – Volume V: Integration of Remote Sensing Imagery and VIEWS^{TM} Field Data for Post-Hurricane Charley Building Damage Assessment," by J.A. Womble, K. Mehta and B.J. Adams, 11/17/08 (PB2009-115532).

MCEER-08-0025 "Building Inventory Compilation for Disaster Management: Application of Remote Sensing and Statistical Modeling," by P. Sarabandi, A.S. Kiremidjian, R.T. Eguchi and B. J. Adams, 11/20/08 (PB2009-110484).

MCEER-08-0026 "New Experimental Capabilities and Loading Protocols for Seismic Qualification and Fragility Assessment of Nonstructural Systems," by R. Retamales, G. Mosqueda, A. Filiatrault and A. Reinhorn, 11/24/08 (PB2009-110485).

MCEER-08-0027 "Effects of Heating and Load History on the Behavior of Lead-Rubber Bearings," by I.V. Kalpakidis and M.C. Constantinou, 12/1/08 (PB2009-115533).

MCEER-08-0028 "Experimental and Analytical Investigation of Blast Performance of Seismically Resistant Bridge Piers," by S.Fujikura and M. Bruneau, 12/8/08 (PB2009-115534).

MCEER-08-0029 "Evolutionary Methodology for Aseismic Decision Support," by Y. Hu and G. Dargush, 12/15/08.

MCEER-08-0030 "Development of a Steel Plate Shear Wall Bridge Pier System Conceived from a Multi-Hazard Perspective," by D. Keller and M. Bruneau, 12/19/08 (PB2010-102696).

MCEER-09-0001 "Modal Analysis of Arbitrarily Damped Three-Dimensional Linear Structures Subjected to Seismic Excitations," by Y.L. Chu, J. Song and G.C. Lee, 1/31/09 (PB2010-100922).

MCEER-09-0002 "Air-Blast Effects on Structural Shapes," by G. Ballantyne, A.S. Whittaker, A.J. Aref and G.F. Dargush, 2/2/09 (PB2010-102697).

MCEER-09-0003 "Water Supply Performance During Earthquakes and Extreme Events," by A.L. Bonneau and T.D. O'Rourke, 2/16/09 (PB2010-100923).

MCEER-09-0004 "Generalized Linear (Mixed) Models of Post-Earthquake Ignitions," by R.A. Davidson, 7/20/09 (PB2010-102698).

MCEER-09-0005 "Seismic Testing of a Full-Scale Two-Story Light-Frame Wood Building: NEESWood Benchmark Test," by I.P. Christovasilis, A. Filiatrault and A. Wanitkorkul, 7/22/09 (PB2012-102401).

MCEER-09-0006 "IDARC2D Version 7.0: A Program for the Inelastic Damage Analysis of Structures," by A.M. Reinhorn, H. Roh, M. Sivaselvan, S.K. Kunnath, R.E. Valles, A. Madan, C. Li, R. Lobo and Y.J. Park, 7/28/09 (PB2010-103199).

MCEER-09-0007 "Enhancements to Hospital Resiliency: Improving Emergency Planning for and Response to Hurricanes," by D.B. Hess and L.A. Arendt, 7/30/09 (PB2010-100924).

MCEER-09-0008 "Assessment of Base-Isolated Nuclear Structures for Design and Beyond-Design Basis Earthquake Shaking," by Y.N. Huang, A.S. Whittaker, R.P. Kennedy and R.L. Mayes, 8/20/09 (PB2010-102699).

MCEER-09-0009 "Quantification of Disaster Resilience of Health Care Facilities," by G.P. Cimellaro, C. Fumo, A.M Reinhorn and M. Bruneau, 9/14/09 (PB2010-105384).

MCEER-09-0010 "Performance-Based Assessment and Design of Squat Reinforced Concrete Shear Walls," by C.K. Gulec and A.S. Whittaker, 9/15/09 (PB2010-102700).

MCEER-09-0011 "Proceedings of the Fourth US-Taiwan Bridge Engineering Workshop," edited by W.P. Yen, J.J. Shen, T.M. Lee and R.B. Zheng, 10/27/09 (PB2010-500009).

MCEER-09-0012 "Proceedings of the Special International Workshop on Seismic Connection Details for Segmental Bridge Construction," edited by W. Phillip Yen and George C. Lee, 12/21/09 (PB2012-102402).

MCEER-10-0001 "Direct Displacement Procedure for Performance-Based Seismic Design of Multistory Woodframe Structures," by W. Pang and D. Rosowsky, 4/26/10 (PB2012-102403).

MCEER-10-0002 "Simplified Direct Displacement Design of Six-Story NEESWood Capstone Building and Pre-Test Seismic Performance Assessment," by W. Pang, D. Rosowsky, J. van de Lindt and S. Pei, 5/28/10 (PB2012-102404).

MCEER-10-0003 "Integration of Seismic Protection Systems in Performance-Based Seismic Design of Woodframed Structures," by J.K. Shinde and M.D. Symans, 6/18/10 (PB2012-102405).

MCEER-10-0004 "Modeling and Seismic Evaluation of Nonstructural Components: Testing Frame for Experimental Evaluation of Suspended Ceiling Systems," by A.M. Reinhorn, K.P. Ryu and G. Maddaloni, 6/30/10 (PB2012-102406).

MCEER-10-0005 "Analytical Development and Experimental Validation of a Structural-Fuse Bridge Pier Concept," by S. El-Bahey and M. Bruneau, 10/1/10 (PB2012-102407).

MCEER-10-0006 "A Framework for Defining and Measuring Resilience at the Community Scale: The PEOPLES Resilience Framework," by C.S. Renschler, A.E. Frazier, L.A. Arendt, G.P. Cimellaro, A.M. Reinhorn and M. Bruneau, 10/8/10 (PB2012-102408).

MCEER-10-0007 "Impact of Horizontal Boundary Elements Design on Seismic Behavior of Steel Plate Shear Walls," by R. Purba and M. Bruneau, 11/14/10 (PB2012-102409).

MCEER-10-0008 "Seismic Testing of a Full-Scale Mid-Rise Building: The NEESWood Capstone Test," by S. Pei, J.W. van de Lindt, S.E. Pryor, H. Shimizu, H. Isoda and D.R. Rammer, 12/1/10 (PB2012-102410).

MCEER-10-0009 "Modeling the Effects of Detonations of High Explosives to Inform Blast-Resistant Design," by P. Sherkar, A.S. Whittaker and A.J. Aref, 12/1/10 (PB2012-102411).

MCEER-10-0010 "L'Aquila Earthquake of April 6, 2009 in Italy: Rebuilding a Resilient City to Withstand Multiple Hazards," by G.P. Cimellaro, I.P. Christovasilis, A.M. Reinhorn, A. De Stefano and T. Kirova, 12/29/10.

MCEER-11-0001 "Numerical and Experimental Investigation of the Seismic Response of Light-Frame Wood Structures," by I.P. Christovasilis and A. Filiatrault, 8/8/11 (PB2012-102412).

MCEER-11-0002 "Seismic Design and Analysis of a Precast Segmental Concrete Bridge Model," by M. Anagnostopoulou, A. Filiatrault and A. Aref, 9/15/11.

MCEER-11-0003 'Proceedings of the Workshop on Improving Earthquake Response of Substation Equipment," Edited by A.M. Reinhorn, 9/19/11 (PB2012-102413).

MCEER-11-0004 "LRFD-Based Analysis and Design Procedures for Bridge Bearings and Seismic Isolators," by M.C. Constantinou, I. Kalpakidis, A. Filiatrault and R.A. Ecker Lay, 9/26/11.

MCEER-11-0005 "Experimental Seismic Evaluation, Model Parameterization, and Effects of Cold-Formed Steel-Framed Gypsum Partition Walls on the Seismic Performance of an Essential Facility," by R. Davies, R. Retamales, G. Mosqueda and A. Filiatrault, 10/12/11.

MCEER-11-0006 "Modeling and Seismic Performance Evaluation of High Voltage Transformers and Bushings," by A.M. Reinhorn, K. Oikonomou, H. Roh, A. Schiff and L. Kempner, Jr., 10/3/11.

MCEER-11-0007 "Extreme Load Combinations: A Survey of State Bridge Engineers," by G.C. Lee, Z. Liang, J.J. Shen and J.S. O'Connor, 10/14/11.

MCEER-12-0001 "Simplified Analysis Procedures in Support of Performance Based Seismic Design," by Y.N. Huang and A.S. Whittaker.

MCEER-12-0002 "Seismic Protection of Electrical Transformer Bushing Systems by Stiffening Techniques," by M. Koliou, A. Filiatrault, A.M. Reinhorn and N. Oliveto, 6/1/12.

MCEER-12-0003 "Post-Earthquake Bridge Inspection Guidelines," by J.S. O'Connor and S. Alampalli, 6/8/12.

MCEER-12-0004 "Integrated Design Methodology for Isolated Floor Systems in Single-Degree-of-Freedom Structural Fuse Systems," by S. Cui, M. Bruneau and M.C. Constantinou, 6/13/12.

MCEER-12-0005 "Characterizing the Rotational Components of Earthquake Ground Motion," by D. Basu, A.S. Whittaker and M.C. Constantinou, 6/15/12.

MCEER-12-0006 "Bayesian Fragility for Nonstructural Systems," by C.H. Lee and M.D. Grigoriu, 9/12/12.

MCEER-12-0007 "A Numerical Model for Capturing the In-Plane Seismic Response of Interior Metal Stud Partition Walls," by R.L. Wood and T.C. Hutchinson, 9/12/12.

MCEER-12-0008 "Assessment of Floor Accelerations in Yielding Buildings," by J.D. Wieser, G. Pekcan, A.E. Zaghi, A.M. Itani and E. Maragakis, 10/5/12.

MCEER-13-0001 "Experimental Seismic Study of Pressurized Fire Sprinkler Piping Systems," by Y. Tian, A. Filiatrault and G. Mosqueda, 4/8/13.

MCEER-13-0002 "Enhancing Resource Coordination for Multi-Modal Evacuation Planning," by D.B. Hess, B.W. Conley and C.M. Farrell, 2/8/13.

MCEER-13-0003 "Seismic Response of Base Isolated Buildings Considering Pounding to Moat Walls," by A. Masroor and G. Mosqueda, 2/26/13.

MCEER-13-0004 "Seismic Response Control of Structures Using a Novel Adaptive Passive Negative Stiffness Device," by D.T.R. Pasala, A.A. Sarlis, S. Nagarajaiah, A.M. Reinhorn, M.C. Constantinou and D.P. Taylor, 6/10/13.

MCEER-13-0005 "Negative Stiffness Device for Seismic Protection of Structures," by A.A. Sarlis, D.T.R. Pasala, M.C. Constantinou, A.M. Reinhorn, S. Nagarajaiah and D.P. Taylor, 6/12/13.

MCEER-13-0006 "Emilia Earthquake of May 20, 2012 in Northern Italy: Rebuilding a Resilient Community to Withstand Multiple Hazards," by G.P. Cimellaro, M. Chiriatti, A.M. Reinhorn and L. Tirca, June 30, 2013.

MCEER-13-0007 "Precast Concrete Segmental Components and Systems for Accelerated Bridge Construction in Seismic Regions," by A.J. Aref, G.C. Lee, Y.C. Ou and P. Sideris, with contributions from K.C. Chang, S. Chen, A. Filiatrault and Y. Zhou, June 13, 2013.

MCEER-13-0008 "A Study of U.S. Bridge Failures (1980-2012)," by G.C. Lee, S.B. Mohan, C. Huang and B.N. Fard, June 15, 2013.

MCEER-13-0009 "Development of a Database Framework for Modeling Damaged Bridges," by G.C. Lee, J.C. Qi and C. Huang, June 16, 2013.

MCEER-13-0010 "Model of Triple Friction Pendulum Bearing for General Geometric and Frictional Parameters and for Uplift Conditions," by A.A. Sarlis and M.C. Constantinou, July 1, 2013.

MCEER-13-0011 "Shake Table Testing of Triple Friction Pendulum Isolators under Extreme Conditions," by A.A. Sarlis, M.C. Constantinou and A.M. Reinhorn, July 2, 2013.

MCEER-13-0012 "Theoretical Framework for the Development of MH-LRFD," by G.C. Lee (coordinating author), H.A Capers, Jr., C. Huang, J.M. Kulicki, Z. Liang, T. Murphy, J.J.D. Shen, M. Shinozuka and P.W.H. Yen, July 31, 2013.

MCEER-13-0013 "Seismic Protection of Highway Bridges with Negative Stiffness Devices," by N.K.A. Attary, M.D. Symans, S. Nagarajaiah, A.M. Reinhorn, M.C. Constantinou, A.A. Sarlis, D.T.R. Pasala, and D.P. Taylor, September 3, 2014.

MCEER-14-0001 "Simplified Seismic Collapse Capacity-Based Evaluation and Design of Frame Buildings with and without Supplemental Damping Systems," by M. Hamidia, A. Filiatrault, and A. Aref, May 19, 2014.

MCEER-14-0002 "Comprehensive Analytical Seismic Fragility of Fire Sprinkler Piping Systems," by Siavash Soroushian, Emmanuel "Manos" Maragakis, Arash E. Zaghi, Alicia Echevarria, Yuan Tian and Andre Filiatrault, August 26, 2014.

MCEER-14-0003 "Hybrid Simulation of the Seismic Response of a Steel Moment Frame Building Structure through Collapse," by M. Del Carpio Ramos, G. Mosqueda and D.G. Lignos, October 30, 2014.

MCEER-14-0004 "Blast and Seismic Resistant Concrete-Filled Double Skin Tubes and Modified Steel Jacketed Bridge Columns," by P.P. Fouche and M. Bruneau, June 30, 2015.

MCEER-14-0005 "Seismic Performance of Steel Plate Shear Walls Considering Various Design Approaches," by R. Purba and M. Bruneau, October 31, 2014.

MCEER-14-0006 "Air-Blast Effects on Civil Structures," by Jinwon Shin, Andrew S. Whittaker, Amjad J. Aref and David Cormie, October 30, 2014.

MCEER-14-0007 "Seismic Performance Evaluation of Precast Girders with Field-Cast Ultra High Performance Concrete (UHPC) Connections," by G.C. Lee, C. Huang, J. Song, and J. S. O'Connor, July 31, 2014.

MCEER-14-0008 "Post-Earthquake Fire Resistance of Ductile Concrete-Filled Double-Skin Tube Columns," by Reza Imani, Gilberto Mosqueda and Michel Bruneau, December 1, 2014.

MCEER-14-0009 "Cyclic Inelastic Behavior of Concrete Filled Sandwich Panel Walls Subjected to In-Plane Flexure," by Y. Alzeni and M. Bruneau, December 19, 2014.

MCEER-14-0010 "Analytical and Experimental Investigation of Self-Centering Steel Plate Shear Walls," by D.M. Dowden and M. Bruneau, December 19, 2014.

MCEER-15-0001 "Seismic Analysis of Multi-story Unreinforced Masonry Buildings with Flexible Diaphragms," by J. Aleman, G. Mosqueda and A.S. Whittaker, June 12, 2015.

MCEER-15-0002 "Site Response, Soil-Structure Interaction and Structure-Soil-Structure Interaction for Performance Assessment of Buildings and Nuclear Structures," by C. Bolisetti and A.S. Whittaker, June 15, 2015.

MCEER-15-0003 "Stress Wave Attenuation in Solids for Mitigating Impulsive Loadings," by R. Rafiee-Dehkharghani, A.J. Aref and G. Dargush, August 15, 2015..

MCEER-15-0004 "Computational, Analytical, and Experimental Modeling of Masonry Structures," by K.M. Dolatshahi and A.J. Aref, November 16, 2015.

MCEER-15-0005 "Property Modification Factors for Seismic Isolators: Design Guidance for Buildings," by W.J. McVitty and M.C. Constantinou, June 30, 2015.

MCEER-15-0006 "Seismic Isolation of Nuclear Power Plants using Sliding Isolation Bearings," by Manish Kumar, Andrew S. Whittaker and Michael C. Constantinou, December 27, 2015.

MCEER-15-0007 "Quiintuple Friction Pendulum Isolator Behavior, Modeling and Validation," by Donghun Lee and Michael C. Constantinou, December 28, 2015.

MCEER
EARTHQUAKE ENGINEERING TO EXTREME EVENTS
University at Buffalo, The State University of New York
133A Ketter Hall ▪ Buffalo, New York 14260-4300
Phone: (716) 645-3391 ▪ Fax: (716) 645-3399
Email: *mceer@buffalo.edu* ▪ Web: *http://mceer.buffalo.edu*
University at Buffalo *The State University of New York*

ISSN 1520-295X